

# 1. LEG 181 SYNTHESIS: FRONTS, FLOWS, DRIFTS, VOLCANOES, AND THE EVOLUTION OF THE SOUTHWESTERN GATEWAY TO THE PACIFIC OCEAN, EASTERN NEW ZEALAND<sup>1</sup>

R.M. Carter,<sup>2</sup> I.N. McCave,<sup>3</sup> and L. Carter<sup>4</sup>

## ABSTRACT

The Late Cretaceous–Cenozoic geology of New Zealand represents the evolution of a post-Gondwana, Pacific-facing passive margin which interacted, first, with the mid-Cenozoic development of the Australian/Antarctic and Australian/Pacific plate boundaries and, second, with the subsequent development of the oceanic thermohaline circulation system. Situated between the Tasmanian and southwest Pacific oceanic current gateways, the stratigraphy of the New Zealand region provides our best record of the evolution of the Pacific Ocean's largest deep cold-water inflow, the Deep Western Boundary Current (DWBC), and also possesses an important record of Antarctic Intermediate Water flow. Prior to Leg 181, our knowledge of southwest Pacific Ocean history and, in particular, the development of the DWBC and its local partner, the Antarctic Circumpolar Current (ACC), was poor. Seven holes were therefore drilled east of New Zealand to determine the stratigraphy, sedimentary systems, and paleoceanography of the DWBC, ACC, and related water masses and fronts. The sites comprised a transect of water depths from 396 to 4488 m and spanned a latitudinal range from 39° to 51°S. Leg 181 drilling provided the data needed to study a wide range of problems in the Southern Ocean Neogene.

Driven by rifting and a new cycle of seafloor spreading along the Mid-Pacific Rise, New Zealand's youngest (Kaikoura) stratigraphic cycle begins with Late Cretaceous rift fill followed by subsidence and marine transgression until the late Eocene. Biopelagic oozes accumulated

<sup>1</sup>Carter, R.M., McCave, I.N., and Carter, L., 2004. Leg 181 synthesis: fronts, flows, drifts, volcanoes, and the evolution of the southwestern gateway to the Pacific Ocean, eastern New Zealand. *In* Richter, C. (Ed.), *Proc. ODP, Sci. Results*, 181, 1–111 [Online]. Available from World Wide Web: <[http://www-odp.tamu.edu/publications/181\\_SR/VOLUME/SYNTH/SYNTH.PDF](http://www-odp.tamu.edu/publications/181_SR/VOLUME/SYNTH/SYNTH.PDF)>. [Cited YYYY-MM-DD]

<sup>2</sup>Marine Geophysical Laboratory, James Cook University, Townsville QLD 4811, Australia.

[bob.carter@jcu.edu.au](mailto:bob.carter@jcu.edu.au)

<sup>3</sup>Department of Earth Sciences, University of Cambridge, Downing Street, Cambridge CB2 3EQ, United Kingdom.

<sup>4</sup>National Institute of Water and Atmosphere, PO Box 14-901 Kilbirnie, Wellington, New Zealand.

Initial receipt: 17 December 2002

Acceptance: 15 October 2003

Web publication: 20 February 2004

Ms 181SR-210

throughout as an abyssal apron around the Pacific perimeter of the New Zealand Plateau, seen as Paleocene siliceous nannofossil chalk, chert, and clay at Site 1121 (water depth = 4488 m) and nannofossil chalk at Site 1124 (water depth = 3967 m). At the Eocene/Oligocene boundary (~33.7 Ma), the spreading ridge between Australia and Antarctica broke through south of the Tasman Rise, linking for the first time the Indian and Pacific Oceans into a continuous Southern Ocean. Powerful wind-forced currents, predecessors to the modern ACC, were funneled through the Tasmanian Gateway and into the Pacific, where their path, combined with that of the thermohaline DWBC, was impeded by the shallowly submergent New Zealand Plateau, centered then at latitude ~55°S. All drill sites within or east of the Tasmanian Gateway and all onland sections in New Zealand record this event as a regional unconformity, the Marshall Paraconformity, across which there is a time gap of ~3–10 m.y., a result of a combination of corrosion, erosion, and non-deposition. Above the paraconformity, sedimentation in both shallow and deep water resumed as late Oligocene (~27–29 Ma) sediment drifts (Site 1124; water depth = 3967 m). Younger deepwater drifts at Sites 1123 (water depth = 3290 m) and 1124 comprise alternating nannofossil chinks containing greater or lesser amounts of terrigenous clay. At Site 1123 on the North Chatham Drift, sediment accumulated essentially continuously from ~20.5 Ma onward. Analysis of this record shows that the stratigraphic rhythms there correspond to 41-k.y. Milankovitch climatic cycles, with faster DWBC flow during colder or glacial intervals. Site 1123 is globally unique. It provides an essentially complete, richly microfossiliferous Miocene to Quaternary record of uniform ~4-cm/k.y. sedimentation that has been astronomically tuned. It also contains an almost complete paleomagnetic record since Chron C6r at 20.5 Ma, including the first record of new magnetic subchron C5ADn1r. Shallower-water Sites 1125 (water depth = 1366 m), 1120 (water depth = 546 m), and 1119 (water depth = 396 m) reveal, respectively, a major productivity bloom between 5.6 and 4.8 Ma on the north side of the Subtropical Front (STF) (Site 1125), foraminiferal nannofossil chalk accumulation punctuated by paraconformities at 16.7–15.8, 5.6–1.9, and 0.9–0.24 Ma (Site 1120), and enhanced frontal flows along a seaward-relocated STF during glaciations (Site 1119). The late Quaternary climatic record at Site 1119 also closely matches that of air temperature in the Vostok ice core, indicating close links between climate change in southern middle and polar latitudes.

From ~24 Ma onward, abundant terrigenous material was shed into the southwest Pacific from rising mountains along the South Island Alpine Fault plate boundary. Gradually changing clay mineral assemblages in DWBC drifts, with chlorite + illite replacing smectite + kaolinite, reflect the increasing influence of newly unroofed basement (Rangitata) graywackes and schists through the Miocene–Quaternary. From 12 Ma onward, sediments were augmented by an influx of mainly rhyolitic tephra from the North Island volcanic arc. Site 1122 (water depth = 4432 m), on the left bank levee of the abyssal Bounty Fan, records a marked increase in the input of terrigenous turbidites and fan building starting at ~1.7 Ma and peaking at average rates >50 cm/k.y. after 0.7 Ma. Site 1124, on the Rekohu Drift near the Hikurangi Channel, records the start of overbank turbidite deposition, and therefore avulsion of the Hikurangi Channel from the Hikurangi Trough following channel deflection by a large submarine landslide from the North Island continental margin at ~1.65 Ma. Geological and oceanographic events that have occurred in the southwest Pacific since the Eocene/

Oligocene boundary (~33.7 Ma) together compose the Eastern New Zealand Sedimentary System (ENZOSS), studies of which are contributing to our understanding of the history of global ocean circulation and climate change.

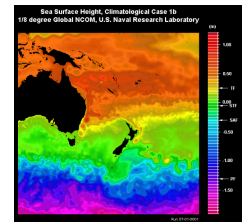
## INTRODUCTION

Had it not been the Land of the Long White Cloud (Aotearoa), in 1769 Young Nick and Captain Cook might have sailed right past the island microcontinent that is New Zealand. Instead, after sighting and then circumnavigating and mapping “the land uplifted high” (see the volume [Frontispiece](#), parts A–C), Cook proceeded westward to chart also the east coast of Australia. He thus demonstrated to his European audience the existence of the Tasman Sea and established the geographic importance of New Zealand as the western margin of the main Pacific Ocean Basin (Fig. F1).

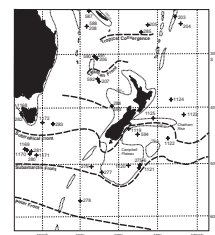
Almost exactly 200 years later, two other Northern Hemisphere vessels sailed New Zealand waters in pursuit of a global understanding of the nature of continents, ocean basins, and the tectonically active volcanic interface between them that is exemplified by the circum-Pacific mobile belt. In 1962, the vessel *Eltanin* was assigned to the U.S. National Science Foundation (NSF) for use as a research ship in support of the Foundation’s Antarctic and Southern Ocean research program. During 1962–1972, the *Eltanin* conducted an extensive series of 55 pioneering voyages that laid the basis for our understanding of the oceanography and geology of the Southern Ocean (e.g., Glasby, 1990). Many of the *Eltanin* results were published in more than 40 volumes of the *Antarctic Research Series* of the American Geophysical Union (for Pacific geology, especially volumes 15 and 19) (cf. Houtz et al., 1967; Ewing et al., 1969; Hayes and Pitman, 1972; and summary in Davey, 1977). These achievements were followed, in 1972–1974, by the accomplishment of drilling Legs 21, 28, and 29 by the *Glomar Challenger* (Fig. F2) under the aegis of the NSF Deep Sea Drilling Project (DSDP), which formed part of the then rapid development of our understanding of the mechanisms of global tectonics and of the new discipline of paleoceanography (e.g., Burns, Andrews, et al., 1973; Kennett, Houtz, et al., 1975; Andrews, 1977; Burns, 1977). At that time, perhaps most astonishing was the fact that shipborne measurements and conclusions, drawn mostly by persons unfamiliar with New Zealand geology, should provide such powerful insights into both global geological mechanisms (Molnar et al., 1975; Weissel et al., 1977) and regional geological history (Ballance, 1976; Carter, R., and Norris, 1976).

The science achieved by these *Eltanin*–*Glomar Challenger* cruises revolutionized our understanding of southwest Pacific geology and oceanography just as surely as Cook, earlier, had revolutionized our appreciation of its geography. The first plate tectonic interpretations made it apparent that the northeast-trending active volcanic and earthquake zones of New Zealand—in the North Island the Taupo Volcanic Zone–Hikurangi Subduction Zone and in the South Island the transform Alpine fault—marked the modern plate boundary between the Pacific and the Australian plates (Isacks et al., 1968; Le Pichon, 1968; Molnar et al., 1975; Sutherland, 1995). The Tasman Sea represents an abandoned spreading center located entirely on the Australian plate (Hayes and Ringis, 1973; Weissel and Hayes, 1977). Thus, the New Zealand Plateau or microcontinent—comprising the emergent islands

F1. Simulation of sea-surface height, p. 83.



F2. Location map for the southwest Pacific region, p. 84.



together with the flanking submarine Campbell Plateau, Chatham Rise, and Lord Howe Rise—forms not only the geographic but also the geologic and oceanographic southwestern margin of the Pacific Ocean Basin.

### Historical Geological Studies

Meanwhile, onland, more than one 100 years of investigation by the staff of the New Zealand Geological Survey (Grindley et al., 1959) and by university and museum researchers had established that New Zealand's younger geology encompassed a richly fossiliferous record with a widely varying representation of both nonmarine and marine sediment facies (e.g., Cotton, 1955; Fleming, 1975; Suggate et al., 1978). The essentially unbroken nature of the postrifting succession of sediments is well summarized in the quotation from Cotton at the head of this review (cf. volume [Frontispiece](#), part D). This Cretaceous–Cenozoic succession was termed the Notocenozoic by Cotton (1955) and classified as the Kaikoura Sequence (now Kaikoura Synthem) by Carter, R., et al. (1974). (Use of the term synthem as a replacement for sequence, in the sense of Sloss, 1963, after the latter term had been usurped by sequence stratigraphers, follows the usage of the International Commission on Stratigraphic Nomenclature. Synthems retain great usefulness as high-level terms for the widespread, unconformity-bounded packets of strata that make up regional geological successions; cf. Chang, 1975).

Compared with land-based geological studies, knowledge of the offshore geology and oceanography of the New Zealand region lagged and only developed during the second half of the twentieth century. Two events were pivotal to improving our knowledge of the geology of offshore territories. The first was the creation in 1954 of the New Zealand Oceanographic Institute (NZOI), initially as a branch of the Department of Scientific and Industrial Research (DSIR) but since 1992 encompassed within the National Institute of Water and Atmosphere (NIWA). The creation of a strong marine geological capability followed, as reflected in the major advances made by NZOI staff in understanding New Zealand's undersea geology and sedimentology during the second half of the twentieth century; Thompson (1994) presented a summary of this activity. Second, increasing numbers of petroleum exploration wells were drilled in New Zealand offshore waters from the 1960s onward. Under a far-sighted licensing policy, the seismic and stratigraphic databases collected during commercial exploration became open file reports, available through the Petroleum Section of the Geological Survey of New Zealand (e.g., McLernon, 1972). Analysis of this offshore data in conjunction with the onland geology had a markedly beneficial effect on the regional understanding of Cretaceous–Cenozoic stratigraphy, as exemplified by the appearance of the first regionally comprehensible and modern account of New Zealand's eight or so major Kaikoura sedimentary basins (Katz, 1968, updated in Ballance, 1993a; Laird, in press).

Each of New Zealand's post-Gondwana sedimentary basins, of course, contains an idiosyncratic local history, but all the eastern basins conform to the same regional pattern of *initiation by rifting* during the Late Cretaceous creation of the Pacific margin of the New Zealand microcontinent; *thermal subsidence* and *marine transgression* during the Cretaceous–Eocene phase of passive margin drift that accompanied mid-Pacific seafloor spreading; *sediment starvation* and *current erosion* during the Oligocene, by which time land areas and terrigenous sediment sources were greatly reduced and Southern Ocean current flows

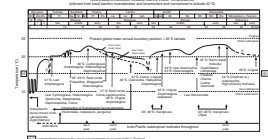
had started; and *increased terrigenous sedimentation* under the accelerating influence of volcanic and tectonic activity along the developing New Zealand plate boundary from the early Miocene onward (volume [Frontispiece](#), part A) (Ballance, 1976; Carter, R., and Norris, 1976; Carter, R., 1988b; Ballance, 1993b; Laird, in press). Most of the sediments from which these generalizations are drawn were deposited in shallow or intermediate-depth marine waters, say <1500 m deep. Nonetheless, even the earliest studies recognized that these waters represented merely the shallow edge of a much larger and deeper Pacific Ocean Basin. This leads us to discuss the development of paleoclimatic and paleoceanographic studies in New Zealand.

### Cenozoic Climatic History of the New Zealand Region

Pelagic marine macro-organisms, such as nautiloids, occur only rarely as Cenozoic fossils. Thus, the abundant and diverse New Zealand Cretaceous–Cenozoic macrofossil record, like most, is overwhelmingly dominated by the remains of benthic organisms of limited zoogeographic distribution. Not surprisingly, the rich New Zealand literature on the interpretation of these fossil assemblages has been concerned mostly with discussion of their evolutionary and geographic origins and overseas affinities, as exemplified, for instance, by Finlay (1925). By the 1960s, however, the greatly increased knowledge of the invertebrate fossil faunas and the development of micropaleontological studies led to a burst of papers in which zoogeographic analysis was used also to infer New Zealand's changing climate history, as summarized by Fleming (1962; updated in 1975) and Hornibrook (1992). About the same time, the first direct physical measurements related to oceanic paleotemperature were provided from oxygen isotope analyses by Devereux (1967), and papers by Kennett (1968) and Vella (1973) provided early assessments of the past distribution of oceanic water masses in the southwest Pacific based on analysis of planktonic microfossils. These studies—which were based on organisms as diverse as mollusks, brachiopods, echinoderms, corals, foraminifers, nannoplankton, and trees (nuts, seeds, and pollen)—converged to provide a clear consensus regarding the history of Cenozoic climate in the New Zealand region (Fig. F3).

In outline, New Zealand fossil assemblages reveal the dominance of warm temperate to subtropical temperatures during the Paleocene and Eocene, followed by a sharp reduction of temperature across the Eocene/Oligocene boundary (33.7 Ma), and then warming in the late Oligocene. Gradual warming continued up until the occurrence of another subtropical climatic optimum in the early middle Miocene (Altonian–Clifdenian; peaking at ~16.5 Ma), followed by reducing temperatures through the remainder of the Miocene and Pliocene, with the final disappearance of most warm-water taxa and the appearance of subantarctic immigrants at ~2.4 Ma. Superimposed on this long-term climatic change, from ~3.5 Ma onward increasing tectonic uplift resulted in the exposure onland of sections containing a superb cyclothem record of Pliocene–Pleistocene glacial–interglacial fluctuations (Fleming, 1953; Beu and Edwards, 1984; Haywick et al., 1992; Abbott and Carter, R., 1994; Naish and Kamp, 1995; Journeaux et al., 1996; Saul et al., 1999).

F3. Climatic history of the New Zealand region, p. 85.



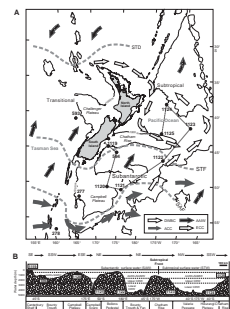
## Paleoceanography in the New Zealand Region

Because of the richly fossiliferous nature of the sedimentary record, environmental inferences about past New Zealand seas are common in the local geological literature from the late nineteenth century onward. Thus Marshall (1912, p. 41) commented that the characteristics of outcropping Oligocene glauconitic marls “tell us that much of the present land was during this period 1200 to 1800 feet below the sea level” and that “limestone succeeds the greensand and indicates deeper submergence and probably the climax of the (downward) movement.” These, of course, are paleoceanographic inferences. Fleming’s comprehensive summary (Fleming, 1975) of this largely qualitative phase of paleoceanographic and paleogeographic study was, appropriately, published a little after the pioneering reconstruction by Devereux (1967) of the world’s first Cenozoic-long oxygen isotope paleotemperature record. Although based on mixed samples from both micro- and macrofossils, Devereux’s New Zealand curve broadly mirrors current high-resolution global isotope curves (e.g., Zachos et al., 2001) and included a clear delineation of the abrupt, major temperature decline across the Eocene/Oligocene boundary.

Modern paleoceanography arose from using similar new and sensitive analytical techniques applied to the long, undisturbed, and uninterrupted oceanic sediment cores that became available from the late 1960s. In this regard, the hydraulic piston corer, precursor of the advanced piston corer (APC), was first deployed successfully during DSDP Leg 64 in the Gulf of California in 1982, and the first volume of the journal *Paleoceanography* appeared in 1986. The 1983 drilling of DSDP Leg 90, a latitudinal transect of sites with paleoceanographic targets, provided the first lengthy piston cores from the New Zealand region (Kennett, von der Borch, et al., 1986). This drilling marked the inception of modern paleoceanographic research in the southwest Pacific Ocean, 10 years after Vella (1973, p. 318) concluded a discussion of the onland evidence for Neogene movements of the subtropical front (STF) with the prescient remark that “...to obtain more direct, more reliable and more complete results, the research must be reoriented towards paleo-oceanography.”

DSDP Sites 593 and 594, drilled during Leg 90, were situated west and east of New Zealand, respectively, in subtropical waters on the Lord Howe Rise and subantarctic waters on the southern flank of the Chatham Rise (Kennett, von der Borch, et al., 1986). Subsequent study of material from these and earlier DSDP sites provided the first high-resolution sedimentary, geochemical, and climatic records for the southwest Pacific (Kennett et al., 1975; Kennett, von der Borch, et al., 1986; Nelson, 1986), contributed to the integration of onland New Zealand stratigraphy with international zonation schemes (Hornibrook, 1980, 1981, 1982, 1984; Scott, 1992), and provided evidence toward establishing the late Neogene timetable of mountain building along the Australian/Pacific plate boundary (Lewis et al., 1985). More expressly, paleoceanographic results from Site 594 were concerned with the synchronicity of glacials and interglacials between the hemispheres (Nelson et al., 1986a), the more general Neogene climatic deterioration (Lazarus and Caulet, 1993), the history of supply of Antarctic Intermediate Water (AAIW), and the historic properties and evolution of the STF and the Subantarctic Front (SAF) (Nelson et al., 1986a, 1993; Kowalski and Meyers, 1997) (Fig. F4). Of the three earlier DSDP sites in the vicinity, Sites 275 and 276 were rotary drilled at locations on the edge of the Camp-

F4. Oceanographic setting of the Leg 181 drill sites, p. 86.



bell Plateau where erosion had removed a large part of the record and DSDP Leg 29 Site 277, in the Emerald Basin just west of the Campbell Plateau, recovered an exceptional late Eocene–early Oligocene isotope record (Shackleton and Kennett, 1975).

The successful completion of DSDP Leg 90 provided a strong impetus for the development of paleoceanographic studies of the New Zealand region, aided by the growth of allied research programs at Waikato University and within NIWA (including a shipborne capability on *Rapahui* and *Tangaroa*), with staff and students often working in collaboration with overseas scientists aboard visiting research vessels such as the *Sonne*, *Atalante*, and *Marion Dufresne*. Consequently, the last two decades have witnessed a burgeoning of papers on the paleoceanography of the southwest Pacific Ocean and Tasman Sea (Thiede, 1979; Griggs et al., 1983; Stewart and Neall, 1984; Nelson et al., 1985, 1986b, 1993, 2000; Hodell and Kennett, 1986; Carter, L., and Mitchell, 1987; Carter, L., and Carter, R., 1988; Dudley and Nelson, 1988, 1989; Carter, L., 1989; Proctor and Carter, 1989; Carter, L., et al., 1990, 1995, 1996, 1999, 2000, 2002a, 2002b; Dersch and Stein, 1991; Fenner et al., 1992; Barnes, 1994; Carter, L., and McCave, 1994, 1997; Head and Nelson, 1994; Hesse, 1994; Heusser and van de Geer, 1994; Martinez, 1994; van der Lingen et al., 1994; Flower and Kennett, 1995; Wright et al., 1995; Weaver et al., 1997, 1998; Ayress et al., 1997; Hiramatsu and De Deckker, 1997; Kowalski and Meyers, 1997; Swanson and van der Lingen, 1997; Thiede et al., 1997; Wells and Connell, 1997; Wells and Okada, 1997; Lean and McCave, 1998; Lewis et al., 1998; Schuur et al., 1998; Wei, 1998; Barrows et al., 2000; King and Howard, 2000; Nelson et al., 2000; Sikes et al., 2000, 2002; Hayward et al., 2001; McGlone, 2001; McMinn et al., 2001; Nelson and Cooke, 2001; Stickley et al., 2001; Cooke et al., 2002; Findlay and Giraudeau, 2002; Kawahata, 2002; Neil et al., submitted [N1]). Increasingly, similar high-resolution stratigraphic studies are being pursued for New Zealand onland sections as well (e.g., Vella, 1973; Hollis et al., 1995; Strong et al., 1995; Kaiho et al., 1996; Morgans et al., 1999, 2002; Graham et al., 2000; Killops et al., 2000; Crouch et al., 2001; Hancock et al., 2003; Hollis, 2003, and papers therein). Paul Vella must be well satisfied!

### Eastern New Zealand Sedimentary System

Globally, it is very clear that geological boundaries have a profound influence on the oceans; after all, land is land, sea is sea, and the continents are geologically different from the ocean basins. Thus the presence of land masses and their submerged extensions plays a dominant role in shaping the disposition of the major ocean currents. Since the advent of plate tectonics, it has been apparent that it is the dance of the geological plates that controls the opening of ocean basins and the position of their gateways and that therefore ultimately shapes the flow of the world ocean (e.g., Berggren and Hollister, 1977) and the distribution of marine organisms that possess planktonic larvae or life habits (e.g., Jenkins, 1993). To a large degree, tectonics also control the location and magnitude of the major sources of terrigenous sediment that is contributed to the world ocean. The resulting interaction between tectonics, sediment supply, and ocean current flows is well epitomized in the New Zealand area. There, the concept of an Eastern New Zealand Sedimentary System (ENZOSS) (Carter, L., et al., 1996) was used to characterize a regionally extensive system within which ~2% of the world's marine terrigenous sediment flux is currently being provided from—

and then recycled by oceanographic, tectonic, and volcanic processes through—the southwest Pacific sector of the Australian/Pacific plate boundary (see **Frontispiece**, parts A–E).

The ENZOSS terrigenous sediment budget is dominated by two major sources. First, a background supply of sediment is derived from the erosion of actively uplifting mountain chains in South and North Islands, and, second, an intermittent but voluminous volcanoclastic contribution was provided by large eruptions in the Coromandel and Taupo volcanic zones of the North Island. The Southern Alps, which are delimited to the west by the Alpine Fault plate boundary, have similar maximum rates of uplift and summit erosion (up to 10 mm/yr) and therefore approximate a “steady-state” mountain chain (Wellman, 1979; Adams, 1980; Koons, 1989; Willett and Brandon, 2002). Sediment is shed eastward from the alpine summits into about eight major river systems, three of which coalesce to form the 300-km-long braid-plain of the Canterbury Plains (e.g., Leckie, 1994). The estimated ENZOSS sediment input from South Island rivers at the east coast is ~40 Mt annually (Griffiths and Glasby, 1985), despite the presence of large sediment traps en route in abandoned glacial lake basins (Carter, L., and Carter, R., 1990). Given adequate precipitation, at glacial lowstands the east coast sediment input can therefore be expected to have been considerably higher (Carter, L., et al., 2000). On reaching the coast, the riverine sediment is entrained within a north-traveling transport system (Carter, L., and Herzer, 1979; Gibb, 1979; Gibb and Adams, 1982), where most of it is initially deposited in coastal or inner shelf depocenters (Andrews, 1973; Herzer, 1981; Carter, R., et al., 1985; Carter, L., and Carter, R., 1986). Abundant terrigenous material is also provided to the North Island shelf (Lewis, 1973). Griffiths and Glasby (1985) estimated that eastern North Island rivers provide ~66 Mt of sediment to the east coast annually. Given such an abundant sediment supply, inshore sedimentation rates are locally very high in eastern New Zealand, for instance attaining >5 m/k.y. in the Clutha River and Poverty Bay depocenters (Carter, L., and Carter, R., 1986; Foster and Carter, L., 1997). Nonetheless, given the efficiency of nearshore sediment entrapment and the presence of vigorous oceanic currents on both the North (south-traveling East Auckland–East Coast Current) and South (north-traveling Southland Current) Island shelves (e.g., Heath, 1985) (Fig. F4), the offshore shelf is commonly starved of terrigenous sediment (Carter, L., 1975). For instance, the outer shelf off northern and western North Island (Nelson et al., 1981; Norris and Grant-Taylor, 1989) and eastern South Island (Powell, 1950; Carter, R., et al., 1985) is the locus of extensive bryozoan-molluscan carbonate deposition (shelly detritus which often overspills onto the adjacent upper slope; Orpin et al., 1998), a major field of phosphatic nodules and glauconite is developed along the crest of the Chatham Rise (Cullen, 1980), glauconitic sediment also occurs on outer shelf highs east of North Island (Pantin, 1966), and current-swept exposed rock platforms occur outside the shore-connected terrigenous prisms on the outer shelf off Kaikoura, South Island (Carter, L., et al., 1982) and under the influence of the East Coast Current off East Cape, North Island (Carter, L., unpubl. data).

If most modern terrigenous sediment is confined to coastal and inner shelf depocenters and the outer shelf is characterized by condensed carbonate-rich sediment or is swept clean by currents, how then does terrigenous sediment from New Zealand reach the deep sea?

Three mechanisms operate to transfer sediment of New Zealand origin to the deep sea. *First* is the direct air fall of volcanic ash. For in-

stance, 120 km<sup>3</sup> of epiclastic material was associated with the historic Taupo eruption of A.D. 186 (Walker, 1980; Carter, L., et al., 1995), and the older Kawakawa (~26.6 ka) and Rangitawa (~340 ka) eruptions are estimated to have ejected ~550 km<sup>3</sup> (Carter, L., et al., 1995) and ~700 km<sup>3</sup> (Froggatt et al., 1986) of ash, respectively (cf. **Frontispiece**, part A, inset). Carter, L., et al. (1996) estimated an average air fall ash input into ENZOSS of ~45 Mt/yr (~0.025 km<sup>3</sup>/yr) since the last glacial maximum, and thus individual large volcanic eruptions contribute volumes of detrital sediment equivalent to ~9,500–12,000 yr of typical riverine supply from North and South Island combined. The *second* transfer mechanism is the collapse of an underconsolidated or oversteepened outer shelf or upper slope seabed, a common accompaniment of rapid sediment deposition (e.g., Herzer, 1979) or accretionary wedge tectonics (Lewis et al., 1998). Seafloor failure is particularly characteristic of the Hikurangi subduction margin in North Island (Lewis, 1971; Barnes and Lewis, 1991; Lewis and Pettinga, 1993), where the Matakaoa and Ruatoria avalanches have been estimated to attain volumes of 600 and 3150 km<sup>3</sup>, respectively (Carter, L., 2001; Collot et al., 2001). Thus, individual slides may transfer material downslope equivalent to ~17,000–88,000 yr of riverine supply to the New Zealand east coast margin. *Third*, and regionally most widespread, sediment is transferred to the deep sea through three recently described submarine channels, each of which debouch into the abyssal Deep Western Boundary Current (DWBC). In the south, erosional products are transferred from the mountainous Fiordland region via Southland rivers, Solander Trough, and Solander Channel to the Emerald Basin and beyond (Carter, L., and McCave, 1997; Schuur et al., 1998). East of South Island, the Bounty Channel (Carter, R., and Carter, L., 1987; Carter, L., and Carter, R., 1988; Carter, L., et al., 1990) forms the conduit between the South Island shelf and East Otago canyon–fan complex and the abyssal Bounty Fan (Carter, L., and Carter R., 1993; Carter, R., et al., 1994), which builds out directly into the path of the DWBC at the mouth of the Bounty Trough (Carter, R., and Carter, L., 1996). Near the northeastern tip of South Island, the head of the third Hikurangi Channel, marked by the Kaikoura and Pegasus canyons, lies at the terminus of the north-traveling South Island shelf sediment system (Carter, L., and Herzer, 1979; Carter, L., et al., 1982; Lewis and Barnes, 1999). This channel then passes north along almost the entire North Island margin (Lewis, 1994) before turning east at latitude 39°S to deliver its sediment load to the Hikurangi Fan-drift, located beneath the DWBC and 1500 km northward and downstream from the Bounty Fan (Carter, L., and McCave, 1994; McCave and Carter, L., 1997). Of the three channels, the Hikurangi Channel is unusual because the nearshore location of its head ensures that it is abundantly supplied with terrigenous sediment today and, therefore, also during past sea level highstands. In contrast, both the Solander (Schuur et al., 1998) and Bounty (Carter, R., and Carter, L., 1992) channels, the heads of which lie well offshore, are inferred to have received a greater terrigenous sediment supply during periods of Quaternary glacial sea level lowstand. Thus, in a sense, a *fourth* mechanism of sediment transfer to the deep sea is eustatic sea level fall, which operated particularly strongly during the Pliocene–Pleistocene. Indeed, it is argued by McCave (2002) that on a global basis and a 10<sup>5</sup> yr timescale, “sea level pumping” was the principal method of sediment delivery from the continents to the deep sea throughout the Pliocene–Pleistocene.

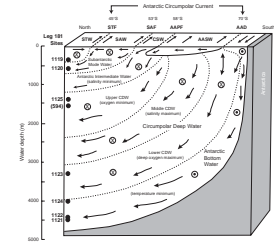
## Modern Oceanographic Setting

The circulation of cold, deep Antarctic Bottom Water (AABW) is one of the controlling factors in the Earth's heat budget and, ultimately, climate (Figs. F4, F5). Today, 40% of the flux of cold bottom water entering the major ocean basins does so through the southwest Pacific Ocean, as the Pacific DWBC (Frontispiece, part E) (Warren, 1981). The DWBC is constituted of Circumpolar Deep Water (CDW), which is derived through dense waters sinking around Antarctica and through the entrainment and mixing of deep Atlantic and Indian Ocean waters by the wind-driven Antarctic Circumpolar Current (ACC). The DWBC attains an average volume transport of  $16 \pm 11.9$  Sv ( $= 10^6$  m<sup>3</sup>/s) at 32°30'S (Whitworth et al., 1999) and, in the southwest Pacific, comprises three main divisions: lower CDW, a mixture of new bottom waters generated around Antarctica (cf. Stickley et al., 2001); middle CDW, derived from North Atlantic Deep Water (NADW) and marked by a characteristic salinity maximum; and upper CDW, derived mainly from Indian Ocean outflow and characterized by strong nutrient enrichment and oxygen depletion. At the approach to the Pacific Ocean, the ACC passes around and through gaps in Macquarie Ridge and then flows northeast along and around the eastern edge of the Campbell Plateau. There, the DWBC is reinforced by the ACC at an estimated rate of 50 Sv and velocities up to 70 cm/s (Carter and Wilkin, 1999; Stanton and Morris, in press). At the southern edge of the Bounty Trough (46°S), the main body of the ACC veers east and continues across the Pacific, leaving the DWBC to flow northward at depths between ~5000 and ~2000 m, across the Bounty Fan, around the eastern end of the Chatham Rise through Valerie Passage, northwestward across the eastern boundary of the Hikurangi Plateau, and finally northward toward the equator along the Tonga-Kermadec Ridge (Fig. F4).

Higher in the water column, north-spreading AAIW, formed by subduction near the Antarctic Polar Front (AAPF), and Subantarctic Mode Water (SAMW), formed by seasonal convection at and north of the SAF, bathe the top and eastern upper flank of the Campbell Plateau at depths of 400–1500 m (Morris et al., 2001).

The upper ocean east of South Island contains two major frontal systems. At ~55°S, the east-flowing ACC is bounded to the north by the SAF (cf. Fig. F1), which here follows the southeastern edge of the Campbell Plateau (Orsi et al., 1995). South of the SAF, the annual mean surface water temperature is <10°C and the nutrient-rich polar ocean is rich in both phosphate and silica. About 10° latitude north of the SAF at 45°S, the STF separates subantarctic water from subtropical water (Heath, 1985; Belkin and Gordon, 1996). Cold (Southland Current) and warm (East Coast Current) currents that have passed around the extremities of New Zealand continue east along the south and north sides of the STF along Chatham Rise and merge east of the rise to form the 5-Sv South Pacific Current of Stramma et al. (1995). (The STF is termed the Subtropical Convergence, STC, in many previous papers, but this term also has a more general usage to describe the broad oceanic zone between ~20° and 50°S where wind stress drives downward Ekman pumping; therefore, we follow Stramma et al., 1995, in preferring to use the term STF for the sharp band of enhanced meridional gradients present at the contact of northern warm and saline subtropical water and southern cool and relatively fresh subantarctic water.) In the open ocean the SAF and STF have been shown to migrate laterally by as much as 6° of latitude during a glacial–interglacial cycle (e.g., Howard and

F5. Water masses, fronts, and circulation patterns, p. 87.



Prell, 1992; Wells and Connell, 1997). However, modern seasonal movements of the fronts of at least 2° of latitude may occur also, as, for example, the STF east of New Zealand (Chiswell, 1994; Kawahata, 2002). In contrast to such seasonal mobility, over the longer term and through climatic cycles the STF appears to have remained topographically aligned along the shallow crest of the Chatham Rise (Fenner et al., 1992; Nelson et al., 1993; Weaver et al., 1998; Sikes et al., 2002).

When referring to ancient water masses whose properties can never be fully reconstructed, some authors prefer not to use the terminology of modern water masses. Thus Wright and Miller (1993) use the term Southern Component Water (SCW) for paleowater masses that originate in the Southern Ocean. Such terminology may be modified to take account of presumed depth of origin, as in Southern Component Intermediate Water (SCIW) or Southern Component Bottom Water (SCBW).

### **Evolution of Flow through the Southwest Pacific Gateway**

With respect to the preceding summary and discussion, the ENZOSS region occupies a key position on the route of the modern global thermohaline circulation system. Nearby tectonic developments affected it in two different, but interrelated, ways.

1. First, the New Zealand plateau lay immediately downstream of the Tasmanian Gateway when, opening to deep water at ~33.7 Ma, it allowed southern Indian Ocean waters to flow through into the Pacific for the first time (Molnar et al., 1975; Cande et al., 2000; Exon, Kennett, Malone, et al., 2001). This event was first recognized as marked by the ubiquitous nondepositional Marshall Paraconformity in shallow marine sections from New Zealand (Carter, R., and Landis, 1972; cf. Carter, R., 1985; Fulthorpe et al., 1996), later proving to be widely present also in the deep sea (Kennett et al., 1972, 1974; Carter, R., McCave, Richter, Carter, L., et al., 1999; Exon, Kennett, Malone, et al., 2001). The paraconformity is associated with a hiatus with a minimum known length of 3.4 m.y. (32.4–29.0 Ma) (Fulthorpe et al., 1996) and everywhere separates pre-gateway onlapping or biopelagic apron sediments below from current-influenced and—from the early Miocene—increasingly terrigenous offlapping sediments above (e.g., Carter, R., et al., 1991, 1998). Thus, from ~33.7 Ma onward, the New Zealand region provides a critical stratigraphic record of the circum-Antarctic and related current flows which developed into the modern thermohaline ocean circulation (Carter, R., et al., 1996).
2. Second, the establishment of Indian-Pacific throughflow at 33.7 Ma marked the start of the thermal isolation of Antarctica (Crowell and Frakes, 1970; Kennett, 1977; Kennett and von der Borch, 1986), which led to glaciation and the development of southern cold, deepwater flows. Today, these flows provide a primary forcing mechanism for the thermohaline circulation (e.g., Schmitz, 1995; Toggweiler and Samuels, 1993, 1995). As an abandoned spreading center (Hayes and Ringis, 1973), the northern end of the Tasman Sea is too shallow to allow throughflow, so the cold, deep flow is steered through gaps in the Macquarie Ridge complex and, encountering the New Zealand Plateau athwart its path, it passes into the Pacific around the

eastern edge of the Campbell Plateau and Chatham Rise, continuing northward through Valerie Passage and along the Kermadec Trench (Carter, L., and Wilkin, 1999). Sediment drifts deposited from the Pacific DWBC were described by Carter, L., and McCave (1994, 1997) and McCave and Carter, L. (1997), and the Leg 181 drilling described below shows that these drifts contain a high-resolution record of climatic and oceanographic cycling back to ~20.5 Ma and, intermittently, beyond to 27 Ma.

To investigate the development of the New Zealand sector of the global thermohaline system as well as related problems such as the eruptive history of the North Island volcanic arc and the integration of local biostratigraphic zonation into a global stratigraphy, a two-leg drilling program was designed. Ocean Drilling Program (ODP) Leg 181 represented the distillation of this wider program, with a particular focus on drilling sediment drifts; Table T1 comprises a listing of the sites drilled, and Table T2 is a summary of the relevant water masses and fronts. As always in frontier areas, stratigraphic surprises awaited the drill bit. Less of a surprise, given the latitudes and the late winter drilling period, was that storms disrupted the intended work program. Nonetheless and despite severe weather-imposed drilling setbacks at Sites 1120 and 1122, much was accomplished from our reconnaissance drilling. Leg 181 results confirm that the southwest Pacific is a critical region within which to pursue future studies of the history of the thermohaline current system, the movements of Southern Hemisphere oceanic fronts, and the production of thermocline water masses.

## PRINCIPAL RESULTS FROM LEG 181

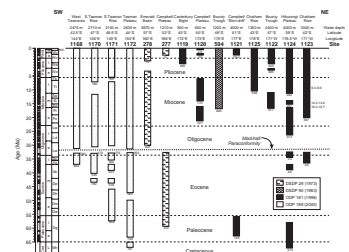
Prior to Leg 181, only one APC-cored drill site, DSDP Leg 90 Site 594, was located in the ENZOSS region and its record only extends back to the early Miocene. In composite, Leg 181 drilling retrieved an almost complete stratigraphic succession of largely deep-marine sediment back to the late Eocene (37 Ma), together with two high-quality cores (Sites 1121 and 1124) of Late Cretaceous to Paleocene age (67–56 Ma) (Fig. F6) (McCave et al., in press; Carter, L., et al., in press b). Although it was unsurprising that the drilling intersected sediments of a wide range of ages, drilling through the Cretaceous/Tertiary (K/T) boundary at Site 1124 and almost reaching it at Site 1121 were perhaps particularly unexpected. Overall, sedimentation rates range widely from a low of 0.001 cm/k.y. during the late Neogene for Site 1121, situated under the energetic ACC-DWBC current system, to highs >50 cm/k.y. on the turbidity current-supplied abyssal Bounty Fan (Site 1122) and >120 cm/k.y. on the Canterbury upper slope (Site 1119). Significant paraconformities with attendant hiatuses lasting up to many millions of years occur at most sites and indicate phases of erosive bottom flow both in the pre-modern (Eocene) Pacific and, after 33.5 Ma, under the ACC-DWBC system.

Including the results of earlier drilling, which sampled sediments of early-middle Eocene and early Oligocene age (Leg 29, Sites 277 and 278), after Leg 181 drilling an almost complete Late Cretaceous to Holocene deep-marine stratigraphic record is now available for the New Zealand region for the first time. Detailed study of this data set has already led to significant advances in regional southwest Pacific stratigraphy, micropaleontology, and paleoceanography. We summarize below

T1. Leg 181 drill sites, p. 109.

T2. Water masses and features, ENZOSS sector, p. 110.

F6. Stratigraphic data for southwest Pacific and Southern Ocean sites, p. 88.



research completed using Leg 181 samples up until mid-2002. As proved to be the case for the earlier Leg 90 cores, however, we anticipate that many further studies will be based on Leg 181 data sets over the next decade, and even beyond.

### Stratigraphy and Biostratigraphy

The primary source for stratigraphic information about sites drilled during Leg 181 is the Leg 181 *Initial Results* volume (Carter, R., McCave, Richter, Carter, L., et al., 1999). Since completion of that volume, however, more refined age models have been prepared for the upper 100 meters composite depth (mcd) of Site 1119 (Carter, R., et al., in press) and for Sites 1121 (Graham et al., in press), 1122 (Wilson et al., 2000a), and 1123 (Wilson et al., 2000b). Detailed paleontologic zonation studies have been completed on Paleocene radiolarians from Site 1121 (Hollis, 2002), Eocene–Oligocene nannofossils from Sites 1123 and 1124 (McGonigal and Di Stefano, this volume), late Miocene bolboforms and planktonic foraminifers from Site 1123 (Crundwell, in press), and Pliocene–Pleistocene phytoplankton (Wei et al., submitted [N2]; Fenner and Di Stefano, in press). These studies are summarized below.

#### Age Model for Upper 100 mcd, Site 1119, Canterbury Slope

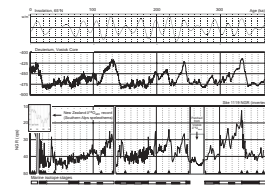
The high terrigenous content of the upper slope muds at Site 1119 is not ideal for microfossil studies. Furthermore, the mineralogy also proved to be unfavorable for preserving a depositional remanent magnetism (Carter, R., McCave, Richter, Carter, L., et al., 1999). Thus the shipboard age model was tentative and predicted an age of ~0.7 Ma at 100 mcd. Utilizing accelerator mass spectrometric radiocarbon dates and the onboard multisensor track (MST) gamma radiation record, Carter, R., et al. (in press) erected a detailed age model for the upper part of the core based on matching climate cycles between Site 1119 and the Vostok ice core (Petit et al., 1999, but using the amended age model of Shackleton, 2000). The upper 86.19 mcd of Site 1119 was deposited in the last 0.252 m.y. during marine isotope Stages (MIS) 1–8. The underlying sediments to 100 mcd, beneath a ~25-k.y.-long intra-MIS 8 unconformity at 86.19 mcd, represent MIS 8.5–11 (0.278–0.370 Ma) (Fig. F7).

#### Age Model and Sedimentation History, Site 1121, Campbell “Skin Drift”

Southernmost Site 1121 is located on a body of sediment that runs along the base of the Campbell Plateau in water depths of ~4500 m. Rather than the anticipated Neogene drift succession, drilling revealed that the extensive sediment body visible on seismic records comprises a Paleocene siliceous biopelagic sediment apron overlain by a thin Fe-Mn nodule-bearing “skin drift” of foraminiferal sand and light to dark brown clay that encompasses the Neogene history of the DWBC. Shipboard paleontological and paleomagnetic data were interpreted to indicate slow sedimentation rates, ages of ~3.6 Ma at ~3.0 meters below seafloor (mbsf) and ~56 Ma at ~30 mbsf, and Paleocene (>55 Ma) radiolarians possibly in situ for all depths below 19.4 mbsf.

Postcruise measurements (Graham et al., in press) showed that  $^{10}\text{Be}/^{9}\text{Be}$  values both for the sediments and for entrapped Fe-Mn nodules decrease systematically with depth, consistent with radioactive decay.

F7. Climatic records compared with the insolation curve, p. 89.



However, the  $^{10}\text{Be}/^9\text{Be}$  sediment and nodule values diverge from ~3 mbsf to the top of the core, allowing several alternative geochronological models. The preferred age model assumes that the measured  $^{10}\text{Be}/^9\text{Be}$  ratios of the nodule rims reflect the initial  $^{10}\text{Be}/^9\text{Be}$  ratio of contemporary seawater, and these ratios are then used to derive the true age of the sediment where the nodules occur. Graham et al. (in press) thus infer an age of ~17.5 Ma (early Miocene) at only ~7 mbsf in the Site 1121 core (Fig. F8). Calculated sedimentation rates range from 8 to 95 cm/m.y., with an overall rate to 7 mbsf of 39 cm/m.y. The lowest rates coincide with the occurrence of trapped nodules and are interpreted to reflect periods of increased bottom current flow that caused net sediment loss. The growth rates of individual nodules decrease toward the top of the core, which is suggestive of an overall increase in the vigor of the DWBC from ~10 Ma to the present. The lithologic Subunit IA/IB boundary at 15.2 mbsf, below which the sediment is uniform yellow clay with nodules and broken layers of chert, therefore probably marks the start of DWBC activity and represents the abyssal manifestation of the Marshall Paraconformity.

Hollis (2002; see further description below) described the detailed radiolarian biostratigraphy of the underlying in situ Paleocene sediments (~40–140 mbsf) at this site that represent the eroded residuum of the postrift pelagic apron of the New Zealand Plateau.

### Age Model and Sedimentation History, Site 1122, Abyssal Bounty Fan

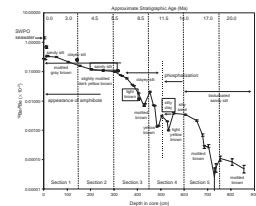
The Bounty Fan developed across the path of the DWBC at the mouth of the Bounty Trough, 800 km east of eastern South Island. Site 1122 (water depth = 4432 m) was cored ~627 m into a left bank fan levee succession that was deposited under the influence of both east-traveling (and north-overspilling) turbidity currents emanating from the Bounty Trough and the north-flowing DWBC. Core recovery was complete using the APC to 104 mbsf but averaged only 47% between 104 and 627 mbsf because of loss of turbidite sands during rotary drilling (Carter, R., McCave, Richter, Carter, L., et al., 1999). Wilson et al. (2000a) showed that above ~520 mbsf shipboard paleomagnetic results are mostly confirmed by measurements of stepwise-demagnetized discrete paleomagnetic samples. However, between ~520 and 610 mbsf, discrepancies between discrete sample and shipboard measurements required the revision of the shipboard magnetostratigraphy.

Integration of the paleomagnetic stratigraphy with 30 shipboard microfossil datums and indicators provides a reliable chronology and age model for the Site 1122 sequence down to ~520 mbsf (Wilson et al., 2000a). Significant unconformities occur at ~5 Ma (~485 mbsf), between middle Miocene and early Pliocene drift sediments, and at ~2.2 Ma (~440 mbsf), which corresponds to an increased sedimentation rate and the arrival of the first turbidite sediment from the Bounty Trough and Channel.

### Age Model and Sedimentation History, Site 1123, North Chatham Rise

Deposition of the North Chatham Drift beneath the DWBC began at 20.5 Ma and has continued virtually uninterrupted up to the present day (Carter, R., McCave, Richter, Carter, L., et al., 1999). The drift is ~600 m thick at Site 1123 and overlies a 13-m.y. hiatus (33.5–21.0 Ma)

F8.  $^{10}\text{Be}$  stratigraphy and age profile, Site 1121, p. 90.



identified as the regionally pervasive Marshall Paraconformity. Core recovery was nearly complete to ~390 mcd, but below that level recovery using the extended core barrel (XCB) was incomplete. Comparison between downhole and core magnetic susceptibility records demonstrates that sediment loss was distributed throughout the length of each core run (Wilson et al., 2000b). Linear stretching of the magnetic susceptibility records from short core recovery runs were matched to downhole logging data, thus allowing the reconstruction of a complete depositional record of the North Chatham Drift. Chronology from shipboard paleomagnetism (Carter, R., McCave, Richter, Carter, L., et al., 1999) was confirmed by measurement of 256 stepwise demagnetized discrete paleomagnetic samples. Integration of the paleomagnetic stratigraphy with 47 shipboard microfossil datums indicates that an almost complete sequence of magnetic polarity reversals (including one new reversal, C5ADn1r) is preserved (Figs. F9, F10).

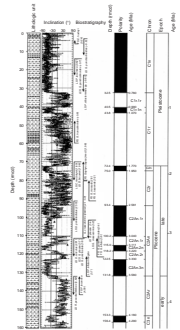
Site 1123 is located adjacent to Valerie Passage and distant from terrigenous sediment sources. The sediment contains 40–80 wt% carbonate throughout the core. The cyclic variations in sedimentation rates observed at the site result from a combination of the waxing and waning of DWBC flow and variation in biopelagic productivity (Hall et al., 2002). The most dramatic variation occurred in the middle Miocene, when sedimentation rates slowed between 15 and 13.5 Ma and then increased fourfold after 13.5 Ma. Sedimentation was fairly constant between 12 and 7.5 Ma, waned slightly at 7.5 Ma, and decreased by half between 7 and 5 Ma. Sedimentation increased again briefly in the early Pliocene (~3.2–2.8 Ma), after which sediment accumulation remained relatively constant throughout the rest of the Pliocene–Pleistocene. Comparison with benthic oxygen isotope and sortable silt records (see Hall et al., 2001) suggests that these variations in sedimentation rate represent fluctuations in bottom water production and DWBC flow rate, driven by variations in a cooling Antarctic climate and/or in ice volume, processes that were well under way by the early Miocene (Hall et al., 2003).

### Paleocene Radiolarian Biostratigraphy, Site 1121

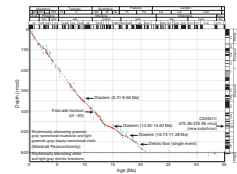
A 100-m-thick Paleocene sequence of pelagic siliceous and nannofossil-bearing chalky sediment was recovered from Site 1121, at the eastern foot of the Campbell Plateau (Carter, R., McCave, Richter, Carter, L., et al., 1999; Hancock and Dickens, this volume). Hollis (2002) showed that the lower 40 m of this succession contains a low-diversity radiolarian fauna of early to early late Paleocene age (Zones RP4 and RP5; ~63–59 Ma), similar to faunas already described from onland New Zealand and at DSDP Leg 21 Site 208 from the northern Lord Howe Rise (Fig. F11). The upper 60 m contains diverse middle–late Paleocene (Zone RP6) assemblages that differ from their counterparts elsewhere in their richness in plagiocanthids and cycladophorids, perhaps suggestive of cool-water conditions. The 150 Paleocene taxa so far recorded from Site 1121 are estimated to represent only about one-half of the complete radiolarian species diversity at the site.

An age model based on well-constrained nannofossil and radiolarian datums indicates that the rate of compacted sediment accumulation doubled from 1.5 to 3 cm/k.y. at the RP5/RP6 zonal boundary (~59 Ma). This results in large part from a sudden and pronounced increase in accumulation rates for all siliceous fossils; overall, radiolarians and larger diatoms increase from <100 to >10,000 specimens/cm<sup>2</sup>/k.y. This in-

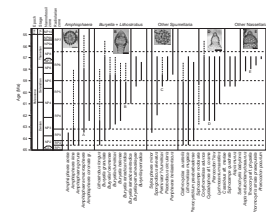
F9. Paleomagnetic and biostratigraphic data, Site 1123, p. 91.



F10. Revised age model, Site 1123, p. 92.



F11. Age ranges of radiolarians in the southern Pacific, p. 93.



crease in biosiliceous productivity corresponds to the 59- to 57-Ma middle Paleocene cooling event, which is marked by the heaviest  $\delta^{13}\text{C}$  values known for the entire Cenozoic (cf. Fig. F19).

Site 1121 radiolarian faunas provide an exciting new opportunity for linking Cretaceous–Cenozoic transition sediments in the South Pacific to the rest of the world. Cores recovered from the site contain the richest and most diverse late Paleocene radiolarian assemblages known from the Southern Hemisphere. Correlation with the North Atlantic in Zone RP6 is indicated by the presence of *Aspis velutochlamydosaurus*, *Plectodiscus circularis*, and *Pterocodon poculum*. Other species, including *Buryella tetradica* and *Buryella pentadica*, are valuable for local correlation but exhibit considerable diachroneity when their ranges are compared between the Pacific, Indian, and Atlantic Oceans.

### **Eocene–Oligocene Nannofossil Biostratigraphy, Sites 1123 and 1124**

Holes 1123C and 1124C penetrated middle Eocene–early Oligocene sediments that contain moderately to poorly preserved calcareous nannofossils. Younger DWBC sediments at these sites consist of alternating white clay-bearing nannofossil chalk and light greenish gray clayey nannofossil chalk (late Oligocene at Site 1124 and early Miocene at Site 1123), which overlie alternating white and light gray micritic limestone (late Eocene–early Oligocene) and red, yellow, pink, and brown mudstone (Paleocene and Eocene). [McGonigal and Di Stefano](#) (this volume) report that although the nannofossil assemblages show signs of dissolution and overgrowth, key marker species can be identified. The early Oligocene sediments are distinctly separated from the overlying Neogene succession by the Marshall Paraconformity, a regional marker of environmental and sea level change (Carter, R., 1985).

Age-depth models were constructed using nine nannofossil age datums and three magnetostratigraphic datums. There is good agreement between the biostratigraphy and magnetostratigraphy. The age model for Site 1123 indicates that the Marshall Paraconformity here spans ~21–33.5 Ma, suggesting that current speeds precluded deposition at the site and perhaps corroded and eroded older sediments for more than the first 10 m.y. of DWBC flow. At Site 1124, the succession is disrupted by three major paraconformities, of which the youngest equates with the Marshall Paraconformity and spans ~26.1–31.8 Ma. Two older hiatuses are a 3-m.y. gap that separates early Oligocene and middle Eocene sediment (~34–37 Ma) and a ~19-m.y. gap between middle Eocene mudstone and middle Paleocene nannofossil-bearing mudstone (~58–39 Ma).

Nannofossil information from Sites 1123 and 1124 indicates that the Eocene–Oligocene transition in eastern New Zealand was a time of fluctuating biota, in sympathy with the pulsed development of bottom currents. The widespread presence of the Marshall Paraconformity is consistent with other evidence for the development of DWBC and other flows along the New Zealand margin at that time. The hiatuses at Site 1124 that predate the Marshall Paraconformity may have developed under the influence of Paleogene south-flowing currents (see discussion in [“Late Cretaceous–Late Eocene Rift-Drift: Start of the Kaikoura Synthem,”](#) p. 38, in [“ENZOSS Revisited: The History of Pacific Deep Flow”](#)).

### Late Miocene Bolboforms and Planktonic Foraminifer Biostratigraphy, Site 1123

Bolboforms are calcareous spinose marine microfossils inferred to have been phytoplankton. Their distinctive and changing morphologies and high resistance to dissolution make bolboforms important index fossils with which to supplement calcareous foraminifers and calcareous nannofossils. They occur particularly in middle to high latitudes in both hemispheres and have a stratigraphic record that extends back to the Paleogene (Cooke et al., 2002).

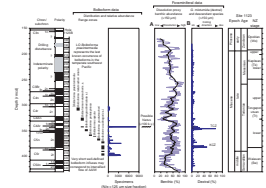
Crundwell (in press) established a high-resolution late Miocene biostratigraphy for the southwest Pacific using bolboforms and planktonic foraminifers from Site 1123, which also has an exceptionally complete magnetostratigraphic and astrochronologic record (Wilson et al., 2000b). The biochronologic model is based on dissolution-resistant species and morphotypes and is constrained by 33 bioevents that also occurred at DSDP Site 593 (Challenger Plateau, northwest of New Zealand). Well-constrained bolboform events include the total range zones of *Bolboforma subfragoris* s.l. (11.56–10.50 Ma), *Bolboforma gruetzmacheri* (10.46–10.31 Ma), *Bolboforma capsula* (10.20–10.13 Ma), *Bolboforma pentaspinosa* (10.15–10.08 Ma), *Bolboforma gracilireticulata* s.l. (9.75–9.61 Ma), lower *Bolboforma metzmacheri* s.s. Subzone (9.54–9.34 Ma), upper *Bolboforma metzmacheri* s.s. Subzone (9.01–8.78 Ma), *Bolboforma metzmacheri ornata* (8.45–8.25 Ma), *Bolboforma praeintermedia* (8.25–8.21 Ma), and distinctive abundance spikes associated with the upper *B. subfragoris* s.l. Subzone (10.61 Ma) and the lower *B. metzmacheri* Subzone (9.44 Ma) (Fig. F12). Planktonic foraminiferal events include well-defined intervals of dextral coiling excursions in *Globoconella miotumida* (10.93–10.82 and 9.62–9.42 Ma), the regional disappearance of *Globoquadrina dehiscens* (8.88 Ma), an acme zone of *Truncorotalia juanai* (7.23–6.23 Ma), and the evolutionary appearances of *Globoconella conomiozea* (~6.87 Ma), *Globoconella mons* (~5.72 Ma), *Globoconella sphericomiozea* (~5.53 Ma), *Globoconella pliozea* (~5.39 Ma), and *Globoconella puncticulata* (~5.28 Ma).

The close fit of the biostratigraphic data to a linear line of correlation between DSDP Site 593 and ODP Site 1123 and the consistency of the stratigraphic ordering of events suggest that most of the biostratigraphic events recognized are near synchronous. This correlation also shows that late Miocene sedimentation rates were in phase between the two sites, despite their 1400-km separation and accumulation beneath different water masses. Although the age model is based on only two oceanic sites, it establishes for the first time a high-quality late Miocene biochronostratigraphic framework for the temperate southwest Pacific Ocean and Tasman Sea regions.

### Pliocene–Pleistocene Nannofossil Biostratigraphy, Sites 594 and 1125

DSDP Site 594 and ODP Site 1125 both have an established stratigraphy which, together with their respective location on the cooler and warmer sides of the STF, makes them particularly useful for calibration of regional nannofossil stratigraphies in the southwest Pacific. Based on correlation between these and other mid-latitude sites (DSDP Leg 90, Sites 593, 590, and 588), Wei and Chen (submitted [N3]) assessed the Southern Hemisphere synchronicity of eight commonly used nannofos-

F12. Late Miocene bolboform and foraminifer data, Site 1123, p. 94.



sil datum levels. These bioevents and their new age assignments are as follows:

1. The first occurrence datum (FAD) of *Emiliana huxleyi* in MIS 8 (~0.26 Ma);
2. The last occurrence datum (LAD) of *Pseudoemiliana lacunosa* in MIS 12 (~0.46 Ma);
3. The LAD of *Calcidiscus macintyreii* at ~0.9–1.1 Ma, which is much younger than its LAD in Southern Hemisphere low latitudes;
4. The FAD of medium-sized *Gephyrocapsa* spp. at ~1.61–1.73 Ma (i.e., slightly younger than the top of the Olduvai Chron);
5. The LAD of *Discoaster brouweri* at 2.17 Ma, slightly older than that for low latitudes;
6. The LAD of *Reticulofenestra pseudumbilica* at 2.57 Ma at Site 1125 and 1.03 Ma at Site 594, which indicates strong diachroneity for this species and, perhaps, a water mass control;
7. The LAD of *Discoaster surculus* at 2.65 Ma, this early disappearance probably being related to a paucity of discoasterids in general; and
8. The FAD of *Pseudoemiliana lacunosa* at 3.95 Ma at Site 594 and 3.58 Ma at Site 1125.

In addition, the timing of two other stratigraphically useful nanno-events remains unchanged from previous determinations, namely

1. The acme of *Emiliana huxleyi* in MIS 3–4 (between 0.06 and 0.08 Ma) and
2. The reentry of medium-sized *Gephyrocapsa* at 1.03–1.05 Ma, within the Jaramillo Subchron.

Because of the rarity of some age-diagnostic species, this biozonation is broader than the conventional low-latitude nannofossil biozonation. Nevertheless, the new southwest Pacific biozones are an important aid for correlating sites within and across the transitional water masses and temperatures of the STF.

### **MIS 1–5 Phytoplankton Stratigraphy for the Eastern New Zealand Region**

Fenner and Di Stefano (in press) used population censuses of late Quaternary calcareous nannofossil and diatom assemblages to develop a quantitative calcareous nannofossil stratigraphy for the area near the STF. Five core sites near Chatham Rise and on both sides of the STF were selected for study (NIWA core Q 858, DSDP Site 594, and ODP Sites 1120, 1121, and 1123). Stratigraphic marker species used to establish the general age of the studied cores include *Emiliana huxleyi* (FAD = 0.28–0.268 Ma), *Fragilariopsis reinholdii* (LAD = 0.65 Ma), *Fragilariopsis fossilis* (LAD = 0.70 Ma), and *Fragilariopsis doliolus* (FAD = 1.8 Ma). The top sections of all cores fall within the stratigraphic range of *E. huxleyi* and are therefore younger than 0.268 Ma (early MIS 7). Detailed age constraints were developed using oxygen isotope stratigraphy, tephrochronology, and <sup>14</sup>C age determinations for two sites north of the Chatham Rise (NIWA piston core Q858 [Fenner et al., 1992] and Site 1123 [Hall et al., 2001]) and one site south of the Chatham Rise (Site 594 [Nelson et al., 1993]). Correlation shows that mid–late Holocene

sediment is missing at both Sites 1123 and 594, perhaps due to core-top drilling disturbance.

Based on this stratigraphy, abundance changes were determined for phytoplankton species that are present both north and south of the Chatham Rise. Five nannofossil abundance shifts were identified that apparently occur synchronously both north and south of the Chatham Rise:

1. A changeover in abundance of *Calcidiscus leptoporus* (dominant in MIS 1) and *Coccolithus pelagicus* (dominant in MIS 2) at the MIS 1/2 boundary.
2. The base of the upper acme of *Emiliania huxleyi* in early MIS 2.
3. The acme of *Helicosphaera carteri* within MIS 3, the stratigraphically lower abundance peak of which is selected as a datum;
4. A large drop in abundance of *Gephyrocapsa muelleri* at or slightly earlier than the MIS 4/3 boundary; and
5. A sharp increase in abundance of *Coccolithus pelagicus* within MIS 5a.

In contrast to the nannofossils, the diatom assemblages largely comprise species that are restricted to one side of the Chatham Rise. No stratigraphically useful diatom abundance changes were found among taxa that are common both north and south of the rise. The only consistent event is a peak of *Thalassionema nitzschioides* in MIS 3 that coincides with the abundance peak of the nannofossil *Helicosphaera carteri* and may correlate with the MIS 3.2 isotope event (Martinson et al., 1987). Despite this lack of quantitative stratigraphic indicators, *T. nitzschioides* and *Rhaphoneis surirelloides* are more abundant in sediments deposited during cooler times (MIS 2–4) and *Paralia sulcata* is more abundant in sediments deposited during warm intervals.

The newly defined calcareous nannofossil datums are based on prominent species' abundance shifts within the past 130 k.y. and can be applied throughout the subtropical to subantarctic region east of New Zealand. Where a stable oxygen isotope record is not available, the nannofossil datums can be used to correlate between cores and to calculate sedimentation rates.

### Other Paleontology

Leg 181 drilling complemented earlier DSDP work in the New Zealand area, especially the exceptional cores that were retrieved from Leg 29 Site 277 and Leg 90 Sites 593 and 594, to provide for the first time a combined deep-ocean record that spans the entire Cretaceous–Cenozoic tectonosedimentary cycle (Kaikoura Synthem). Substantial advances are thereby being made in our knowledge of Southern Hemisphere mid-latitude biostratigraphy (see previous section) and in the wider application of Leg 181 micropaleontologic analysis. Other post-cruise studies, summarized below, apply paleontology to evolutionary and paleoceanographic problems.

### Evolution Rates in Deep-Sea Benthic Foraminifers

Deep-sea foraminifer species have an estimated low background turnover rate of 2%/m.y. (McKinney, 1987). The most severe extinctions of deep-sea foraminifers, with a loss of 30%–50% of species, occurred during the Paleocene/Eocene Thermal Maximum (PETM) (~55

Ma) (van Morkhoven et al., 1986; MacLeod et al., 2000) and is inferred to have resulted from oxygen-poor, warm bottom waters coupled with changes in surface productivity (Katz et al., 1999). Extended periods of slightly enhanced extinction rate have also been identified globally in the late Eocene–early Oligocene (36–30 Ma), the middle Miocene (16–12 Ma) (Weinholz and Lutze, 1989), and the middle Pleistocene (dubbed the “*Stilostomella* extinction” after the family Stilostomellidae, which died out at this time; Schonfeld, 1996).

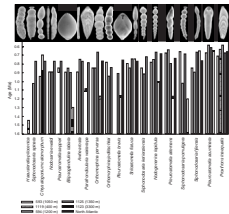
The *Stilostomella* event was first identified in the Atlantic Ocean, where 10 benthic foraminiferal species from six genera are reported to have disappeared between 1.0 and 0.6 Ma (Lutze, 1979; Thomas, 1987); extinctions occurred 0.1–0.2 m.y. earlier at depths >3000 m and in southern latitudes (Weinholz and Lutze, 1989; Schonfeld, 1996). Middle Pleistocene extinctions of some of these taxa have also been recorded from several sites in the Indian Ocean (Gupta, 1993) and the Pacific Ocean (Schonfeld and Spiegler, 1995). Hayward (2001, 2002) used new samples available from Leg 181 sites to reassess the nature of the *Stilostomella* event in the southwest Pacific. This event is associated with the disappearance of at least 2 families, 15 genera, and 48 species of dominantly uniserial, elongate foraminifers with distinctive apertural modifications (i.e., ~15%–25% of the fauna). These taxa progressively dwindled in number and became extinct during glacial periods throughout the late Pliocene to middle Pleistocene (~2.5–0.6 Ma), with most extinctions occurring between 1.0 and 0.6 Ma, at the time of the middle Pleistocene transition (MPT) (Fig. F13). Hayward’s are the first high-resolution studies of the *Stilostomella* extinction event, and they indicate that the event was far more significant for deep-sea diversity loss than the 10-species extinction previously reported. The middle Pleistocene extinction of elongate benthic foraminifers was the most dramatic last phase of a worldwide decline in their abundance that began during cooling near the Eocene/Oligocene boundary and continued until at least the middle Pleistocene.

### Modern Benthic Foraminiferal Associations and Their Paleooceanographic Implications

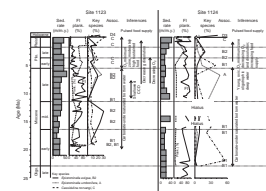
Hayward et al. (2001) used cluster analysis and correspondence analysis to study the distribution of benthic foraminiferal faunas from grab samples, piston core tops, and DSDP and ODP core tops at sites located east of New Zealand over a water depth range of 90–4700 m. A total of 465 benthic taxa were identified, of which 139 are new records for the New Zealand region. The relative abundance of common species, species associations (six of which are delimited by the cluster analysis), upper depth limits of key benthic species, and the relative abundance of planktonic foraminifers are the most useful proxies for estimating paleobathymetry. In a further development, Hayward et al. (2002) reported on the environmental factors that principally determine benthic foraminiferal associations in the southwest Pacific area. Important factors—all of which are related to water depth—include dissolved oxygen content, seasonality of food supply, organic carbon flux, advection of water masses, bottom water carbonate corrosiveness, benthic energy state at the boundary layer, and grain size distribution of the seabed.

Hayward et al. (in press) performed benthic foraminiferal censuses (336 species) and fragmentation estimates on 85 Neogene samples from Site 594 and Sites 1120–1125 (Fig. F14). Sample associations were determined using cluster analysis and canonical correspondence analysis,

**F13.** Benthic foraminifers affected by the “*Stilostomella* event,” p. 95.



**F14.** Neogene sedimentation rates, foraminifers, and key species, p. 96.



which showed that the foraminiferal groupings are most strongly influenced by bathymetric depth, reflecting water mass stratification, and age, reflecting biotic evolution. Three intervals of foraminiferal taxonomic turnover occur at 16–15, 11.5–10, and 2–0.5 Ma and are inferred to correspond to intervals of enhanced cooling and increased surface water productivity; the late Pliocene–middle Pleistocene *Stilostomella* extinction culminated at the MPT. Significant differences between lower bathyal faunas north and south of the Chatham Rise suggest the presence of an oceanic front (predecessor of the STF) along the rise since at least the early Miocene. Modern AAIW benthic associations were established north of the Chatham Rise at 10–9 Ma and south of it at 3–1.5 Ma. Middle–upper bathyal faunas on the Campbell Plateau are dominated by reticulate bolivinids during the early and middle Miocene, indicative of sustained productivity above relatively sluggish, poorly oxygenated bottom waters. Faunal changes and sediment hiatuses indicate increased current vigor over the Campbell Plateau since the latest Miocene.

Downcore studies for planktonic foraminiferal fragmentation indices show significant amounts of abyssal carbonate dissolution throughout most of the Neogene, peaking at upper abyssal depths in the late Miocene (11–7 Ma), with the lysocline progressively deepening thereafter. Peak abundances of *Epistominella umbonifera* indicate an increased input of cold SCW to the DWBC at 7–6 Ma. Faunal association changes imply establishment of the modern oxygen minimum zone (upper CDW) in the latest Miocene. Faunal assemblage changes are consistent with stepped increases in productivity at 16–15, 3–1.5, and 1–0.5 Ma, whereas benthic taxonomic turnover was concentrated at 16–15, 11.5–10, and 2–0.5 Ma. These microfaunal changes are interpreted in terms of the pulsed, sequential development of southern, and later northern, polar glaciation, with consequent cooling of bottom waters, increased vertical and lateral stratification of ocean water masses, and increased surface water productivity.

### **Middle–Late Pliocene Foraminiferal Censuses and Sea-Surface Temperatures, Site 1125, North Chatham Rise**

Sabaa et al. (in press) conducted planktonic foraminiferal census counts to estimate middle–late Pliocene (4.0–2.37 Ma) sea-surface temperatures (SSTs) in cool subtropical waters at Site 1125, presently just north of the STF. Using the modern analog technique (MAT), SSTs at this location are estimated to have often been cooler than both modern and last glacial SSTs, although there were brief periods when temperatures were 1°–2°C warmer than today. Specifically, summer temperature maxima were 1°–2°C warmer than present day and winter temperature minima were 6°–10°C cooler, but the warm maxima were brief and spasmodic. Major cooling excursions of 6°–10°C occurred at 3.35, 3.0, and 2.8 Ma, and minor coolings of shorter duration and lower magnitude (~4°C cooling) occurred at 2.7 and 2.4 Ma. These results demonstrate episodes of strong cooling in the middle–late Pliocene of the subtropical southwest Pacific. The coolings might be a regional effect or, alternatively, could stem from increased upwellings of cold intermediate water or from northward migrations of the STF. Sabaa et al. (in press) prefer the regional cooling interpretation because of the evidence that exists for mid-Pliocene cooling in other regions of the western Pacific (e.g., Andersson, 1997; Heusser and Morley, 1996), despite the in-

ferred occurrence of an overall global warming at this time (Dowsett et al., 1996).

### Deep-Sea Record of New Zealand Pliocene–Pleistocene Palynomorphs, Site 1123

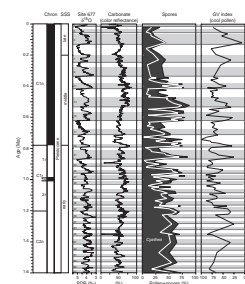
Site 1123 possesses a robust chronology, the upper part of which is based on the astronomical tuning of the benthic foraminiferal  $\delta^{18}\text{O}$  record (Hall et al., 2001, 2002). The ~180-m-thick Pliocene–Pleistocene sequence at the site represents the best continuous record of climate and vegetation change covering the last 5.25 m.y. in the New Zealand region. Mildenhall (2003) and Mildenhall et al. (in press) used censuses of the terrestrial pollen and spore record at the site in order to determine (1) how variations in terrestrial palynomorph assemblages are related to global climate cycles and regional climatic/oceanographic processes and (2) the degree to which New Zealand's terrestrial vegetation was influenced by major climatic changes associated with the MPT at ~0.92–0.62 Ma. Despite the long distance from shore and relatively great water depth (3290 m), palynomorph abundance is more than adequate at Site 1123 to demonstrate a strong correlation between the orbitally tuned marine record and climatically controlled changes in terrestrial vegetation (Fig. F15).

Pollen and spores from a range of terrestrial environments are present in all samples, but overall the recovered palynomorph assemblages are derived from regional podocarp/hardwood forest vegetation from the southern part of North Island, New Zealand. Angiosperm pollen, although generally sparse, are dominated by *Nothofagus*, whereas robust buoyant spores such as *Cyathea* and bisaccate pollen such as *Podocarpus/Prumnopitys* are overrepresented. This overrepresentation probably results from the ability of these taxa to float great distances. Gradual changes occur in the dominant pollen types, with more mesothermal taxa (e.g., *Brassospora*) in the Pliocene and early Pleistocene and fewer mesothermal taxa (e.g., *Fuscospora* and podocarp conifers) in the middle and late Pleistocene. This suggests a gradual change from warm, humid, and perhaps cloudy conditions to a cooler, drier climate as the global climate deteriorated. Superimposed on this long-term change are more intense glacial–interglacial cycles in which glacial periods are enriched in *Halocarpus*, *Phyllocladus*, *Nothofagus fusca* type, and *Coprosma* pollen relative to the interglacial flora with *Cyathea*, tall tree *Podocarpus/Prumnopitys*, and *Dacrydium cupressinum*. Time series analysis indicates that the vegetation record is covariant with marine climate proxies (as represented by carbonate content) and that it is strongly coherent at the 41- and 100-k.y. Milankovitch frequencies. This is the first time that terrestrial pollen changes have been shown to occur almost exactly in phase with a marine climatic signal. A pronounced increase in amplitude and a coeval lengthening of climate cycles from 41 to 100 k.y. occurs between 0.92 and 0.62 Ma and provides a rare vegetation record during the fundamental MPT reorganization of Earth's climate system.

### Planktonic Foraminiferal Evidence for Late Pliocene–Quaternary Paleocirculation about Chatham Rise, Site 1123

Scott and Hall (in press) used MAT, ordinations, and minimum spanning trees to compare 32 foraminiferal assemblages from Site 1123 with 35 core-top assemblages collected between 35° and 61°S east of New

F15. Pollen and spores, Site 1123, p. 97.



Zealand (Fig. F16). Many Site 1123 faunas in the 2.7-m.y. interval sampled are transitional between colder- and warmer-water assemblages, similar to core-top faunas along the crest of the Chatham Rise. This result is consistent with earlier studies from this region and suggests that the STF was positioned over the Chatham Rise through glacial and interglacial periods at least back to the late Pliocene. Other assemblages are rare, but one at 1.165 Ma closely resembles core-top assemblages between 44° and 48°S and may identify cooler surface water.

The dominance of *Globoconella inflata* is a principal feature of Site 1123 assemblages, but across the MPT this species is generally present in subordinate numbers to dextral specimens of *Neogloboquadrina pachyderma*. There are no close core-top analogs for such faunas, but other data show that they develop in high biomass water associated with upwelling or mixing. The proportion of sinistrally coiled *N. pachyderma* rises to 0.6 between 2.45 and 2.57 Ma, soon after the intensification of Northern Hemisphere glaciation. Although the coiling data indicate subantarctic near-surface water, the species remains rare and the assemblage overall is still of transitional character. Therefore, probably only minor entrainment of subantarctic water occurred.

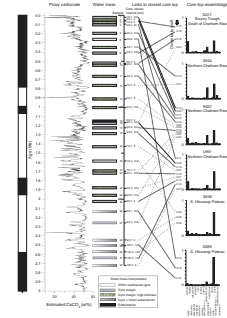
A new high-resolution census study of planktonic foraminifers across the MPT has begun (M.P. Crundwell and G.H. Scott, unpubl. data). This MIS 27–12 (0.44–1.00 Ma) interval is relatively free from carbonate dissolution, and the coiling signature of *N. pachyderma* in the census probably identifies further periods in which subantarctic near-surface water was introduced into the subtropical gyre. Such colder-water assemblages also contain increased proportions of sinistral *N. pachyderma*, to the extent that they are sometimes present in subequal numbers to dextral specimens.

### Deep Ocean Record of Late Neogene Volcanism: Coromandel and Taupo Volcanic Zones

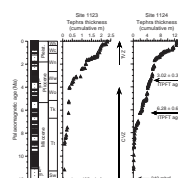
The Quaternary Taupo Volcanic Zone (TVZ) is Earth's most productive modern rhyolitic center (Wilson et al., 1995a, 1995b), but many details of its history—and those of its western predecessor, the Miocene–Pliocene Coromandel Volcanic Zone (CVZ)—remain unknown. Previous research was based mainly on terrestrial records, which are affected by tectonism, erosion, and burial beneath successive volcanic deposits (Shane, 2000; Wilson, 1994). Leg 181 provided the most complete record of major volcanic events available to date in the form of tephra layers preserved at Sites 1122–1125, which in prevailing conditions lie downwind of the CVZ and TVZ. Thus, Leg 181 drilling provided a new standard history of the evolution of these major plate boundary volcanic zones (Carter, L., et al., 2003, in press a). This information, together with that from DSDP Leg 29 Site 284 (Kennett et al., 1979), Leg 90 Sites 590–594 (Nelson et al., 1986b), and existing piston core data (e.g., Ninkovich, 1968; Lewis and Kohn, 1973; Froggatt et al., 1986; Watkins and Huang, 1977; Carter, L., et al., 1995), has given us a firm understanding of ash dispersal for the offshore New Zealand region.

Carter, L., et al. (2003) used glass shard geochemistry and isothermal plateau fission track dating, supported by robust chronologies developed from paleomagnetic stratigraphy, orbitally tuned reflectance profiles, and benthic isotope records, to demonstrate that near-continuous rhyolitic volcanism occurred within the CVZ and TVZ since ~12 Ma (Fig. F17). This history is particularly well preserved at Site 1124, which,

F16. Planktonic foraminifers, Site 1123, p. 98.



F17. Ash record, Sites 1123 and 1124, p. 99.



although 600 km from the inferred volcanic sources, contains 134 macroscopic tephra layers with individual tephra up to 92 cm thick.

### Tephrochronologic Record

Volcanic activity related to the development of the Australian/Pacific boundary began in western North Island in the Oligocene and early Miocene (e.g., Hayward, 1993). Yet, despite continuous core records that stretch back to the early Miocene (Site 1123) and late Oligocene (Site 1124), the Leg 181 macroscopic tephra record only begins at ~12 Ma. Nearby onland, tephra also appear at ~12–13 Ma in a well-exposed Miocene terrigenous succession at Mahia Peninsula (Schneider et al., 2001). The absence of discrete tephra in sediments east of New Zealand prior to this time is attributed to the following factors:

1. The occurrence of relatively nonexplosive volcanism in the Northland volcanic arc (25–11 Ma) and CVZ (18–9 Ma), where basalts, andesites, and minor dacite eruptions prevailed at the time (Adams et al., 1994; Hayward et al., 2001);
2. A greater distance than today between the active volcanoes and Leg 181 sites, as indicated by Neogene reconstructions of the Australian/Pacific plate boundary (King, 2000); and
3. Diagenetic alteration of tephra, as represented by dark green layers composed mostly of clay minerals with only trace amounts of volcanic glass (Site 1124 smear slide data in Carter, R., McCave, Richter, Carter, L., et al., 1999) (cf. Gardner et al., 1985); altered tephra of this type, and older than 12 Ma, are present, most conspicuously between ~27 and 23 Ma (late Oligocene) at Site 1124.

### Neogene Volcanism

At Site 1124, the earliest rhyolitic tephra (~12 Ma) predates the earliest known terrestrial ignimbrite in the CVZ by more than a million years. Thereafter, through the Miocene and Pliocene, the data show that episodes of volcanism were punctuated by periods of subdued activity or quiescence. The longest break in activity is 0.7 m.y., with most breaks being <0.5 m.y. The first phase of pronounced tephra deposition occurred at ~7.7–7.0 Ma, which coincides with a major phase of caldera development in the CVZ (Adams et al., 1994). Quiescence between 7.0 and 6.3 Ma was followed by short bursts of activity at 6.30–6.24 Ma and ~5.2 Ma, about the respective ages of the Pumpkin Rock Ignimbrite/Wheuakite Rhyolite and Ahu Ahu Rhyolite eruptions onshore. The ensuing Pliocene ash record indicates 2 m.y. of near-continuous but more intense activity than in the late Miocene. This contrasts with the terrestrial record, which places the end of CVZ volcanism at ~4 Ma and the start of TVZ volcanism at ~2 Ma (Adams et al., 1994).

From ~1.6 Ma onward, major rhyolitic activity was centered in the TVZ (Wilson et al., 1995b). Again, new Leg 181 data show that large rhyolitic eruptions were more frequent than previously known from terrestrial studies. Wilson et al. (1995b) noted that large TVZ eruptions were associated with major caldera-forming periods, although such events were probably interspersed with smaller eruptions. The Site 1124 record demonstrates, however, that tephra of intervening age and of similar thickness to those deposited during the *known* periods of caldera collapse are present, suggesting that some hitherto unknown calderas

in the TVZ (and CVZ) are buried by younger eruptives or occur integrated within larger and partly younger caldera complexes (Wilson et al., 1995b). Another possibility is that other eruptive sources may lie within the offshore extension to the TVZ, or beyond. Given the close similarity between the major oxide glass geochemistry of ashes from the CVZ and TVZ and the near-continuum of eruptions implied by the Leg 181 tephra record, it is difficult to attribute particular ashes or groups of ashes to a definitive source. The two closely related volcanic zones may have succeeded one another in time or, alternatively, there may have been an overlapping interval when both zones were active together.

### Ash Dispersal and Distribution

That tephra layers are more frequent and thicker off eastern, compared to western, New Zealand confirms the dominance of prevailing westerly winds on ash dispersal (cf. *Frontispiece*, part A, inset). For example, Site 1124 contains 134 tephra layers averaging 9.6 cm thick, whereas DSDP Leg 90 Site 593, the closest western drill site to the volcanic sources, bears only four macroscopic tephra layers that average <3.5 cm thick (Nelson et al., 1986a).

Within such a pattern of preferential eastward dispersal, some variability might be expected, resulting from fluctuations in paleowind patterns. Thus the increased thickness and frequency of tephra during the Pliocene may not only reflect increased volcanic activity but also a general strengthening of the westerly wind regime at ~3–4 Ma (Kennett and von der Borch, 1986; Zhou and Kyte, 1992). Other variability may be associated with El Niño–Southern Oscillation (ENSO) events, with some models suggesting that periods of strong ENSO activity lasted for at least 0.5 m.y. (Clement et al., 2001). Vigorous El Niño conditions favor the eastward dispersal of ash, whereas La Niña weather encourages westward transport. Interestingly, the Rangitawa eruption of  $0.345 \pm 0.012$  Ma (Pillans, 1996), which has a wide distribution, coincides with a shutdown of ENSO, as proposed by Clement et al. (2001). The weakened westerlies (or La Niña easterlies) of the shutdown period may explain the (unusual) presence of the Rangitawa (Mt. Curl) tephra on both sides of New Zealand (Froggatt et al., 1986; Shane, 2000). Superimposed on these large but short-scale climatic variations is the regular rhythm of the Milankovitch glacial–interglacial cycles. At the Leg 181 sites, most macroscopic tephra accumulated during glacial periods, suggestive of increased windiness at those times (e.g., Stewart and Neall, 1984; Hesse, 1994). More frequent eruptions during glaciations may also have been caused by the hydrostatic unloading of magma chambers during falls in sea level, leading to decompression melting (Paterne et al., 1990).

Eruption size can play a prominent role in ash dispersal (Nelson et al., 1985). Major events may be accompanied by ash columns that extend through the low-level winds of the tropopause, currently 20–22 km high at the latitude of the TVZ (Trenberth, 1992), and penetrate the stratosphere, especially in the austral spring-summer when stratospheric winds have a strong westward component while lower level winds continue to the east. Examples of inferred stratospheric penetration include the ~41- to 45-km-high eruption column estimated for the 26.17-ka Oruanui eruption (Wilson, 1994) and the ~35- and 50-km-high columns estimated for the 3.47-ka Waimihia and 1.718-ka Taupo eruptions (Pyle, 1989). Nonetheless, eruption columns apparently only

rarely penetrated into the stratospheric zone of easterly winds, as 97% of all marine tephra are observed in the east.

The latitudinal limits of tephra distribution from the CVZ/TVZ extend south from 30°S (Ninkovich, 1968; Lewis and Kohn, 1973; Pillans and Wright, 1992; Watkins and Huang, 1977) to somewhere between 46°S (Site 1122) and 50°S (Site 1120) (Carter, R., McCave, Richter, Carter, L., et al., 1999). Although Site 1120 displays no obvious tephra, the presence there of several late Cenozoic hiatuses means that the absence of tephra may be more apparent than real. Nonetheless, the isopachs for several recent large eruptions presented by Carter, L., et al. (1995) show that Site 1120 must be located close to the edge of the tephra distribution area. Such minor ambiguities notwithstanding, it is certain that below 60°S southwest Pacific ash-bearing sediments have an Antarctic rather than a New Zealand provenance (Shane and Froggatt, 1992).

### Mineralogy, Geochemistry, and Physical Properties

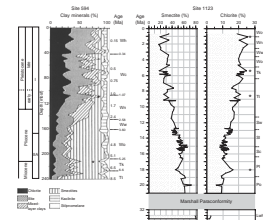
Since completion of the Leg 181 *Initial Reports* volume (Carter, R., McCave, Richter, Carter, L., et al., 1999), studies have been completed on Site 1123 clay mineralogy (Winkler and Dullo, this volume), Site 1123 major element analyses (Weedon and Hall, this volume, in press), dissolved manganese concentrations (Dickens, this volume), Site 1121 carbonate percentages (Hancock and Dickens, this volume), microbial sulfate reduction (Böttcher et al., this volume, in press), biogenic opal concentrations (Suzuki et al., this volume), the use of color reflectance as a carbonate proxy (Millwood et al., this volume), stable isotope measurements (Hall et al., 2001; Harris, this volume; Carter, R., et al., in press; Yang et al., 2002; Wei et al., submitted [N2]; Mii et al., unpubl. data [N4]) and petrophysical properties of muds from Site 1125 (Kim et al., 2001). These studies are summarized below.

### Miocene–Holocene Patterns of Clay Mineralogy, Site 1123

Site 1123, located on the northeastern flank of the Chatham Rise, contains an almost uninterrupted record of sedimentation under the DWBC from the early Miocene onward (~20.5–0 Ma). Systematic mineralogical analyses by Winkler and Dullo (this volume) confirm the very fine grained, carbonate-rich nature of the Site 1123 succession. Clay mineral assemblages are dominated by smectite and illite, with high smectite values in the Eocene decreasing upcore (Fig. F18, right). Accompanying a smectite decrease from 21 Ma, illite and chlorite concentrations progressively increase, with a significant step at 6.4 Ma. An abrupt tenfold increase in the percentage of >63- $\mu\text{m}$ -diameter sediment grains that occurs at ~1.3 Ma is apparently not accompanied by changes in the clay assemblage.

The early Miocene start and gradual nature of the long-term changes in clay mineralogy beneath the DWBC at Site 1123 contrasts with the more recent (middle Pliocene; ~3.5 Ma) change to chlorite-illite-dominated sediments documented at Site 594, which lies under AAIW (Dersch and Stein, 1991) (Fig. F18, left). The Site 1123 change reflects a regionally uniform sedimentation process that was driven by long-term factors, whereas sediment deposited at Site 594 was subjected to a more sudden change to chlorite-illite-rich assemblages, which was probably caused by the arrival of the first turbidity current overspills from the Bounty Channel.

F18. Clay mineral assemblages, Sites 594 and 1123, p. 100.



Overall, the mineralogic changes observed at Sites 1123 and 594 are consistent with regional evidence for progressive uplift along the Alpine plate boundary from the early Miocene (~25 Ma) onward, with increased rates of plate collision since the Pliocene (Walcott, 1978; Tippett and Kamp, 1993; Sutherland, 1996; Batt et al., 2000). These events caused progradation of the eastern South Island terrigenous sediment prism and the activation of channel systems that fed detritus onto the slope and, ultimately, into the DWBC (Carter, R., 1988b). Initially, the prism was derived mainly from the erosion of low-grade metagraywackes and chlorite schists, but from the Pliocene onward there has been an increasing contribution from higher-grade schists. Despite previous assertions, no *unique* date marks the intensification of South Island plate boundary uplift. Rather, the stratigraphic evidence clearly demonstrates a regional early Miocene (~25 Ma) start to the provision of “new” terrigenous sediment (e.g., Finlay, 1953; Lewis et al., 1980), an early middle Miocene (~17 Ma) acceleration of supply (e.g., Cutten, 1979; Turnbull et al., 1993), and, with the precise age depending upon location, a Pliocene (~3–5 Ma) start to the deposition of higher-grade metamorphic detritus, consequent upon marked mountain uplift (e.g., Sutherland, 1996; Batt et al., 2000).

### **Carbonate Content of Paleocene Sediments, Site 1121**

**Hancock and Dickens** (this volume) analyzed 39 samples from the Paleocene biopelagic sediments at Site 1121. Carbonate concentrations vary widely between 3.7 and 51.4 wt% (average = 31 wt%). Site 1121 was at ~3800 m water depth or deeper during the deposition of these sediments. The occurrence of such relatively high carbonate percentages here indicates that the Paleocene carbonate compensation depth (CCD) in the southwest Pacific was significantly deeper than previous studies suggested (e.g., van Andel, 1975).

### **Major Element Analyses (0–1.2 Ma), Site 1123**

**Weedon and Hall** (this volume, in press) report on a high-resolution analytical study of mid–late Pleistocene drift sediments from Site 1123. In order to capture Milankovitch cyclicity, ~1000 samples were taken at a close spacing of 5–10 cm from four selected intervals: 0–1.2 Ma (Pleistocene), 13.9–15.4 Ma (middle Miocene), 20.0–20.6 Ma (early Miocene), and 32.8–33.1 Ma (early Oligocene). Samples were analyzed for elemental concentrations by inductively coupled plasma–atomic emission spectrophotometry. After analysis, results were normalized using aluminium concentrations to provide proxies for nutrient levels, siliciclastic and volcanoclastic sediment composition, and bottom water redox conditions.

The results of Ba/Al for the Pleistocene interval were discussed by Hall et al. (2001), and a geochemical interpretation of the additional elemental ratios and the more extensive age range of host sediment is given by Weedon and Hall (in press). One important result is that samples located close to macroscopic tephra layers, presumed therefore to contain bioturbated ash, are characterized by relatively high Si/Al and K/Al, low Ti/Al, and, in some cases, low calcium carbonate contents. Such tephra-bearing samples were removed from the Pleistocene data set prior to time-series analysis for determination of the pelagic sediment history. None of the pre-Pleistocene samples were detected to be contaminated by tephra.

In the late Pleistocene, productivity variations at the 41-k.y. orbital obliquity frequency are apparent in the Ba/Al and P/Al time series, which are coherent but not in phase (Ba/Al leading P/Al). In the middle Miocene, a trend of increasing carbonate, Ba/Al, P/Al, and Si/Al may reflect gradually increasing surface water nutrient supply (i.e., higher productivity). Carbonate and P/Al are here highly coherent but do not reflect orbital cyclicity. However, Ba/Al does show 41-k.y. cyclicity, so orbital-scale changes may have affected productivity too. No evidence for regular cyclicity exists in any of the variables for the older early Miocene and early Oligocene intervals sampled. Based on comparative values of carbonate, Si/Al, Ba/Al, and P/Al and the presence of biogenic silica, the early Oligocene was more highly productive than the younger sampled intervals or today.

The simplest explanation of the long-term trend is that surface water nutrient levels systematically increased during the middle Miocene, perhaps because of the growth of ice in Antarctica. However, it is an important point that the highest inferred nutrient levels and productivity at Site 1123 occurred prior to DWBC activity during the early Oligocene.

### **Dissolved Manganese, Sites 1119, 1122, 1123, and 1125**

Shipboard pore water and gas analyses show that sediments from the seven Leg 181 sites span an exceptional range of chemical environments. Pore water alkalinity,  $\text{NH}_4^+$ ,  $\text{SO}_4^{2-}$ , and  $\text{PO}_4^{3-}$  concentrations as well as headspace  $\text{CH}_4$  concentrations indicate significant differences in sediment redox conditions across the region (Carter, R., McCave, Richter, Carter, L., et al., 1999). The distribution of solid and dissolved manganese plays an important role in geochemical interpretations of such sedimentary environments, and [Dickens](#) (this volume) therefore measured the dissolved  $\text{Mn}^{2+}$  concentrations of pore waters at Sites 1119, 1122, 1123, and 1125. He reports  $\text{Mn}^{2+}$  concentrations ranging between 0.1 and 26.5  $\mu\text{M}$  and averaging 1.8, 3.3, 3.8, and 1.0  $\mu\text{M}$  at the four sites, respectively.  $\text{Mn}^{2+}$  concentrations are relatively high at the deep-water sites (1122 and 1123) and relatively low at the shallow sites (1119 and 1125), perhaps reflecting higher inputs of reducible solid Mn phases at the deeper locations.

### **Microbial Sulfate Reduction**

[Böttcher et al.](#) (this volume, in press) analyzed 79 interstitial water samples from Sites 1119–1125 for stable isotopes of dissolved sulfate ( $\delta^{34}\text{S}$ ) and for major and minor ions. Sulfate from the interstitial fluids had  $\delta^{34}\text{S}$  values between +20.7‰ and +60.0‰ (i.e., were enriched in  $\delta^{34}\text{S}$  with respect to modern seawater;  $\delta^{34}\text{S} = \sim +20.6\text{‰}$ ). Microbial sulfate reduction is therefore inferred to have occurred at all sites with an intensity that depended upon the availability of organic matter. This availability is controlled by sedimentation rate, which is itself related to factors such as productivity and the presence or absence of turbidity or bottom currents. Böttcher et al. also showed that the amount of reduced inorganic sulfur (essentially pyrite, which is the product of microbial sulfate reduction) varied commensurately between 0.05 and 0.63 wt%.

### Biogenic Opal, Sites 1123–1125

Suzuki et al. (this volume) measured biogenic opal concentrations from bulk sediment samples using wet alkaline extraction of freeze-dried bulk sediment. Samples were taken throughout Sites 1123 and 1125 and from the uppermost 100 mcd of Site 1124. The first and last sites lie within the influence of the DWBC, whereas Site 1125 lies within AAIW. Site 1124 showed opal contents of 2–8 wt%, which is relatively high compared to the other two sites, where values mostly range 1–4 wt%. A subbottom maximum in biogenic opal content occurring between 1.0 and 1.5 mcd at all three sites represents the position of the Last Glacial Maximum (LGM) and is suggestive of enhanced silica productivity during glacials (cf. Fenner et al., 1992; Nelson et al., 1993). The sampling resolution used by Suzuki et al. did not allow capture of the full detail of the climatic signature below the LGM.

### Core Color Reflectance as a Carbonate Proxy

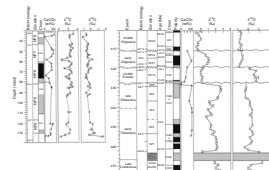
It is well established that color reflectance measurements can provide an estimate of the component mineralogy of sediment cores, especially with respect to calcium carbonate content (Mix et al., 1995; Balsam et al., 1999). Leg 181 was the first ODP voyage during which a new automated Minolta spectrophotometer system was used for routine core logging. Because of several teething problems, the data collected at Site 1119 were of poor quality. Accordingly, Millwood et al. (this volume) collected postcruise reflectance data from the Site 1119 core. Empirical regression relationships between reflectance (400- and 550-nm wavelength) and carbonate content were then formulated separately for each Leg 181 site using the available shipboard and laboratory carbonate determinations from Carter, R., McCave, Richter, Carter, L., et al. (1999). These regressions were then applied to calculate a model carbonate percentage curve for each site based on the reflectance data.

### Stable Isotope Analysis

Because of the primary role that the marine oxygen isotope stages play in stratigraphic correlation and the richness of their information content, stable isotope analysis has become “master-proxy” for paleoceanographic studies. Thus, a prime intention of Leg 181 drilling was to recover multicored, continuous sequences that were suitable for high-resolution foraminiferal stable isotope studies. Sites 1119, 1121, and 1123 have so far yielded such results (Figs. F19, F21).

Site 1119 (water depth = 396 m) penetrated 495 m of micaceous, terrigenous mud with interbeds of bottom current–emplaced sand, generally <1 m thick. Carter, R., et al. (in press) provided a high-resolution (~2 k.y./sample) planktonic stable isotope record through the ~47-m-thick MIS 1–5 interval at this site, based on *Globigerina bulloides*. A lower-resolution (~5 k.y./sample) data set for MIS 6–10 extends the isotope record to 100 mcd, but the record is interrupted by a ~25-k.y. unconformity that cuts out part of MIS 8. Although the Site 1119 MIS 1–9 oxygen isotope record broadly matches the established SPECMAP pattern, site-specific oscillations correspond to movements of the STF across the site during periods of rapid climatic and sea level change. When combined with the color reflectance and natural gamma ray logs, the paleoceanographic proxies from the upper part of Site 1119 define a climatic record that accords closely to Antarctic continental air

F19. Carbon and oxygen isotope values for bulk sediments, p. 101.



temperature, as represented by the Vostok deuterium record (Petit et al., 1999). Thereby, the Site 1119 record demonstrates a close correlation between changes in Southern Hemisphere mid-latitude oceanographic proxies and south polar air temperatures, consistent with strong intra-hemispheric atmospheric coupling.

Sites 1121 and 1124 penetrated a pre-DWBC succession corresponding to the postrifting Cretaceous–Oligocene sediment apron. Mii et al. (unpubl. data [N4]) and Wei et al. (submitted [N2]) made stable isotope measurements on bulk nannofossil-rich sediment samples, 64 from Site 1121 (early–late Paleocene) and 58 from Site 1124 (Late Cretaceous–Oligocene) (Fig. F19). Despite the age and (for Site 1124) burial depth of the sediments sampled, the isotope values do not vary systematically with carbonate content or with burial depth, nor do the carbon and isotope values show any systematic linear relationship with each other. Any diagenetic or dissolution effect is therefore minimal, except possibly for the deepest sample from Site 1121 (133.52 mbsf), which displays an anomalous 2‰ negative excursion in  $\delta^{18}\text{O}$  accompanied by a smaller negative change in  $\delta^{13}\text{C}$ . This sample apart, the Site 1121 samples span ~62.2–56.2 Ma and display a slight overall positive trend in both  $\delta^{13}\text{C}$  (~2.7‰–3.3‰) and  $\delta^{18}\text{O}$  (~0.0‰–0.5‰). Fluctuations in magnitude as large as 1‰ occur on either side of this trend, with a particularly marked  $\delta^{13}\text{C}$  depletion spike of 2.26‰ at 58.51 mbsf, just above the Chron C26n/C25r boundary. At Site 1124,  $\delta^{13}\text{C}$  values range 1.7‰–3.4‰ and  $\delta^{18}\text{O}$  values range –1.3‰–0.9‰. Prominent in the  $\delta^{13}\text{C}$  record is a 1.1‰ negative shift across the K/T boundary, followed immediately by a 1.0‰ increase in the early Paleocene. Values of  $\delta^{13}\text{C}$  then decrease by 1.3‰ at the Paleocene/Eocene boundary, increase by 0.5‰ in the late Eocene, and finally decrease by 0.8‰ at the Eocene/Oligocene boundary. Values of  $\delta^{18}\text{O}$  decrease by 1.0‰ in the latest Cretaceous and remain around –1.0‰ into the early Paleocene before increasing again by 1.4‰ later in the early Paleocene. Values of  $\delta^{18}\text{O}$  then fluctuate around –0.3‰ until they increase to 0.7‰ near the Paleocene/Eocene boundary. A 1.4‰ decrease occurs in the early Eocene, after which  $\delta^{18}\text{O}$  values increase to 0.9‰ at the Eocene/Oligocene boundary, before settling at ~0.8‰ in the Oligocene.

Although the Site 1121 record covers a relatively short time span and the Site 1124 record is punctuated by three major paraconformities, these results show throughout a pattern that is closely comparable to previously published oceanic foraminiferal isotopic records (e.g., Zachos et al., 2001). Both records show negative carbon and isotope shifts across the K/T boundary followed by a gentle cooling trend through the Paleocene, and Site 1121 displays well the established Cenozoic carbon isotope maximum value at ~57 Ma. Site 1124 also displays notably enriched isotope values during the middle Eocene and—albeit within a lengthy paraconformity—contains a sharp cooling enrichment across the Eocene/Oligocene boundary. These results show that stable isotope ratios within Paleogene bulk sediments from the southwest Pacific mimic the global oceanic pattern. The waters of the southwest Pacific Ocean were therefore in free communication with those of the world ocean, and isotope measurements from the region provide a good means of chemostratigraphic correlation (Wei et al., submitted [N2]).

Site 1123 contains an almost continuous early Miocene–Holocene (0–20.5 Ma) record of sedimentation under the DWBC. A benthic stable isotope record with a resolution of 3–5 k.y./sample was generated for the site to 109 revised mcd (rmcd), or ~3.0 Ma (early Pliocene), based

on *Cibicides* spp. (Harris, this volume; Hall et al., 2001) (Fig. 21B). The isotope measurements were evaluated in the context of the complete composite record available for the site to ~4.7 Ma, which has been tuned to an orbital timescale (Hall et al., 2001). The stable isotope measurements record the influence of North Atlantic and Southern Ocean deepwater masses on water properties at Site 1123. In addition, the Site 1123 record closely matches that of ODP Leg 138 Site 849 in the eastern equatorial Pacific (Mix et al., 1995), and the resulting age model agrees with the excellent paleomagnetic reversal record established for Site 1123 (Carter, R., McCave, Richter, Carter, L., et al., 1999; Wilson, 2000b).

For Site 1125, Yang et al. (2002) determined the oxygen and carbon isotope values of *Globigerina bulloides* and *Uvigerina* spp. for 207 samples spaced at ~24-k.y. intervals through the upper ~200 mbsf (0–5 Ma). The  $\delta^{18}\text{O}$  results delineate two episodes of middle Pliocene warmth between 4.7 and 3.2 Ma and the start of a cooling trend at ~2.9 Ma, a little earlier than the 2.4 Ma accepted as the initiation of Northern Hemisphere glaciation (e.g., Raymo, 1994). During the middle Pliocene warm interval, the  $\delta^{13}\text{C}$  profile of *Uvigerina* spp. shows a significant depletion trend, whereas the planktonic *G. bulloides* record displays relatively heavy values compared to the glacial times. These results are consistent with an increase in shallow-water and shelf biomass, perhaps supplied to Site 1125 via an invigorated East Cape Current system. During the late Pliocene global cooling, an enrichment of  $^{12}\text{C}$  in the surface ocean results in a decreasing trend of  $\delta^{13}\text{C}$  in *G. bulloides*. The  $\delta^{13}\text{C}$  profile of *Uvigerina* spp., however, shows a different trend from that of *G. bulloides* and indicates stronger production of AAIW during glaciations.

### **Petrophysical Properties of Muds, Site 1125, North Chatham Slope**

The effect of consolidation on sediment microfabrics and petrophysical properties is of considerable interest. In order to study these changes, Kim et al. (2001) subjected samples from Site 1125 to scanning electron microscope (SEM) observation both prior to and after laboratory consolidation tests. Preliminary X-ray diffraction and grain size analyses demonstrated that the samples studied were mineralogically and texturally similar and thus ideal for study. Porosity was measured before and after each consolidation test, and permeability was estimated based on the theoretical model of Bryant et al. (1986).

SEM images show that as porosity decreases the geometry and distribution of intergranular pores change significantly in concert. Clay plates with randomly distributed voids and abundant edge-to-edge and edge-to-face contacts in unconsolidated sediment lose these characteristics on consolidation. After consolidation, bedding-parallel fabrics and bedding-elongate voids are characteristic. Visual estimates of the porosity loss imposed by consolidation from SEM images generally agree with measured values. The results of this study therefore confirm the classic descriptions of clay fabric changes and porosity reduction during consolidation and show that consolidation is the major control on the petrophysical properties of buried sediments.

## HISTORY OF SEDIMENTATION UNDER THE DEEP WESTERN BOUNDARY CURRENT

The history of the DWBC since the early Miocene is contained in abyssal sediment drifts located east of New Zealand (Carter, L., and McCave, 1994). The four key drift drill sites are Site 1121 (winnowed veneer accompanied by long erosion), Site 1122 (contourite followed by fan deposition), Site 1123 (continuous 20.5- to 0-Ma record of drift deposition), and Site 1124 (drift deposits since 27 Ma punctuated by erosional paraconformities). Fluctuations in DWBC flow are reflected in variations of the terrigenous grain size (Hall et al., 2001; cf. McCave et al., 1995), variations in linear sedimentation or mass accumulation rates (Handwerger and Jarrard, in press), and variations in magnetic fabric (Joseph et al., 1998). The mean grain diameter for sortable silt grain sizes is expected to rise with increasing flow until, at speeds of more than ~0.15 m/s, erosion outweighs deposition. In general, the magnitude and frequency of individual erosion and deposition events cannot be resolved in the record. In the late Quaternary age control points are several thousand years apart, whereas in the Oligocene and Miocene they are several million years apart, so sedimentation rates and hiatuses can only be tightly resolved for intervals where an orbitally tuned time-scale has been achieved.

### Site 1121—Campbell Skin Drift

Graham et al. (in press) showed from  $^{10}\text{Be}$  dating that the skin drift at this site has an age of ~18 Ma (early Miocene) at ~7–8 m depth (Fig. F7). The low average sedimentation rates this implies (<0.5 m/m.y.) indicate that throughout the Neogene the area behaved more as a sediment source than a sink. At Site 1123, over the same period ~535 m of sediment accumulated. Particularly low sedimentation rates occurred between 15 and 12, 10 and 8, and 1.5 and 0 Ma. As seen in other records (e.g., Flower and Kennett, 1995; Zachos et al., 1992), the period around 15–13.50 Ma is associated with growth of the East Antarctic Ice Sheet. Zhou and Kyte (1992) described the geochemistry of abyssal clays from DSDP Leg 91 Site 596 on the central Pacific plain and inferred (1) a period of development of Mn crusts and vigorous bottom currents between ~14.0 and 8.4 Ma and (2) an erosional interval at ~8.4 Ma, which is also the time of onset of a strong cooling trend identified from isotope data by Shackleton and Kennett (1975; cf. Zachos et al., 2001). Lastly, 1.5–0 Ma spans the development of the intense cooling of the Quaternary glacial period.

It is a significant result that the same timing applies to inferred periods of bottom erosion—and therefore to increased cold-water flow and enhanced Fe-Mn deposition—in both the southwest and west Central Pacific Ocean. If the Site 1121 record is representative of the erosional remnants of the whole Campbell sediment apron, then the apron represents a very large sediment source with an area  $>5 \times 10^4 \text{ km}^2$  (Carter, L., and McCave, 1997) that supplied material to regions farther north for >20 m.y. through the Neogene. The record of rapidly accumulated radiolarian-rich Cretaceous–Paleocene sedimentation at Site 1121 predates 55 Ma, and former overlying sediments up to early Oligocene in age are inferred to have been removed by DWBC/ACC erosion after the ~33.7-Ma opening of the Tasmanian Gateway to deep flow (cf. Carter, R., McCave, Richter, Carter, L., et al., 1999).

### Site 1122—Mouth of Bounty Trough, Pre-Bounty Fan

The Bounty Fan developed across the path of the DWBC at the mouth of the Bounty Trough. Site 1122 was cored into the left bank levee succession of the fan, which was deposited under the influence of east-traveling, north-overspilling turbidity currents from the Bounty Channel and the north-traveling DWBC (Carter, R., and Carter, L., 1996).

Using the updated age model of Wilson (2000a), a ~5-m.y. hiatus separates early Pliocene from middle Miocene drift sediments at 485 mbsf. At ~2.2 Ma (~440 mbsf), injection of sediment from the Bounty Trough, and perhaps also from erosion near Site 1121 farther south, resulted in a change in sedimentation style beneath the DWBC, increased sediment accumulation rates (to ~10 cm/k.y.), and inception of the abyssal Bounty Fan. Despite this increase in sedimentation rate, discrete turbidites do not appear in the Site 1122 record until ~1.7 Ma (~380 mbsf). The first turbidites are interbedded with cross-laminated sediments that record a continuing influence of DWBC/ACC flow. The increase in sediment injection from the Bounty Trough at ~2.2 Ma occurs also, though a little earlier at ~2.5 Ma, at DSDP Site 594 (Nelson et al., 1985). These changes may result from late Pliocene climatic deterioration or, alternatively, may be related to increased uplift along the Southern Alps plate boundary in the west. At ~0.7 Ma, turbidite frequency and thickness increases, as turbidity currents from the Bounty Trough cause average sedimentation rates to increase to >40 cm/k.y., probably in response to further uplift along the Southern Alps.

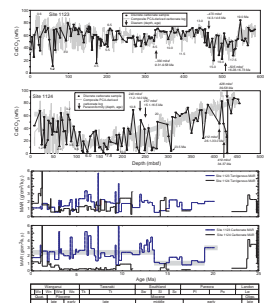
### Site 1123—North Chatham Drift

Handwerker and Jarrard (in press) used downhole logging data for the record younger than 25 Ma at Sites 1123 and 1124 to estimate the relative proportions of carbonate and terrigenous sediment using principal component analysis. The logging data analyzed were bulk density, *P*-wave velocity, total gamma ray, spectral gamma ray (K, U, and Th), resistivity, photoelectric factor, and depth. The Site 1123 records show relatively high carbonate percentages (~70 wt%) and MARs (~2.5 g/cm<sup>2</sup>/k.y.) during the periods 0.6–13.5 and 19–20.5 Ma and lower carbonate percentages (~40 wt%) and MARs (1.5 g/cm<sup>2</sup>/k.y.) during the intervening period (14.5–17.5 Ma) (Fig. F20). Milankovitch-scale 41-k.y. cyclicity occurs superimposed on these background averages, within which particularly strong depletions in carbonate content occur at ~17.5, 16, 15, 11.5, 10, 4.5, and 1.2 Ma. Assuming that carbonate accumulation at this drift site is controlled primarily by DWBC transport vigor, this suggests the occurrence of generally slower flow late in the early Miocene between 14.5 and 17.5 Ma.

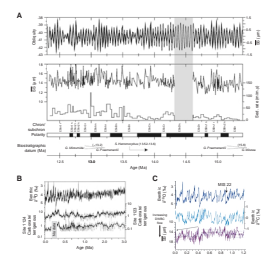
Three other postcruise studies of the Site 1123 core used grain size records as a proxy for changing flow speeds under the DWBC (cf. McCave et al., 1995), one for the middle Miocene (Hall et al., 2003), one for the last 3 m.y. (Hall et al., 2002), and one focusing at high resolution on the last 1.2 m.y. of the Quaternary (Hall et al., 2001) (Fig. F21).

Between ~15.5 and 12.5 Ma (middle Miocene), fluctuating sortable silt mean grain sizes indicate current variations at the period of 41-k.y. orbital obliquity forcing, with faster flow speeds during intervals of colder climate (Hall et al., 2003) (Fig. F21A). In addition to the Milank-

F20. Calcium carbonate and MARs, p. 102.



F21. Selected time series records, Sites 1123 and 1124, p. 103.



ovitch-scale forcing, longer-term changes of current speed occur, with increasing DWBC strength between ~14.8 and 14.3, ~14.3 and 13.8, and 13.8 and 13.15 Ma, and a decreasing trend between 13.2 and 12.5 Ma. The trends of increased DWBC speed that culminate at ~14.3 and ~13.8 Ma correspond to the known middle Miocene cooling phases Mi3b (= CM4; Woodruff and Savin, 1989) and Mi3a (Flower and Kennett, 1995), respectively.

Orbital-scale flow changes in the DWBC also occurred in the Pliocene–Pleistocene (Hall et al., 2001, 2002). Sortable silt grain sizes clearly indicate that faster flow occurred in glacial compared to interglacial periods. Spectral analysis of the sortable silt record shows significant spectral peaks, coherent with both planktonic and benthic oxygen isotope records, at each orbital frequency. There is no phase lag between sortable silt and benthic  $\delta^{18}\text{O}$  at the 100-k.y. period. Although the DWBC has a very large flux, data from current meters, nepheloid layers, and bottom photographs show that it is presently sluggish around the New Zealand margin. In contrast, very large current scours occur at the seabed around volcanic pinnacles (Carter, L., and McCave, 1994; McCave and Carter, L., 1997). The Leg 181 results suggest that these scours most probably formed under stronger bottom flows during glaciations, and farther downstream these enhanced flows may also have driven the glacial increase in sediment focusing that has been recorded in the central equatorial Pacific over the past 300 k.y. (Marcanonio et al., 2001).

Collectively, these variations indicate that a strong coupling exists between changes in the speed of the deep Pacific inflow and high-latitude climatic forcing (Fig. F21B). We conclude that this coupling has probably been a persistent feature of the global thermohaline circulation system for at least the past 15 m.y. Furthermore, longer-term changes in the mean flow speed suggest that intensification of the DWBC occurred in parallel with increases in the production rate of the intermediate-depth SCW, as indicated by isotopic data at DSDP sites north of New Zealand (Flower and Kennett, 1995). Site 1123 results, therefore, provide evidence that the middle Miocene growth of ice on Antarctica caused a significant increase in the production of deep cold water, thus in turn increasing the vigor of the DWBC and perhaps global thermohaline circulation and marking an important step in the development of Neogene icehouse climate. A particularly elegant detail of the Site 1123 record is the increase in grain size recorded at 14.8–14.6 Ma, followed by a short hiatus at 14.6–14.3 Ma, which is precisely the pattern that would be expected from increasing current flow that eventually exceeded the erosion threshold of seafloor sediment. The hiatus is then followed by sedimentation of finer grain sizes, indicating the resumption of accumulation once the flow had slowed.

Using the Pleistocene oxygen isotope stratigraphy as a stratigraphic control, Hall et al. (2001) also recorded three long-term periods of differing mean flow speeds of the DWBC at Site 1123 (Fig. F21C). First, a period of moderately high flow occurred prior to the termination of glacial MIS 22 (which is the first large 100-k.y. cycle in the record); second, a transitional period of lower-speed flow occurred during 0.87–0.45 Ma; and third, another phase of higher-speed mean flow occurred from 0.45 Ma to the present. The mean current speeds for these inferred flow periods are significantly different ( $P < 0.001$ ). The middle flow phase corresponds to the MPT, marking the change in response of the Earth's climate from orbital obliquity (41 k.y.) to eccentricity (100 k.y.) forcing; at Site 1123, this change extended over several hundred thousand years

rather than comprising a sharp event. This gradual change in a proxy record indicative of the strength of the DWBC demonstrates that a changing global thermohaline circulation accompanied the MPT. Over the most recent period, the strength of DWBC flow in the interglacials has clearly increased as part of a long-term trend that has typified the last 0.9 m.y.

The benthic  $\delta^{13}\text{C}$  record at Site 1123 is in phase with  $\delta^{18}\text{O}$  at major orbital frequencies, with light  $\delta^{13}\text{C}$  associated with heavy  $\delta^{18}\text{O}$ . Nutrient-enriched carbon values of  $-0.6\text{‰}$  are present in glacial sediment and depleted values of  $+0.8\text{‰}$  in interglacial sediment. Deepwater  $\delta^{13}\text{C}$  spatial gradients can be used to shed light on water mass aging trends, and Site 1123 is ideally located for the assessment of Pacific  $\delta^{13}\text{C}$  gradients because it represents the entrance of CDW. As CDW travels across the Pacific, it mixes with the overlying waters and progressively accumulates nutrients through the remineralization of sinking organic material—thus depleting the  $\delta^{13}\text{C}$  signal. The gradient between Site 1123 and eastern equatorial Leg 138 Site 849,  $\delta^{13}\text{C}_{(1123-849)}$ , varies by  $>0.5\text{‰}$  and displays a larger gradient during interglacial periods. The spectrum of  $\delta^{13}\text{C}_{(1123-849)}$  shows strong obliquity power and is coherent with  $\delta^{18}\text{O}$ , with the records in phase. A clear relationship is also seen between  $\delta^{13}\text{C}_{(1123-849)}$  and the sortable silt index, with periods of reduced ventilation (high  $\delta^{13}\text{C}_{(1123-849)}$ ) associated with reduced DWBC flow speeds. An important related feature is a very large glacial–interglacial variation of  $\sim 1.4\text{‰}$  in the  $\delta^{13}\text{C}$  of the water emanating from the ACC and flowing into the Pacific, part of which is attributable to changes in the global carbon reservoir.

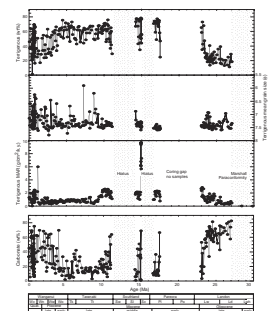
Overall, the carbon isotope and sortable silt data demonstrate strong glacial–interglacial variability in the strength of flow and water mass properties of the southwest Pacific DWBC sector of the global thermohaline system. The data are consistent with greater DWBC flow, and therefore enhanced formation of AABW and greater Pacific ventilation, as a persistent feature of glacial periods over the past 1.2 m.y. This Pleistocene record provides a solid basis for studies going back further in time if reliable isotopic data can be assembled.

### Site 1124—Rekohu Drift

Using the same techniques as for Site 1123, Handwerger and Jarrard (in press) also analyzed sediment accumulation rate proxies at Site 1124. The Site 1124 record (Fig. F20) displays a long-term decline in average carbonate percentage from  $\sim 85$  to  $15\text{ wt\%}$  ( $25\text{--}10\text{ Ma}$ ), a late Miocene period of low ( $10\text{--}20\text{ wt\%}$ ) carbonate content ( $10\text{--}5\text{ Ma}$ ), a rise from  $\sim 15$  to  $55\text{ wt\%}$  ( $5\text{--}3.2\text{ Ma}$ ), and a final period during which carbonate values oscillate repeatedly and rapidly between  $\sim 10$  and  $55\text{ wt\%}$  ( $3.2\text{--}0\text{ Ma}$ ). The long-term decline in carbonate during the Miocene continues across the core gap at  $22.5\text{--}17.6\text{ Ma}$  and the hiatuses at  $16.5\text{--}15$  and  $14\text{--}11\text{ Ma}$ . High carbonate peaks occur superimposed on the long-term trends at  $\sim 20$ ,  $10.5$ , and  $3.2\text{ Ma}$ , and notable lows occur at  $\sim 23.6$ ,  $11$ ,  $2.4$ , and  $1.2\text{ Ma}$ . Mass accumulation rates of both carbonate and terrigenous material show a sharp reduction at  $\sim 23.7\text{ Ma}$ , and terrigenous MAR shows highs at  $14.8\text{--}14.2$  and  $10.9\text{--}9.7\text{ Ma}$  and a sharp increase at  $\sim 1.1\text{ Ma}$ .

The Site 1124 core was also studied by Joseph et al. (in press), who used grain size and magnetic fabric measurements as proxies for DWBC intensity. These data (Fig. F22) clearly show sharp increases in terrige-

F22. Sediment characterization, Site 1124, p. 104.



nous:carbonate ratio starting at ~23.6 and 10.4 Ma, a longer-term but markedly fluctuating decrease in the same ratio between ~5 and 1.5 Ma, and finally another significant increase in the ratio over the last 1.5 m.y. Higher-frequency fluctuations are also apparent throughout the Joseph et al. data set and represent an orbital signal, though the sampling interval was not quite close enough to capture the full 41-k.y. Milankovitch cyclicity.

The changes in sediment parameters at Site 1124 documented by Jarrard and Handwerger (in press) and Joseph et al. (in press) are consistent with our other conclusions regarding the ~23.7-Ma settling of the DWBC along pathways at speeds similar to those of today as the strong predecessor current through the Tasmanian Gateway waned with the widening of the Southern Ocean and perhaps the opening of Drake Passage (Fulthorpe et al., 1996). The grain size and fabric measurements seem to be particularly sensitive to fluctuations of the DWBC between 23 and 9 Ma, in accord with major Antarctic episodes of glacial development and associated circulation changes (e.g., Miller et al., 1991). The hiatus between 22.5 and 17.6 Ma represents an increase in ACC circulation around Antarctica (perhaps caused by the opening of deep circum-Antarctic gateways) (cf. Rack, 1993; Handwerger and Jarrard, in press), whereas the hiatuses at 16.5–15 and 14–11 Ma encompass the late middle Miocene cooling events described by several earlier writers (Woodruff and Savin, 1991; Wright and Miller, 1992; Flower and Kennett, 1993) and represent glacial deepening in Antarctica. The time period between 11 and 9 Ma is characterized by the signature of formation and stabilization of the West Antarctic Ice Sheet. A decrease in carbonate and terrigenous MAR at this time is most marked at the deeper Site 1124, an effect that may indicate the presence of a stronger and more corrosive DWBC there. Again at Site 1124, a Pleistocene surge in accumulation rate occurs after 1.5 Ma, which probably marks the diversion of the Hikurangi Channel onto the abyssal Pacific floor close to Rekohu Drift (cf. Lewis et al., 1998; Hall et al., 2002).

## Other Paleoceanographic Changes

### Ice-Rafted Debris on the Campbell Plateau

Records of ice-rafted debris (IRD) in seven site survey cores and at Site 1120 reveal a pattern of periodic iceberg incursion into the southwest Pacific over the last 200 k.y. (Carter, L., et al., 2002b). Modern icebergs originate in Antarctica and are moved east and north to the margins of the Campbell Plateau by the ACC. Once they are in the southwest Pacific, local currents and winds disperse icebergs as far north as Chatham Rise at 43°S (Cullen, 1965; Brodie and Dawson, 1971). The shallowness of the rise crest, the rise-parallel circulation, and the strong thermal gradient associated with the nearby STF inhibit further northward transport. Although IRD concentrations are very low in the studied cores (926 grains/g), a  $\delta^{18}\text{O}$  chronology reveals distinct IRD peaks (1) at the transition from MIS 7 to 6, (2) during late MIS 5, and (3) during the LGM (MIS 2). Smaller peaks occur in MIS 4 and 3. A similar pattern is also known off Antarctica, suggesting that the periodic destabilization of ice shelves was the main driving force behind Campbell Plateau IRD events. Differences between the Antarctic and New Zealand IRD records probably reflect paleoceanographic influences on iceberg dispersal. For instance, the MIS 5 event is more strongly represented near Antarctica, as would be expected. Conversely, the MIS 2 event is relatively better

shown on Campbell Plateau, consistent with a more vigorous oceanic circulation then causing more icebergs to reach the distant plateau. Comparison of IRD records from the Campbell Plateau with those from the southeast Atlantic and southwest Indian Oceans suggests that IRD events can be correlated across the Southern Ocean over at least the last 70 k.y.

### Changes in the Position of the STF near Site 1119

Site 1119 lies just seaward of the modern STF, east of South Island. The upper 86.19 mcd of Site 1119 was deposited in the last 0.252 m.y., during MIS 1–8 (Fig. F7). The underlying sediments to 100 mcd, beneath a ~25-k.y.-long unconformity, represent MIS 8.5–11 (0.278–0.370 Ma). Interglacial MIS 5, 7, and 9 are represented by silty clay, which encompasses small groups of 5- to 65-cm-thick, sharp-based, *Chondrites*-burrowed, olive-gray, graded fine sands-muds. The sands are shelly (especially *Tawera*) and conspicuously rich in foraminifers, sometimes including temperate-water forms (*Orbulina universa*, *Globorotalia inflata*, and *Globorotalia truncatulinoides*). The intervening micaceous glacial muds may be bedded on a centimeter scale but are more usually massive and bioturbated; they contain the cold-water scallop *Zygochlamys delicatula* and an enhanced siliceous and impoverished calcareous microfauna.

During interglacials, the water at Site 1119 was deeper, the shoreline was distant from the site, and the broad shelf was ventilated by the subtropical Southland Current. At these times, transgressive shelly sand followed by highstand mud accumulated at low rates of 5–32 cm/k.y. along the upper slope, which was bathed in colder SAW. As climatic cooling progressed, the falling sea level was accompanied by a narrowing of the shelf; sedimentation rates rose successively through the MIS 10, 6, and 2 glaciations to 45, 69, and 140 cm/k.y., respectively, as a result of the delivery of river-borne sediment directly to lowstand shorelines.

Against this lithologic background, the upper 100 m of the Site 1119 core records the seaward movement of the STF during glacial periods, accompanied by the incursion of warmer STW above the site and landward movement during interglacials, resulting in a dominant influence then of colder SAW. Counterintuitively and forced by the bathymetric control of a laterally moving shoreline during glacial–interglacial and interglacial–glacial transitions, the Site 1119 core records a *southerly* (seaward) movement of the STF during glacial periods accompanied by the incursion of *subtropical water* (STW) above the site and *northerly* (landward) movement during interglacials, resulting in a dominant influence then of *subantarctic surface water* (SAW). These different water masses are clearly delineated by their characteristic  $\delta^{13}\text{C}$  values (Carter, R., et al., in press). Intervals of thin, sharp-based, graded sands-muds occur within the cold periods MIS 2–3, 6.2, and 7.4. During these glaciations, an increased flow of ACC cold water circulated clockwise in the head of the Bounty Trough (Carter, L., et al., 2000; Neil et al., submitted [N1]) and the glacial STF east of South Island was marked by a zone of intense oceanographic gradients (Weaver et al., 1998). The currents that developed along the glacial STF transported sand beds with grains up to 150  $\mu\text{m}$  in diameter and are therefore inferred to have reached speeds of at least 40 cm/s in waters to ~250 m deep. The beds of very fine sand that occupy the cold-climate intervals at Site 1119 are marked also by conspicuous gamma ray lows, color reflectance (carbonate content)

highs, and stable isotope signatures. In common with other Southern Hemisphere records, the cold period that represents the LGM commenced at ~22.4 ka at Site 1119, at which time the STF and SAF may have coalesced into a single zone of enhanced oceanographic gradients around the head of the adjacent Bounty Trough.

The deeper parts of Site 1119 comprise a succession of silty clay punctuated by thin sand intervals, similar to the lithologies described above for the uppermost 100 m. Shipboard observations indicate that the 495-m base of the core terminates in the late Pliocene at ~3.9 Ma (Carter, R., McCave, Richter, Carter, L., et al., 1999), and research is continuing on the interpretation of the earlier parts of this important climatic record.

### Glacial–Interglacial Changes in Salt Sources for Deep Water

Pore water samples from the upper 100 m of Site 1123 were measured for chloride concentration and oxygen isotopic composition by Adkins et al. (2002), in order to reconstruct the salinity and temperature of the CDW during the LGM. By comparing the results from Site 1123 with similar measurements made at sites elsewhere in the Southern and Atlantic Oceans, these authors showed that LGM deep ocean temperatures were homogeneous everywhere and within error of the freezing point of seawater at the sea surface. In contrast, glacial salinity values varied, with the saltiest deep water present in the Southern Ocean rather than the North Atlantic (NADW). These results have been termed “a landmark change in our understanding of deep-ocean circulation” (Boyle, 2002) because they imply that during Termination I (~20–10 ka) the salt source for the deep sea switched from the Antarctic to the North Atlantic, with concomitant circulation changes.

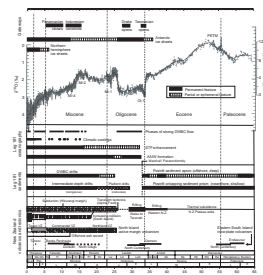
## ENZOSS REVISITED: THE HISTORY OF PACIFIC DEEP FLOW

Leg 181 drilling confirmed the utility of delineating the Eastern New Zealand Sedimentary System (ENZOSS) as a self-contained, dynamic sedimentary system. Like all regional stratigraphies and as summarized below, that of ENZOSS was at times affected by major events for which the cause lay outside the immediate area. Leg 181 drilling confirmed the timing of several of these influential regional events and additionally provided us with a detailed record of many hitherto undocumented changes in Neogene climate and in oceanographic flows for the ENZOSS region of the Southern Ocean (Figs. F23, F24, F25; also see the “[Supplementary Material](#)” contents list).

### Late Cretaceous–Late Eocene Rift-Drift: Start of the Kaikoura Synthem

The New Zealand continental fragment split from the Gondwana supercontinent in the Late Cretaceous (Anomaly 33; ~83 Ma) (Cande and Kent, 1995) by rifting and subsequent seafloor spreading in the South Pacific and Tasman Oceans (Molnar et al., 1975; Cande et al., 2000). The onland geology of New Zealand, especially in South Island, contains an excellent and well-understood record of these events as they affected the western margin of the proto-Pacific (Carter, R., and Norris,

F23. Stratigraphic and climatic events vs. oxygen isotope curve, p. 105.



1976). Scattered fault-controlled Late Cretaceous rift basins with a fan-glomeratic and immature fluviatile fill (e.g., Bishop and Laird, 1976; Laird, 1993) are succeeded by quartzose coastal plain coal measures and shallow-marine transgressive sediments (e.g., Macpherson, 1949; Wilson, 1956; Gair, 1959; Carter, R., 1988a, 1988b; Warren and Speden, 1978; Bishop and Turnbull, 1996). In eastern South Island, where the Canterbury Basin represents the very inner edge of the rift-stretched Pacific margin, total subsidence was small, resulting in a thin marine transgressive succession, generally <500 m thick, which is entirely of shallow-water origin and characterized by condensed sediment facies and many paraconformities (e.g., McMillan and Wilson, 1997).

Leg 181 drilling was primarily targeted at the paleoceanographic record contained in Neogene current drifts. Nonetheless and because of the rudimentary knowledge of the offshore stratigraphy prior to Leg 181, drilling at Sites 1121 and 1124 unexpectedly penetrated through important Late Cretaceous–late Eocene successions that represent the deep-sea counterpart to the well-understood postrift transgressive sections onland. The offshore sediments are mostly fine-grained claystones rich in biopelagic microfossils and represent part of the deep-marine peri-continental apron that accumulated along the western fringe of the Pacific Ocean after rifting. Drilling at Site 1124 penetrated the Cretaceous/Tertiary boundary, though regrettably, the boundary succession itself, which was imaged on downhole logs, lay between two successive cores and was therefore not retrieved (Carter, R., McCave, Richter, Carter, L., et al., 1999). Late Cretaceous siliceous, nannoplankton-rich claystones below the boundary change above to Paleocene nannofossil chalks with intervals of claystone. Similar nannofossil chalks with diatom-rich interbeds characterize the middle–late Paleocene section at Site 1121, farther south along the margin. The Paleocene chalks are overlain at Site 1124 by a 10-m-thick interval of middle Eocene dark brown mudstone, similar to sediment facies described from Gondwanan immediate postrift margins by Andrews (1977) and similarly inferred to represent a period of low oxygenation and sluggish bottom water movement. At intermediate depths, dysaerobic conditions became established during the late Paleocene, as marked by the deposition of the organic carbon-rich Waipawa (“Black Shale”) Formation (Lillie, 1953), which Killips et al. (2000) suggested was formed between ~59 and 55.5 Ma on the outer shelf and upper slope during episodes of upwelling of warm, saline, nutrient-rich deep water (WSDW). A dysaerobic peak also occurred at a major extinction of intermediate-water benthic foraminiferal species that accompanied a 2‰ decrease in  $\delta^{13}\text{C}$  at the ~55.5-Ma PETM, as recorded within siltstones of the Tawanui Formation in eastern North Island (Kaiho et al., 1996) and siliceous marl of the Amuri Limestone in Marlborough (Hancock et al., 2003). More vigorous Paleogene bottom flows are, however, suggested by the presence of Paleocene–early Eocene and middle–late Eocene paraconformities at Site 1124. Nonetheless and as may also be true globally (Moore et al., 1978; Wright and Miller, 1993), a period of stagnant circulation and low surface productivity characterized the southwest Pacific Ocean margin in the late middle Eocene (~37–39 Ma), after which the deposition at Site 1124 of a thin (8 m) interval of late Eocene (~34–37 Ma) nanochalk represents the offshore resumption of more normal biopelagic sedimentation prior to the dramatic ocean circulation changes marked by the Marshall Paraconformity at ~33 Ma.

Late Cretaceous and Paleogene fine-grained terrigenous and biopelagic sediments of deep marine origin occur extensively in northern

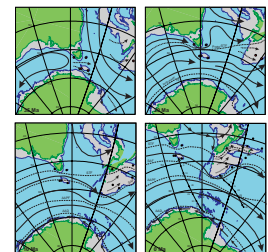
South Island (Herring-Woolshed siltstone and Amuri chalk/chert formations) (Hollis et al., 1995; Field and Browne, 1989; Field et al., 1997) and eastern North Island (Whangai, Waipawa, and Wanstead Formations) (Lillie, 1953; Field et al., 1997). Characteristic Late Cretaceous transgressive shelf facies (Reay and Strong, 1992; Isaac et al., 1991) pass up into this fine-grained, deepening-upward, hemipelagic and biopelagic succession (Moore and Morgans, 1987; Field et al., 1997; Rogers et al., 2001), which accumulated as a regional sediment apron during the postrift foundering of the continental margin to abyssal depths. Today, these sediments occur within the tectonically disturbed East Coast Fold Belt, where they were emplaced by collision or accretion since the establishment of the New Zealand plate boundary in the late Oligocene (~25 Ma).

Leg 181 drilling yielded important in situ samples of the postrift sediment apron and thereby provides insight into the deepwater processes that operated then along the southwest Pacific margin. Earlier studies, including deterministic computer models (Barron and Peterson, 1991; Mikolajewicz et al., 1993), have suggested that the Paleogene Pacific Ocean circulation was dominated by a large anticlockwise gyre that distributed warm water southward from low western latitudes into the New Zealand area (Berggren and Hollister, 1977; Frakes, 1979; Kennett and Stott, 1991). The sediments drilled during Leg 181, and their on-land equivalents in New Zealand, are consistent with these earlier hypotheses regarding Pacific circulation, containing warm-water faunas and yielding no particular evidence for the operation of a northward-flowing DWBC prior to the early Oligocene.

### Opening of the Tasmanian Gateway: ENZOSS is Born

The ENZOSS commenced at the Eocene/Oligocene boundary, when eastward-propagating rifting through the Great Australian Bight and Tasmanian Gateway formed the first ocean passage between the Indian and Pacific Oceans and thereby created the proto-Southern Ocean (Molnar et al., 1975; Cande et al., 2000; Exon, Kennett, Malone, et al., 2001; Exon et al., 2002) (Fig. F24; see the “**Supplementary Material**” contents list). This event had two immediate, climatically profound consequences. First, it resulted in the wind forcing of strong eastward-flowing seabed to sea-surface currents through the gap, creating the precursor circum-Antarctic current. Second, the commencement of this energetic zonal current system began the process of the thermal isolation of Antarctica. The ensuing climatic deterioration may have been accentuated, or even primarily caused, by a marked decline in atmospheric CO<sub>2</sub> content that occurred over the same time period (Pearson and Palmer, 2000; cf. DeConto and Pollard, 2003). Together, these events were a prelude to the Oi-1 oxygen isotope event that marks the Eocene/Oligocene boundary (Devereux, 1967; Shackleton and Kennett, 1975; Miller et al., 1991), which is associated with a spike in ice-rafted debris at Leg 120 Site 748 on the Kerguelen Plateau (Zachos et al., 1992) and also with an associated short-term boost in productivity at Southern Ocean sites (Diester-Haass and Zahn, 1996; Robert et al., 2002). The Oi-1 event has therefore been widely interpreted as marking the formation of the first southern-sourced deep cold-water flows, which were followed by stronger cooling and ice-cap development in the Neogene (e.g., Barrett, 1996). However, recently published benthic foraminiferal

F24. Reconstructed frontal systems and surface circulation, p. 106.



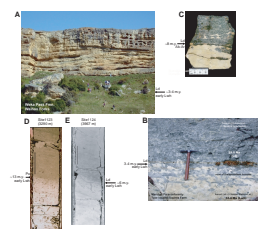
Mg/Ca paleotemperatures (Lear et al., 2000) do not show a significant temperature fall at the Eocene/Oligocene boundary, suggesting that the Oi-1 isotope event may correspond entirely to the growth of new ice on Antarctica without concomitant generation of cold deep water. Irrespective of this ocean temperature ambiguity, however, at 33.7 Ma the center of the New Zealand Plateau lay at paleolatitude  $\sim 55^{\circ}\text{S}$  in the southwest Pacific Ocean, immediately downstream from the throat of the developing Tasmania–Antarctica Gateway (Lawver et al., 1992; Exon, Kennett, Malone, et al., 2001) where “circumpolar...bottom waters were restricted to a relatively narrow channel and, hence, must have had very high current velocities,” thereby producing “numerous and widespread disconformities” (Watkins and Kennett, 1971, p. 817).

### Oligocene Starvation and Erosion: Marshall Paraconformity

Sites 1123 and 1124 were cored through relatively thick Neogene successions but penetrated beyond to terminate in late Eocene and Late Cretaceous sediment, respectively. Drilling at Site 1121 also encountered a Paleogene succession, which, in contrast, lay below thin, condensed Neogene deposits (Graham et al., in press). At these three sites and also at all other deepwater sites in the southwest Pacific that penetrate to the Eocene (Kennett, Houtz, et al., 1975; Exon, Kennett, Malone, et al., 2001), a paraconformity or complete facies change always separates Oligocene or younger sediments above from Eocene or older sediments below. This, the Marshall Paraconformity, has long been recognized to be present in all onland New Zealand sedimentary sections and to mark the inception of southern-sourced current flows into the Pacific consequent upon the opening of the Tasmanian Gateway (Carter, R., and Landis, 1972). Subsequent DSDP (Kennett, Houtz, et al., 1975; Kennett and von der Borch, 1986) and ODP (Carter, R., McCave, Richter, Carter, L., et al., 1999; Exon, Kennett, Malone, et al., 2001) drilling established the ubiquitous presence of the paraconformity in deep marine sections throughout the southwest Pacific. Deepwater unconformities of similar stratigraphic significance have also been identified in the Indian Ocean (Edwards, 1973), off South Africa (Tucholke and Embley, 1984), and on the southern Kerguelen Plateau (Diester-Haas et al., 1993; Diester-Haas and Zahn, 1996). These Southern Ocean unconformities mark the establishment of strong flows around the Antarctic perimeter (cf. Watkins and Kennett, 1971; Kennett et al., 1974) and probably also the start of the modern thermohaline ocean circulation system.

The deepwater manifestation of the Marshall Paraconformity is illustrated in Figure F25 and by Exon, Kennett, Malone, et al. (2001; frontispiece 2). As is the case for its onland shallow-water manifestation (Carter, R., 1985, fig. 3), the paraconformity at Sites 1123 and 1124 is subtle and at first glance it is hard to believe that it represents a sedimentation hiatus of many million years. The break is ubiquitously marked by *Chondrites* (or, in shallow water, *Thalassinoides*) burrows that penetrate into underlying nannofossil chalk and that are filled with the conspicuously younger greenish gray nannofossil chalk that overlies the unconformity. Both below and above the unconformity the sediments are extensively burrow mottled, and their shallow-water counterparts are also richly glauconitic, all pointing to low sedimentation rates. Estimated periods of  $\sim 13$  and  $\sim 6$  m.y. are unrepresented by sediment at Sites 1123 and 1124, respectively, the break commencing in the earliest

F25. Marshall Paraconformity in the ENZOSS region, p. 107.



Oligocene (~33.6 Ma) (Carter, R., McCave, Richter, Carter, L., et al., 1999; **McGonigal and Di Stefano**, this volume). On land, at the type locality of the Marshall Paraconformity at Squires Farm, Sr isotope dating established the duration of the gap as a shorter but still significant ~3.4 m.y. between 32.40 and 29.00 Ma (Fulthorpe et al., 1996). Elsewhere on land, however, the gap across the unconformity may extend for 10 m.y. or longer because of (1) minor marginal tilting and erosion of the sediments beneath the unconformity (Benson, 1969; McLennan and Bradshaw, 1984), which probably relates to the late Eocene–Oligocene propagation of the plate boundary through western South Island (e.g., Carter, R., and Norris, 1976; Turnbull, 1991; Sutherland, 1995); or, as exemplified at Site 1121, (2) extensive synparaconformity erosion under the influence of powerful and probably corrosive seabed currents.

Three agents are capable of causing a profound interruption to the accumulation of biopelagic sediments in both deep and shallow water. These are a complete switch-off of pelagic productivity, the introduction of cold and corrosive water (including possibly a shift in the CCD), or an increase in bottom currents to a level that precludes the deposition of fine-grained sediment. Changes to productivity almost certainly occurred along with the profound ocean reorganization that occurred at the Eocene/Oligocene boundary (e.g., Cifelli, 1969; Benson, 1975; Burns, 1977; Miller, 1992) and at deep Site 1124 corrosion of foraminifers is clearly intensified in sediments from above the Marshall Paraconformity compared with those from below (Carter, R., McCave, Richter, Carter, L., et al., 1999), which is strong evidence for a new cold bottom water source. However, abundant evidence exists that seafloor current activity was the primary cause of the Marshall Paraconformity in shallow water (Carter, R., 1985; Fulthorpe et al., 1996; Carter, R., et al., 1996; see also discussion above) and we infer a similar origin for its deepwater manifestations (cf. Kennett, 1977). Situated as it was, as a shallowly submergent plateau just beyond the Tasmanian Gateway, the ENZOSS region was subjected to the impact of the partial ACC system as soon as it developed. The abyssal seabed to sea-surface character, and the strength, of early Oligocene current activity, which is a key feature of the modern ACC, is demonstrated by the fact that sediment accumulation was inhibited for a minimum of several million years *at all depths* between a few tens of meters on the interior of the continental platform and several thousand meters on the peri-continental abyssal sediment apron.

### **Implications of the Revised Age of the Eocene/Oligocene Boundary**

Three major features that reflect far-reaching oceanographic change characterize late Eocene to mid-Oligocene sediments of the southwest Pacific. They are

1. The cooling of shelf and oceanic waters, as marked by the sharp Oi-1 oxygen isotope enrichment at the Eocene/Oligocene boundary (Devereux, 1967; Benson, 1975; Shackleton and Kennett, 1975; Wei, 1991);
2. The ubiquitous presence of the regional “mid-Oligocene” Marshall Paraconformity (Carter, R., and Landis, 1972; see also the appendix in Carter, R., et al., 1982) and other probably equiva-

- lent “early Oligocene” oceanic and continental margin unconformities (Edwards, 1973; Carter, A., 1978); and
3. A claimed global sea level fall, also of “mid-Oligocene” (~32 Ma) age (Haq et al., 1987; Miller et al., 1985).

Establishing the exact relationships between these events has been bedeviled by problems of accurate dating, with added uncertainty coming from ambiguity in the age of the Eocene/Oligocene boundary itself. For example, Boersma and Shackleton (1977) suggested that the apparently later age of the Oi-1 enrichment in the southwest Pacific (early Oligocene) was caused by diachroneity of zone fossils between tropical and southern locations, a discrepancy that was later partly resolved by adopting the isotope shift as itself marking the Eocene/Oligocene boundary (e.g., Keigwin, 1980; Miller, 1992). Later, Kamp et al. (1990) confirmed the existence of such problems by demonstrating that the traditional late Eocene indices *Globigerapsis index* and *Subbotina linaperta* continued well into the early Oligocene, as judged by their occurrence above the Oi-1 event in southern Australian sections. More generally, correlation using New Zealand Oligocene stages (e.g., Morgans et al., 1996) has long been unsatisfactory because of an inadequate type locality for the Dunroonian Stage, which has an unconformable base at the Marshall Paraconformity and comprises a condensed greensand containing reworked microfossils (e.g., Hornibrook, 1966). There is also a lack of any alternative onland sections that are known to be continuous through the Oligocene (Waghorn, 1981).

Resolution of these problems began when the estimate of 32.4–29.0 Ma was established for the age gap across the Marshall Paraconformity at its type locality (Fulthorpe et al., 1996), shortly after the revision of the age of the Eocene/Oligocene boundary to 33.7 Ma (Berggren and Aubry, 1995), but ambiguities nonetheless remain. Leg 181 and 189 drilling demonstrated that the youngest sediments below the paraconformity offshore are 33.5 Ma (Site 1123) and 33.0 Ma (Site 1124) at Leg 181 sites (McGonigal and Di Stefano, this volume), ~33.0 Ma at Leg 189 Sites 1170–1172 (Exon, Kennett, Malone, et al., 2001), and ~33–32 Ma at DSDP Leg 29 Site 277 (Jenkins, 1974; Murphy and Kennett, 1986). Thus the “early Oligocene” isotope event (Shackleton and Kennett, 1975), widespread Southern Ocean “Eocene–Oligocene” deep marine paraconformities (Edwards, 1973; Tucholke and Embley, 1984), and the “mid-Oligocene” Marshall Paraconformity (Carter, R., and Landis, 1972) are actually closely similar in age, with the isotope shift lying at the Eocene/Oligocene boundary at 33.7 Ma and the basal surface of the Marshall Paraconformity following in the early Oligocene no more than 1–2 m.y. later. The indications after Leg 181 drilling are that in the southwest Pacific the paraconformity developed in deep water ~1 m.y. before it spread to shallow water, which might suggest that the proto-DWBC preceded the origin of the proto-ACC. However, the age difference of ~0.6 m.y. for the youngest sediments below the unconformity in deep and shallow water is of the same order as the likely error on the biostratigraphic dating, and alternatively, such a difference could also result from the occurrence of greater seabed erosion at the deepwater sites.

Two new Eocene–Oligocene stratigraphies for the Tasmanian Gateway region have been published since the appearance of the Leg 189 cruise report (Exon, Kennett, Malone, et al., 2001). The first, by Exon et al. (2002) omits the early Oligocene (32–33.5 Ma) hiatus depicted at Sites 1170–1172 by Exon, Kennett, Malone, et al. (2001). Instead, Exon

et al. (2002) show continuous deposition across the Eocene/Oligocene boundary at the three Tasman Plateau sites, followed by a middle Oligocene (~27–31 Ma) paraconformity at Sites 1170 and 1171; a similar pattern of Eocene–earliest Oligocene continuity followed by middle Oligocene hiatus occurs at Site 277 on the western edge of the Campbell Plateau (Shackleton and Kennett, 1975) and Site 744 on the Kerguelen Plateau (Barron, Larsen, et al., 1989; Robert et al., 2002). The second reinterpretation, by Pfuhl and McCave (2003), recognizes the Marshall Paraconformity at all Leg 189 sites except Site 1168 (see additional comments in the caption to Fig. F6). Different regional interpretations will apply, depending upon the correctness of these differing stratigraphies on the Tasman Plateau and particularly upon the amount of early Oligocene seafloor erosion that actually occurred at particular sites throughout the Southern Ocean. Overall, however, the Marshall Paraconformity (1) is present in all, or all but one, oceanic drill sites in the region and (2) in its type area is centered in the early to middle Oligocene in shallow water (~29–32.5 Ma) (Fulthorpe et al., 1996) and appears to start slightly earlier offshore (33.0–33.5 Ma) (McGonigal and Di Stefano, this volume). At some locations (perhaps including Sites 1123 and 1124), seafloor erosion prior to resumed late Oligocene sediment deposition may have extended the apparent length of the hiatus down to the Eocene/Oligocene boundary, or beyond (i.e., a nondepositional, as opposed to erosional, hiatus of early Oligocene age may never have existed). Alternatively, two separate unconformities may be involved, the older “Eocene–Oligocene” one centered in the earliest Oligocene (~33 Ma) (Edwards, 1973; Exon, Kennett, Malone, et al., 2001) and the younger Marshall Paraconformity centered in the middle of the Oligocene (~29–32 Ma) (Fulthorpe et al., 1996). The existing data are inadequate to resolve the issue, especially because most of the relevant sections lack good magnetostratigraphic, isotopic, or astrochronologic control.

Two other significant stratigraphic conclusions follow from this discussion. First, the Vail-EXXON “mid-Oligocene” sea level fall, where it is present at all, may, like the base of the Marshall Paraconformity, prove to be of early Oligocene age on the revised timescale (Pekar, in Prothero et al., 2000). Second, within the local New Zealand stage classification, the early Whaingaroan, which was assigned formerly to the early Oligocene and for which *Globigerina angiporoides* is a key indicator species, is actually partly late Eocene. Furthermore, *Globigerapsis index*, the extinction of which has traditionally been taken as marking the end of the Eocene in Australasia, is now known to persist well into the Oligocene (Kamp et al., 1990). These facts may help resolve the apparent enigma of alleged “early Oligocene” macrofossils of tropical affinities (including *Cocos* nuts, *Lingula*, and cypraeid and coniid gastropods) (cf. Beu and Maxwell, 1990; Hornibrook, 1992; Edwards, 1991) and the conflicts between faunal and oxygen isotope data reported by Burns and Nelson (1981), Adams et al. (1990), and Buening et al. (1998). The isotope data, once displayed against an accurate timescale, probably accurately reflect the global oceanic climatic trend. Many—though not necessarily all (since shallow-water warm refugia could certainly have existed)—of the tropical taxa reported from “early Oligocene” localities in New Zealand may be miscorrelated and actually have lived during the latest Eocene warm interval. Similarly, the widespread occurrence of fossils of modern subantarctic affinities (cetacean whales, penguins, and *Notorotalia*) in the condensed greensands and limestones that overlie the Marshall Paraconformity (Marples, 1952; Fordyce, 1977, 1981;

Carter, R., 1985) is a clear indication of the regional change in oceanography and of post-Eocene cold water influence.

### **Biopelagic Accumulation Resumes: Late Oligocene Drifts, Site 1124**

Seismic evidence indicates that the first deepwater ENZOSS drifts began to accumulate along the path of the DWBC north of Chatham Rise (Carter, L., and McCave, 1994). The oldest sediments above the Marshall Paraconformity at nearby Site 1124 comprise cyclic alternations of darker- (terrigenous) and lighter- (carbonate rich) colored, greenish gray nannoplankton-rich chalk of late Oligocene (22.4–27.0 Ma) age (Carter, R., McCave, Richter, Carter, L., et al., 1999). The darker mudstones contain fewer and more corroded foraminifers, an increased siliceous microfauna of cold-water affinity, and reworked Eocene–Oligocene diatoms. These materials are inferred to have been derived partly by erosion from upstream sources such as the Paleogene sediment apron cored at Site 1121, and their concentration in the darker mudstones suggests increased cold water inflow at such times.

Clearly, if the Marshall Paraconformity at this site resulted from current erosion, then that activity must have waned sufficiently by ~27 Ma to allow the accumulation of these cyclic chalks. By comparison of their lithologies with the similar but younger sediments at Site 1123 and given their relatively high accumulation rates of >20 cm/k.y., the Site 1124 late Oligocene chalks represent the earliest DWBC deposits in the Leg 181 record and their cyclicity indicates that, like the younger drifts, they were deposited under the influence of the 41-k.y.-long astronomical cycle. Toward their top, these chalks show decreased rates of accumulation (Handwerger and Jarrard, in press) (Fig. F20), perhaps indicative of an increasing current speed toward the overlying paraconformity. The marked increase in the proportion of terrigenous material after 25 Ma (Joseph et al., in press) (Fig. F22) also indicates the arrival of “new” sediment into the path of the DWBC. This sediment may have been derived from the newly uplifting plate boundary in the west, but no definite pathways are known. Alternatively, therefore, the sediment may be derived from the seabed farther south, as evidenced by the eroded sediment apron and moat at Site 1121 and reworked Eocene–Oligocene microfossils at Site 1124.

Unfortunately, because of the great depth and the inferred influence of corrosive bottom water, post-Marshall Paraconformity microfossils at Site 1124 are poorly preserved. Nonetheless, the late Oligocene section at the site, together with the equivalent parts of Sites 1168 and 1172 (Exon, Kennett, Malone, et al., 2001), will be of particular importance for future research into the earlier history of ACC-DWBC evolution, for which they represent both the earliest and the only records available.

### **Opening of Drake (Powell) Passage**

The modern mean flow of water passing through Drake Passage above 3000 m is  $97 \pm 13$  Sv (Orsi et al., 1995). Sensitivity modeling indicates that this vigorous ACC flow depends upon the presence of the passage (Gill and Bryan, 1971), which therefore clearly plays a pivotal role in the maintenance of a fully circum-Antarctic, Southern Ocean circulation. Despite contributions by many authors, it has been surprisingly difficult to achieve a consensus regarding the date at which the passage opened to oceanic circulation.

1. Eocene South American marsupial fossils on the Antarctic Peninsula indicate a connection across Drake Passage up until that time (Woodburne and Zinsmeister, 1982). Relationships between marine benthic organisms on either side of the passage have been used in support of opening ages as widely different as late Eocene (~37–40 Ma) (echinoid distribution, Foster, 1974; increased biopelagic productivity at Maude Rise, Weddell Sea, Diester-Haas and Zahn, 1996) and late Miocene (~6 Ma) (benthic foraminifers; Boltovskoy, 1980).
2. As an increasing number of ocean cores became available from the region, estimates of the age of the passage based on sediment facies distributions or paleoceanographic reasoning mostly came to lie in the range of Oligocene to early Miocene (~30–20 Ma) (e.g., Tucholke et al., 1976; Ciesielski and Wise 1977; Kennett, 1978).
3. About the same time, the first detailed analyses of ocean floor magnetic anomalies near the passage also suggested an opening age for shallow waters in the late Oligocene (~29 Ma) but with continental fragments impeding deepwater flow until the early Miocene (~23.5 Ma) (Barker and Burrell, 1977, 1982). Most recently, Barker (2001) reviewed this evidence and inferred an ACC origin between 17 and 22 Ma.
4. It has been suggested that somewhat earlier passage opening occurred through the Powell Basin, a marginal basin that lies immediately south of the modern Drake Passage, along the Antarctic Peninsula (Lawver et al., 1994; Lawver and Gahagan, 1998). Based on the regional geology, combined with heat flow measurements and age/depth calculations, these authors concluded that a middle- to deepwater passage opened by ridge spreading in the Powell Basin in latest Eocene to Oligocene time (~37–30.5 Ma). This interpretation was refined by Eagles and Livermore (2002), who document continental margin rifting along the Antarctic Peninsula between ~40 and 29.7 Ma and identify seafloor magnetic lineations that indicate the creation of the Powell Basin by spreading between 29.7 and 21.8 Ma.

The best current estimate, therefore, is that a deepwater marine gap opened up between South America and Antarctica, initially through Powell Basin, at ~29.7 Ma (i.e., ~4 m.y. after the opening of the Tasmanian Gateway).

Because of the control it exercises over the relative strengths of meridional (thermohaline) and circum-Antarctic zonal (ACC) flows, the effects of the opening of Drake Passage can be expected to be recognizable in southwestern as well as southeastern Pacific Ocean successions. In that light, one of the most striking aspects of the Marshall Paraconformity is the gap of 3–4 m.y. (32.7–29.0 Ma) or longer that occurs across it, which we take to indicate strong corrosive and erosive seabed current flows. When sedimentation resumed at ~29–28 Ma, sediment drifts were deposited ubiquitously in the New Zealand region in both shallow-water (Ward and Lewis, 1975; Anastas et al., 1997) and deepwater (Carter, R., McCave, Richter, Carter, L., et al., 1999) locations. Noting this, Carter, R. (1985) and Fulthorpe et al. (1996) argued that the early Oligocene proto-ACC-DWBC flowed into the Pacific directly across and along the eastern edge of the New Zealand microcontinent, where it precluded the deposition of biopelagic sediment for a period of several million years, forming the paraconformity in the pro-

cess. The resumption of sedimentation in the mid-Oligocene (local Duntroonian stage) reflects lessening current flows, possibly caused by a southward migration of the ACC core into its more strictly circum-Antarctic path consequent upon the opening of Drake Passage. As discussed above, the best-estimate mid-Oligocene date of opening of Drake (Powell) Passage is consistent with these previous interpretations, which were based on sediment facies evidence. Indeed, if this line of reasoning is correct, the conspicuous regional sedimentation changes that occur at ~28 Ma (resumption of greensand and calcarenite deposition above the Marshall Paraconformity) and ~23 Ma (change from coarse-grained calcareous drifts to fine-grained terrigenous drifts) in shallow-marine sediments in eastern New Zealand may represent our most accurate indication of the start and the complete establishment of true circum-Antarctic flow. A similar major sub-early Miocene unconformity overlain by terrigenous sediment drifts also occurs on both the upstream and downstream side of Drake Passage in the southeast Pacific and South Atlantic, respectively (Tucholke et al., 1976; Wright and Miller, 1993).

Prior to the opening of Drake Passage, enhanced northward meridional flow is expected to have occurred in the Southern Hemisphere, with a greater outflow of AABW to the world ocean and a weaker ACC, both factors that today act to suppress NADW production (Mikolajewicz et al., 1993). Thus, prior to ~5 Ma, which approximates to the closure of the Isthmus of Panama and the start of NADW production (Warren, 1983; Wright et al., 1991; Haug and Tiedemann, 1998; Collins et al., 1996; Haug et al., 2001; Lear et al., 2003), the primary source of global ocean deepwater production was probably cooling in the high latitudes of the Southern Hemisphere (Katz and Miller, 1991). Accordingly, during the period ~33.7–5 Ma, the Pacific DWBC constituted an even more important limb of the thermohaline circulation than it does today and variations in heat flux, modulated by its changing flow, may have been a primary determinant of global climate change.

### **Miocene DWBC Drift Accumulation**

Late Oligocene drift deposits at Site 1124 are interrupted by a 5.4-m.y.-long paraconformity that starts at ~22.4 Ma. Above this break, cyclic nannofossil chalks similar to those below accumulated from 17.6 Ma onward, with two further paraconformities at ~16.5–15.0 Ma and ~14–11 Ma (Carter, R., McCave, Richter, Carter, L., et al., 1999). Meanwhile at nearby Site 1123, North Chatham Drift sedimentation commenced at ~21 Ma and continued almost unbroken to today (Carter, R., McCave, Richter, Carter, L., et al., 1999; Wilson et al., 2000b). At both Sites 1123 and 1124, deposition occurred in concert with a prominent 41-k.y. climatic beat, as shown by the cyclic lithologic logs and the orbitally tuned grain size record of Hall et al. (2003). Intervals with reduced biogenic carbonate correspond to enhanced corrosive bottom-water flow from southern sources, as inferred from the increased size of terrigenous sortable silt and the presence of reworked subantarctic diatoms. Like the diatoms, some of the terrigenous component was probably derived from seafloor erosion farther south rather than from the main New Zealand landmass.

The regular Milankovitch obliquity cycles are superimposed upon other episodic shifts that are manifest in the drift record, for instance, the sharp increase in carbonate flux at ~13.5 Ma (Sites 1123 and 1124), which Handwerger and Jarrard (in press) associate with increased pro-

ductivity and which occurs ~1 m.y. after the marked middle Miocene cooling step recorded in the global oxygen isotope curve (Zachos et al., 2001). Latest Miocene to early Pliocene (~7.0–4.6 Ma) warming and resumed cooling between ~4.0 and ~2.5 Ma are marked at Leg 181 core sites in manifold ways (see the “**Supplementary Material**” contents list), yet none of these events disrupted the background functioning of the DWBC. From at least 27.0 Ma and probably from 33.7 Ma, the Pacific DWBC current continued its metronomic supply of deep cold water to the Pacific Ocean; waxing—occasionally to the point of seabed erosion—and waning awhile, but always present.

### **Post-Middle Miocene Volcanic Supply**

Calc-alkaline volcanic activity commenced in New Zealand in the mid-Cenozoic at the same time as regional tectonism related to the inception of the North Island plate boundary (Stoneley, 1968; Delteil et al., 1996). An active andesitic volcanic chain became established in the Auckland-Northland region at ~25 Ma in the late Oligocene (Ballance et al., 1985), associated with other dramatic geological changes including the emplacement of the Onerahi Chaos Breccia (Kear and Waterhouse, 1967) as part of the Northland Allochthon (Ballance and Sporli, 1979). This, the first of the three active chains of arc volcanoes related to subduction beneath the North Island, now lies far to the west because it was rotated away from the modern trench by intra-arc extension along the younger Coromandel and Taupo Volcanic Zones (cf. Walcott, 1984). Fragmental ejecta from the Northland arc are widely preserved in the nearby Oligocene–Miocene Waitemata Basin (e.g., Hayward, 1993), and altered green clay layers of late Oligocene–late Miocene age from Leg 90 drill sites on the Lord Howe Rise can be interpreted as altered ashes derived from the Northland arc (Gardner et al., 1985). Northland arc ashes may occur in the ENZOSS record as similar altered green clay layers at Site 1124.

Early remnants of ash notwithstanding, the record of unaltered macroscopic tephra derived from the Coromandel and Taupo Volcanic Zones starts at Site 1124 at ~12 Ma, near the middle/late Miocene boundary. Thereafter, the offshore ash record is semicontinuous, with 134 macroscopic tephra layers punctuating the background hemipelagic sediments. As outlined in more detail earlier in this review, these tephra provide a significant source of particulate sediment into the ENZOSS and represent an excellent record of major volcanic eruptions from the North Island arc.

### **ENZOSS Climatic Record and Origin of Ocean Circulation and Fronts**

We described earlier the evidence for the early Oligocene (~33.7 Ma) initiation of a strong southern-sourced current system across the southwest Pacific region. Ubiquitous seafloor erosion in both shallow and deep waters suggests that this protothermohaline system resembled the modern ACC, in that it occupied the entire seabed to sea-surface water column. Burns (1977), using microfossil evidence from DSDP Legs 21, 28, and 29, gave the first summary of the development of Southern Ocean water masses and fronts that followed the pivotal Eocene/Oligocene change.

Prior to the Oligocene, an undifferentiated calcareous, open ocean microfossil assemblage was regionally widespread. During the Oli-

gocene, a cool nannoflora (including *Isthmolithus recurvus*) and siliceous cool-water microfauna developed in coastal locations around Antarctica, followed by marked change in the early Miocene when the first siliceous assemblages characteristic of modern Antarctic waters appeared near Antarctica (Leg 28, Site 267); farther north, away from Antarctica, the undifferentiated oceanic microfauna was replaced by an early Miocene assemblage similar to that of modern cool subtropical water (Leg 21, Site 281). Burns (1977) identified a precursor fauna to that of modern Circumpolar Subantarctic water at Leg 29 Site 278 during the early Miocene, but not until the end of the Miocene did this zonal water mass become regionally extensive. Summarizing, the first proto-Polar Front probably appeared during the Oligocene (cf. Kaneps, 1975) and signaled the start of the regional differentiation of water masses away from a cooling Antarctica. A precursor southwest Pacific Ocean water circulation similar to today's appeared in the early Miocene, and the differentiation of this system took place by northward expansion and strengthening of oceanographic gradients, including an intensification of subtropical gyral circulation (Kennett et al., 1985), during the middle and late Miocene. By the Pliocene, the belt of Subantarctic water intermediate between Antarctic and Subtropical waters was established as a circum-Antarctic feature and the direct predecessor water masses and fronts of the modern circulation were all in place (Kennett, Houtz, et al., 1975; Burns, 1977; Lazarus and Caulet, 1993).

Leg 181 results are consistent with earlier onland studies regarding New Zealand paleoclimate (Hornibrook, 1992) (cf. Fig. F3), which suggests the occurrence of a middle Miocene subtropical climatic optimum at ~16–17 Ma followed by climatic deterioration into the Pliocene–Pleistocene. As discussed earlier, from the Oligocene onward phases of enhanced DWBC flow generally correspond to marked climatic coolings. Increased biopelagic productivity and foraminiferal census counts also demonstrate the existence of early Pliocene climatic warming, albeit followed by further cooling at ~4 Ma. After 4 Ma, all proxy indicators reveal short-period, often Milankovitch-scale, alternations of warmer and colder climate, though only small parts of the record have yet been examined in detail (e.g., Hall et al., 2002, 2003; Sabaa et al., in press; Scott and Hall, in press). Oxygen isotope results suggest that significant surface cooling affected nearshore ENZOSS waters over the last 0.7 m.y. (Site 1119) (Carter, R., unpubl. data), consistent with the intensified winnowing reported for this period for intermediate-depth waters on Lord Howe Rise by Kennett and von der Borch (1986). However, the average peak glacial and interglacial temperatures of oceanic surface waters over the same time interval remained essentially unchanged (Site 1123) (Hall et al., 2001).

Regarding the initiation of oceanic frontal zones in the southwest Pacific, we agree with earlier writers that the number of drill sites available is insufficient to tightly constrain the origins of the STF and SAF. Murphy and Kennett (1986) argued from an analysis of the Eocene–early Oligocene isotope records at Leg 29 Site 277 and Leg 90 Sites 592 and 593 that no frontal structure can have lain between these sites prior to the Oligocene. They inferred from diverging intermediate and surface water isotope records between Site 277 and sites farther north that, after ~33 Ma, intermediate water flows had commenced as part of the enhancement of the latitudinal thermal gradients that eventually led to the formation of the STF and SAF. However, Murphy and Kennett (1986, p. 1359) also noted that “... biogeographic similarities in calcareous microfossils suggest that the Subtropical Convergence (= STF) had

not yet formed by the end of the Paleogene” and that “biostratigraphic evidence suggests formation of this convergence in the middle Miocene.” In contrast, Kamp et al. (1990), Hornibrook (1992), and Buening et al. (1998) used shallow-marine faunal distributions and isotope data to infer that a proto-STF had already developed off Southern Australia and eastern South Island by the early Oligocene and Nelson and Cooke (2001) recently argued for the existence of this front since the latest Eocene. Any such early-established front would have initially marked a simple separation between increasingly cold circumpolar water and the major warm tropical-subtropical gyre water, and its modern descendant may therefore be the more northerly Tasman Front that separates warm from cool subtropical water (20°C summer isotherm) rather than the later-developing STF (15°C summer isotherm).

Data from Leg 181 and other available data do not closely constrain the time of formation of either the STF or the SAF in the southwest Pacific but are consistent with the formation of the AAPF in the early Oligocene and the STF and SAF some time between the early Oligocene and the early Miocene. Relevant information includes

1. Oligocene and younger shallow and intermediate-depth sediment drifts occur throughout eastern New Zealand, changing from carbonate facies in the late Oligocene to terrigenous facies in the early Miocene (Carter, R., 1985; Carter, R., et al., 1996). Drilling at Site 1119 confirmed the Pliocene–Pleistocene age of the upper part of the terrigenous drift succession, which shows a consistent (seismic) drift facies back to the early Miocene. We infer that the subduction of AAIW water at the ancestral AAPF was occurring from at least the early Miocene, after which time its northward passage caused the deposition of the Canterbury terrigenous drifts (cf. Fulthorpe and Carter, R., 1991; Lu et al., 2003).
2. Flower and Kennett (1993, 1994) used isotope data to infer that Tethyan-sourced warm, saline deep water was competing with cold southern-sourced deep water between ~16 and 14.9 Ma in the southwest Pacific, just prior to the major increase in oxygen isotope values that represents Antarctic ice sheet growth from 14.5 to 14.1 Ma. Leg 181 data, which come from rather more southerly sites, are consistent with a fluctuating but continuing southern source through the middle and late Miocene (e.g. Fig. F21A). However, bolboforms, which are reliable cold-water indicators and may also specifically mark the presence of AAIW, first appear at Site 1123 at ~13 Ma and have a regular presence after 11.7 Ma (Crundwell, in press) (cf. Fig. F12). Leg 90 Site 593 in the Tasman Sea contains a similar bolboform stratigraphy and also exhibits a slightly older (15–18 Ma) condensed and oxygenated “orange interval,” which Kennett and von der Borch (1985) and Nelson (1986) interpreted as marking the start of northward-flowing AAIW in the Tasman. Site 1120 on the Campbell Plateau contains a small hiatus at this time (16.7–15.8 Ma). These various events may mark the site-specific strengthening of a general regional increase in AAIW flow strengths, and AAPF frontal structure, during the middle Miocene.
3. Detailed census studies of foraminifers at Sites 1123 and 1124 (Hayward et al., in press) show that there are significant differences between lower bathyal faunas north and south of Chatham Rise, suggesting the presence of a proto-STF in eastern

New Zealand since at least the early Miocene. Major microfaunal changes also occur between ~5.0 and 6.5 Ma (cf. Fig. F14), when the planktonic foraminiferal fragmentation index shows a marked decline at Site 1123 and benthic foraminiferal assemblages at both sites show a marked shift of key species. Hayward et al. interpret these changes as marking a deepening of the CCD, a decrease in dissolution, a decrease in water oxygen content, and an increase in food supply; all these features are consistent with a latest Miocene restructuring of water masses into essentially the modern system (Kennett and von der Borch, 1985; Nelson and Cooke, 2001), after which both the SAF and STF were strong and permanent frontal features.

4. Detailed isotope and MAR studies at Site 1125 (Grant and Dickens, 2003) have demonstrated the presence there of a strong late Miocene–Pliocene “biogenic bloom” starting at ~5.8 Ma, consistent with the initiation of strong frontal (STF) structure at that time; a biogenic bloom of similar age, the “Chron 6 carbon shift,” is widespread in the world ocean (Haq et al., 1980; Kennett and von der Borch, 1985; Hodell and Kennett, 1986; Wei, 1998; Dickens and Owen, 1999; Grant and Dickens, 2003), consistent with the ocean restructuring and the global strengthening of frontal zones at that time.
5. After a period of steady middle–late Miocene nannofossil ooze accumulation, the Site 1120 record displays a major paraconformity at 1.9–5.6 Ma, above which occurs only 12 m of Pleistocene sediment, itself punctuated by further paraconformities (Carter, R., McCave, Richter, Carter, L., et al., 1999). These features are consistent with the commencement of steady intermediate-depth cool-water flows across the Campbell Plateau from the latest Miocene onward.

We conclude that southern-sourced intermediate-depth water flows deriving from a proto-AAPF traversed the New Zealand region from the early Oligocene onward, strengthening after the climatic cooling that followed the ~16-Ma climatic optimum (cf. Flower and Kennett, 1993, 1995). Somewhat later, in the latest Miocene (~7–5 Ma), the direct antecedents of today’s SAF and STF developed, stimulated by a marked climatic deterioration (e.g., Zachos et al., 2001) and as part of the global ocean restructuring that is inferred to have occurred at that time (e.g., Wright et al., 1991).

### **Bounty, Hikurangi, and Solander Channels and Other Late Neogene Sediment Sources to the DWBC**

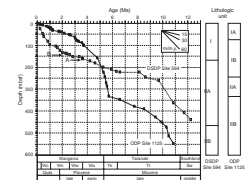
The Solander, Bounty, and Hikurangi Channels are the three main conduits through which sediment is today delivered from the New Zealand landmass into the path of the DWBC (Carter, L., et al., 1996).

The modern Bounty Channel is fed by tributary canyons and channels in the head of the Bounty Trough (Carter, R., and Carter, L., 1996), a basin that was created during the Late Cretaceous rifting of the margin (Davey, 1993). The bulk of the trough remains unfilled, despite the advance of the South Island shelf sediment prism into its western head since the early Miocene (Carter, R., and Norris, 1976). The trough center has undoubtedly been present as a marked bathymetric low since the Late Cretaceous, and evidence exists for the presence since the early Eocene of a proto-Bounty Channel in a now-filled subsidiary headward

rift (the Great South Basin) (Carter, R., and Carter, L., 1987). Nonetheless, seaward of the Late Cretaceous–Eocene shore-connected, transgressive sediment prism, the ENZOSS deep seafloor continued to receive mainly biopelagic detritus until the late Oligocene–early Miocene. Then, at ~23.4 Ma and almost simultaneously with the beginning of terrigenous regression in the South Island (Finlay, 1953; Lewis et al., 1980; Fulthorpe et al., 1996) and the inception of subduction in the North Island (Ballance, 1976; Field et al., 1997), rhythmic terrigenous–carbonate DWBC sedimentation commenced at Site 1124 (Fig. F22; also see the “[Supplementary Material](#)” contents list). The route by which the terrigenous sediment reached the DWBC is unclear, though some was undoubtedly provided from seafloor erosion along the edge of Campbell Plateau. Another possibility is that of transport through a paleo-Bounty Channel, but the presence at Site 1122 of early Pliocene contourites containing reworked diatoms from farther south suggests that a Bounty source only became significant during and after the late Pliocene.

The presence of 41-k.y.-long cycles of clay-rich and clay-poor layers throughout the post-Oligocene successions at Sites 1123 and 1124 indicates that fine-grained terrigenous sediment was continually fed into the DWBC from the late Oligocene onward. In addition, the gradual post-Oligocene enrichment of illite + chlorite at the expense of smectite at Site 1123 ([Winkler and Dullo](#), this volume) is indicative of a “steady-state” system undergoing a progressive change in provenance lithology. Such background flux to the DWBC notwithstanding, the Leg 90 Site 594 record (Dersche and Stein, 1991) shows that during the Miocene–early Pliocene the southern slopes of Chatham Rise continued to accumulate mainly biopelagic chalk, after which the record shows the same enrichment of illite + chlorite that occurs over a longer period at Site 1123. Site 594 clearly lay outside the main zone of terrigenous supply to the offshore until ~4 Ma (age model of Grant and Dickens, submitted [[N5](#)]) (Fig. F26), when terrigenous material first started to become a significant sediment component at ~170 mbsf (Kennett, von der Borch, et al., 1986). This date coincides with the start of the strong global Pliocene oxygen isotope enrichment trend (e.g., Zachos et al., 2001) and therefore probably represents lowered sea levels and the direct delivery of terrigenous material to the Bounty Trough. Consequently, overspilling turbidites may have reached Site 594 for the first time then. Sediment movement away from a Bounty Channel source would have been accentuated by the accelerated northward-flowing AAIW contour currents and STF frontal currents that developed within the Bounty gyre as climatic deterioration developed. Terrigenous sediment transported along-slope to Site 594 becomes even more marked at ~2.5 Ma (145 mbsf), above which are strong rhythms of alternating nannochalk/ooze and hemipelagic mudstone that correspond to the established Pliocene–Pleistocene climatic and oxygen isotope cycles (Nelson et al., 1985). McMinn et al. (2001) show that the 145-mbsf facies change at Site 594 corresponds to MIS 100 (~2.53 Ma) and that diatom and dinoflagellate assemblages change at that time in a way that “may reflect the fundamental reorganization of the pelagic ecosystem in response to...major climate change.” These interpretations, and the inference of latest Pliocene climatic deterioration, are consistent also with data from Site 1122, on the left-bank levee of the abyssal Bounty Fan. There, a paraconformity straddles the period of ~5.0–2.2 Ma, pointing to enhanced DWBC/ACC flow at this time. The paraconformity separates early Pliocene DWBC contourite sediments below from higher

F26. Timescales, Sites 594 and 1125, p. 108.



sedimentation–rate turbidites above, within which fan turbidites come to dominate the depositional facies from ~1.7 Ma onward.

Whereas the course of the Bounty Channel through the Neogene was largely determined by the location of the rift axis of the Bounty Trough, the location of the Hikurangi Channel was strongly influenced by the position of the axis of the Hikurangi Trough, which the headward channel course still follows (Lewis, 1994). It is likely, therefore, that a proto-Hikurangi Channel has existed along the eastern North Island margin ever since subduction commenced at ~25 Ma in the late Oligocene. Like other known trench channels, however, the terminus of the paleo-Hikurangi channel was probably “captured” by the trench (e.g., Surveyor Channel) (Ness and Kulm, 1973), to which it delivered an aggradational turbidite fill (Lewis et al., 1998). For the Hikurangi Channel to provide sediments into the DWBC as it does today requires that its path was diverted out of the trench toward the east. This is unlikely to have occurred by simple channel avulsion both because of the height of the oceanward slope up onto the Hikurangi Plateau and because Coriolis-induced turbidity current overspill, and therefore avulsion is preferentially concentrated on left channel banks in the Southern Hemisphere (e.g., Carter, L., and Carter, R., 1988; cf. Menard, 1955). Rather, Lewis (1994) and Lewis et al. (1998) show that diversion of the channel was caused by the catastrophic collapse of a large portion of the inner trench slope, which Hall et al. (2002) estimated to have occurred in the early Pleistocene, at ~1.7 Ma. The resulting Ruatoria seashide blocked the axis of the Hikurangi Trough and diverted the north-flowing Hikurangi Channel 400 km east across the Hikurangi Plateau to Rekohu Drift, which diverted it northeastward for a further 200 km to Rapuhia Scarp and into the path of the DWBC. Sediment flux records at Site 1124 (Carter, R., McCave, Richter, Carter, L., et al., 1999), on the crest of Rekohu Drift, suggest that overspilling distal turbidites from Hikurangi Channel first reached the drift at ~1.65 Ma and thereby confirm the earlier geological estimates of the timing of channel diversion from the Hikurangi Trough.

Farther south, the Solander Channel/Fan complex prograded toward the DWBC/ACC flow from about the late Miocene onward. However, it was a change in deep circulation that instigated the Solander contribution to the abyssal sediment budget, when the creation of a tectonic seaway through Macquarie Ridge in the Pliocene allowed the ACC to enter the lower Solander Trough, erode the Solander Channel/Fan complex (Schuur et al., 1998), and shift material east and north out of the basin. This eroded sediment contributed to drift deposition in the Emerald Basin (Carter, L., and McCave, 1997).

The establishment of these three major channel sediment injection points, the increased tectonic (e.g., Sutherland, 1996; Mortimer et al., 2001) and volcanic (e.g., Carter, L., et al., 2003, in press a) activity along the New Zealand plate boundary, and powerful paleoclimatic oscillations, all contributed to the major changes that occurred throughout the ENZOSS during the Pliocene–Pleistocene. The combined effect of these changes was to add a prominent terrigenous component to the previously biopelagic-dominant drift deposits of the DWBC (Hall et al., 2001, 2002; Joseph et al., in press; Handwerker and Jarrard, in press). In contrast to the older carbonate-rich Oligocene–Pliocene DWBC drifts at Sites 1123 and 1124, the Hikurangi Fan–Drift and Bounty Fan are dominantly terrigenous (McCave and Carter, L., 1997; Carter, R., McCave, Richter, Carter, L., et al., 1999; Carter, L., and McCave, 2002), though they do contain a small percentage of biopelagic material concentrated

in interglacial intervals. In the case of Bounty Fan, at least, the DWBC redistributes some of its sediment north along the DWBC path, as shown by mineralogical tracer studies (Carter, L., and Mitchell, 1987).

Despite the dominance of channel sediment supply, flux studies by Hall et al. (2002), Joseph et al. (in press), and Carter, L., et al. (2000) as well as palynological analysis of Site 1123 (Mildenhall et al., in press) show that the ENZOSS also has a number of nonchannel sediment sources. In particular, Site 1123, which is located well above the discharge depth of Bounty Channel, received pulses of sediment over the past 3 m.y. that Hall et al. (2002) relate to periodic remobilization of sediment upstream by an invigorated ACC. Site 1123 also contains water-borne pollen derived from the North Island, which perhaps indicates transport to the site via the warm, south-flowing East Cape Current (Mildenhall et al., in press), and a minor eolian component was identified also by Thiede (1979) and Stewart and Neall (1984). Finally, the increasing tectonic tempo at the New Zealand plate boundary during the Quaternary was associated with an increase in the frequency of large volcanic eruptions from the Taupo Volcanic Zone (Carter, L., et al., 2003, in press a). Such activity contributed much air fall material to northern ENZOSS, and at Site 1124 macroscopic tephra make up 6% of the late Cenozoic sequence.

### **Glacial-Interglacial Influences on Sediment Supply and Distribution**

In addition to evidence for the longer-term changes summarized above, the Leg 181 record preserves a striking record of cyclic glacial-interglacial change in the ENZOSS area for the last ~2.6 m.y. and of parallel 41-k.y.-modulated cold-warm climate cycles back to the late Oligocene (cf. see the [“Supplementary Material”](#) contents list).

During late Cenozoic glacial lowstands, the seaward extension of New Zealand river mouths to feed directly into the heads of canyons and submarine channels introduced a flush of sediments to ENZOSS fans and drifts. Not surprisingly, therefore, glacial sediment fluxes can exceed interglacial counterparts by factors of 2–3 (e.g., Lean and McCave, 1998; Carter, L., et al., 2000; Hall et al., 2001). In addition, the glacial ENZOSS received more eolian detritus under the strong winds of the times (e.g., Stewart and Neall, 1984), more hemipelagic detritus under an enhanced wind-forced surface circulation, and possibly even more volcanic ash. All this sediment interacted with an invigorated glacial DWBC/ACC. Accordingly, sortable silt (Hall et al., 2001) and Antarctic diatoms, including reworked forms (Stickley et al., 2001), increased in abundance, whereas calcium carbonate content decreased because of both reduced productivity and corrosion under the expanding and accelerating Antarctic bottom waters (Hall et al., 2001). In contrast, interglacial sediment intervals record a reduction of terrigenous input and a reversal of the other factors listed above.

Detailed glacial-interglacial studies completed to date have been based mainly on the Site 1119 and 1123 records. The upper part of Site 1119 contains an expanded succession of the last ~250 k.y. (MIS 1–7), which confirms that topographic steering was a controlling influence on the location of the STF in the late Pleistocene and shows that strong along-front current flows were developed during glacial periods (Carter, R., et al., in press). Studies of the orbital sedimentary signal at Site 1123 show that the strength of DWBC flow also varied through time, with

stronger flows during glacial periods back to 1.2 Ma (Hall et al., 2001). An alternating flow pattern applies between warm and cold period cycles in the early middle Miocene at Site 1123, which also contains a clear record of longer-term (>41 k.y.) changes in DWBC flow strength (Hall et al., 2003). Undoubtedly, more research will be accomplished in the future on specific aspects of glacial–interglacial cycling in the Leg 181 cores.

## TEN PRINCIPAL CONCLUSIONS: SUMMARY OF ODP LEG 181

The results of Leg 181 demonstrate well the synergy that results from placing offshore paleoceanographic research within a well-understood onshore–offshore basinal context. The New Zealand region, set within the mid-latitudes (~35°–55°S) of the Southern Hemisphere, possesses an outstandingly complete and well-studied onland Late Cretaceous–Cenozoic stratigraphic succession. The surrounding marine realm comprises subtropical to polar surface water masses and their separating SAF and STF frontal systems. At depth, the cold, powerful, north-traveling Pacific DWBC passes along the submerged eastern edge of the microcontinent. All major changes in global climate during the last half of the Cenozoic have been reflected in—and in some instances caused, buffered, or reinforced by—concomitant changes in these major Southern Ocean oceanographic features. Of special significance are those changes that were associated with the early Oligocene start of the thermohaline circulation system and the subsequent global climatic deterioration into the late Cenozoic ice ages.

Leg 181 set out (1) to improve our knowledge of the timing of the establishment and evolution of a major segment of the ocean thermohaline circulation system and (2) to provide an understanding of how different parts of the ocean system, especially the DWBC and its overlying mid-latitude frontal systems, respond to climatic cycling at Milankovitch and other periodicities. These goals were achieved, and, relating to them, we draw the following 10 principal conclusions:

1. ***Cretaceous–Paleogene Sediment Apron (Sites 1121, 1123, and 1124).*** After the initial rifting of the western margin of the South Pacific Ocean, Late Cretaceous–late Eocene radiolarian and nanofossil oozes and clays accumulated as a deepwater sediment apron along the edge of the subsiding New Zealand Plateau. Microfossil data indicate warm surface waters and both deep- and shallow-water circulation into the region may have been southward on the anticlockwise western limb of a proto-Pacific current gyre. Phases of current activity vigorous enough to cause hiatuses occurred in both the Paleocene and Eocene, and an episode of clay deposition of inferred stagnation origin occurred at ~39–37 Ma in the late middle Eocene (Site 1124). By the late Eocene, nanofossil ooze (chalk) deposition was regionally pervasive.
2. ***Start of Thermohaline Circulation: Marshall Paraconformity (Sites 1121, 1123, and 1124).*** Rifting between Australia and Antarctica and the creation of a deepwater link between the Indian and Pacific Ocean was completed at the Eocene/Oligocene boundary (~33.7 Ma). All Southern Ocean drill sites in and east

of the Tasmanian Gateway record this event as the Marshall Paraconformity, a several million-year-long early–late Oligocene sedimentation gap across which occurs a profound change of depositional environment and style.

In both deep- and shallow-water successions, sediments above the Marshall Paraconformity are ubiquitously affected by vigorous current activity consequent upon a restructured ocean circulation. The Marshall Paraconformity represents the start of a fast, cold current around at least part of Antarctica and the production of increased volumes of cold bottom water. It also marks the start of the ENZOSS, the stratigraphy of which records a dynamic interplay between evolving oceanic hydrography, which today includes two major frontal systems, and sediments provided by biopelagic productivity and by erosion along the evolving New Zealand plate boundary.

3. ***Oligocene and Younger ACC/DWBC Erosion (Sites 1121, 1123, and 1124)***. Erosion and corrosion of the seabed dominated the first 3–10 m.y. of ACC/DWBC activity in the southwest Pacific. At Site 1121, situated beneath the highly energetic combined ACC/DWBC, strong post-Eocene erosion removed the entire late Paleocene–late Eocene top of the Paleogene sediment apron. Sediments above the Marshall Paraconformity at this site comprise only a 15.2-m-thick skin drift of abyssal clay and extensively reworked foraminiferal and quartz sand with episodic layers of small manganese nodules down to 5.40 mbsf.  $^{10}\text{Be}$  dating of the nodules and sediment matrix indicates an age of ~18 Ma at ~7 mbsf and identifies probable phases of enhanced DWBC flow at ~15–12, 10–8, and 1.5–0 Ma (Site 1121). At Site 1123, a gap of 13 m.y. (33.6–20.5 Ma) separates late Eocene–early Oligocene nannofossil chalk from the early Miocene DWBC drifts above, whereas a shorter gap of 6 m.y. (33–27 Ma) is present at Site 1124. Earliest Oligocene sediment below the Marshall Paraconformity at these two sites and at DSDP Leg 29 Site 277 suggests that the onset of seafloor erosion generally postdated the Oi-1 isotope event by up to ~2 m.y.
4. ***Late Oligocene and Younger DWBC Sediment Drifts (Sites 1123 and 1124)***. Beneath the path of the DWBC, sediments above the Marshall Paraconformity everywhere comprise abyssal biopelagic (~66% carbonate) drifts. The oldest drifts yet sampled are late Oligocene to early Miocene (~26.1–16.5 Ma) nannofossil chinks at Site 1124, which exhibit color-banded sedimentary couplets with alternately greater and lesser terrigenous clay and biosiliceous contents. These chinks and the similar ~21.0- to 0.0-Ma drift sediments at Site 1123 contain a high-resolution record of 41-k.y. Milankovitch climatic cyclicity and DWBC variability since the late Oligocene. Grain size analyses and MST logs show that throughout this succession DWBC current speeds were coupled to the climate system at 41-k.y. frequency. Longer-term trends in DWBC mean flow in the middle Miocene occur in parallel with increases in the production of intermediate-depth cold waters at sites north of New Zealand and, hence, probably reflect periods of growth of the East Antarctic Ice Sheet.

Micropaleontological studies, controlled since 4 Ma against a detailed stable isotope history and prior to that by astrochronologic tuning of physical properties and by paleomagnetic chronology, provide strong evidence for progressive climatic

deterioration after ~15 Ma, with a warm period between ~5 and 3.3 Ma in the Pliocene and notable cold punctuations (prior to the 2.5-Ma start of enhanced glacial cycles) at 10.93, 10.61, 9.62, 9.44, 7.00, 6.20, 3.37, 3.03, 2.83, and 2.70 Ma.

5. ***Neogene Fluctuations in SAMW/AAIW (Site 1120)***. At shallower depths across the submerged eastern New Zealand continental rim (Campbell Plateau) but outside the realm of terrigenous influence, slowly accumulating foraminiferal nanofossil chalks are punctuated by hiatuses at ~16.7–15.8, ~5.6–1.9, and ~0.90–0.24 Ma, indicative of strong ancestor SAMW/AAIW flows at these times.
6. ***Front Establishment, Intermediate Water Production, and Their Variation (Sites 1119 and 1125)***. Foraminiferal evidence indicates the presence of a front in the vicinity of the modern STF that curves around east of South Island and along the Chatham Rise since at least the early Miocene (~20 Ma) and a proto-STF that may have been present back to ~30 Ma. Site 1119, at 396 m water depth on the subantarctic side of the STF, records periods of seaward (southeastward) movement of the STF and strongly enhanced water flows along the front during recent glacial periods. Site 1125, at intermediate depth on the subtropical side of the STF, records a strong frontal productivity signal in the late Miocene–early Pliocene with enhanced sedimentation rates up to 13 cm/k.y. and a nutrient-enriched  $\delta^{13}\text{C}$  signature between 5.6 and 4.8 Ma that gradually returns to more typical levels by ~3 Ma.

Deeper sediments at Site 1119 contain a record of SAMW/AAIW activity back to ~3.5 Ma. Because these water masses are formed, respectively, at the SAF and AAPF, their presence indicates the presence also of these two frontal features. The base of Site 1119 lies just within the top of a thick interval of large terrigenous sediment drifts that are inferred to have been deposited from north-flowing AAIW since the early Miocene (~23 Ma). These drifts represent the intermediate-depth equivalents of the deeper-water DWBC drifts located farther east. The thickness and restricted presence of the drifts across the head of the Bounty Trough shows that vigorous northeasterly intermediate flows, sourced from a proto-AAPF, have occurred along the eastern South Island margin since the early Miocene. These flows evolved from the erosive early Oligocene and depositional late Oligocene–early Miocene DWBC-ACC, which deposited the regional Kekenodon Group greensand and carbonate drifts (cf. Fig. F24) that underlie the terrigenous Canterbury Drifts. The further climatic deterioration that occurred during the late middle Miocene (~15–12 Ma) and the late Miocene–Pliocene (~7–2.5 Ma) had the effect of strengthening the STF and AAPF, leading to the development of the SAF, probably sometime during the early–middle Miocene. In turn, the development of these fronts and changes in associated water masses caused (a) intensification of northeasterly flow along the closely spaced density gradients of the STF, which was probably locked onto the eastern South Island and Chatham Rise bathymetry from the early Miocene onward, and (b) intensification of AAIW subduction and SAMW formation at the AAPF and SAF, respectively, thus increasing the supply of intermediate water around and across the Campbell Plateau and into the Bounty gyre.

7. *Glacial–Interglacial Cycling (Sites 1119, 1123, and 1125)*. The detailed comparison of sediments between late Quaternary glacial and interglacial intervals indicates that glacial periods were characterized by (a) stronger DWBC current flows, as marked by an increased grain size of sortable silt and a higher rate of reworking of microfossils, including Antarctic diatoms; (b) nutrient-enriched  $\delta^{13}\text{C}$  values and a smaller cross-Pacific  $\delta^{13}\text{C}$  gradient, the latter consistent with enhanced formation of AABW and ventilation of CDW; (c) enhanced inputs of waterborne terrigenous sediment, eolian dust, biopelagic opal, and volcanic ash; (d) reduced biopelagic carbonate entombment, caused both by lower surface carbonate productivity and (in deeper water) by increased dissolution under cold, corrosive flow; (e) freezing cold and highly saline deep water, sourced from CDW rather than from NADW; and (f) enhanced frontal current flows along the South Island sector of the STF, as marked by the deposition of thin beds of sand in the mud-dominated, upper slope environment.

The Site 1119 gamma ray record, which is a proxy for the size of the South Island ice cap, closely matches the deuterium isotope (atmospheric temperature) profile of the Vostok polar ice core back to MIS 11 (~400 ka). This indicates the existence during climate cycling of strong intra-hemispheric coupling between Southern Hemisphere middle and high latitudes.

8. *Sediment Delivery via Submarine Channels (Sites 1122 and 1124)*. Today, terrigenous sediment is delivered into the AAIW and DWBC sediment drifts by the Solander, Bounty, and Hikurangi Channels, which in glacial times was augmented by eolian input of dust and eruptive ash. “New” terrigenous sediment first appears in both the shallow- and deepwater ENZOSS record in the latest Oligocene, at ~23.4 Ma, closely following the ~25-Ma start of uplift along the South Island alpine plate boundary. This near-coincidence of timing notwithstanding, some of the terrigenous material in the DWBC drifts is undoubtedly derived from seafloor erosion along the southern sector of the ancestral DWBC + ACC system. Outside the area of either a contemporary shore-connected sediment supply or the influence of DWBC-supplied sediment, biopelagic nannofossil ooze accumulated regionally well into the Pliocene. At ~4 Ma, coincident with the start of global  $\delta^{18}\text{O}$  enrichment and probable sea level fall, fine-grained terrigenous sediment overspilling from the eastern South Island shelf first reached DSDP Leg 90 Site 594 in the northeastern corner of the Bounty Trough, its transport probably augmented by AAIW and STF advection. At the same time, enhanced DWBC flow is indicated by the presence of a ~5.0- to 2.2-Ma paraconformity at Site 1122 at the abyssal mouth of the Bounty Trough that separates early Pliocene DWBC drifts from latest Pliocene turbidite-augmented drifts. Bounty Channel turbidite activity accelerated at ~2.4 Ma, driven by South Island mountain uplift and by enhanced glacioeustatic sea level lows. Concomitantly, Site 594 exhibits strong terrigenous–carbonate sediment rhythms that are in phase with climatic cycles, and at ~1.7 Ma the main phase of Bounty Fan accumulation commenced.

Within the Hikurangi Channel system, an increase in terrigenous sediment flux at Site 1124 suggests that right bank over-

spilling turbidites from the channel first reached Rekohu Drift in the earliest Pleistocene, at ~1.65 Ma. This date refines earlier geological estimates of the timing of diversion of the Hikurangi Channel out of the Hikurangi Trough, which became blocked then by the giant Ruatoria submarine landslide off Poverty Bay.

9. ***Plate Boundary Volcanism (Sites 1123, 1124, and 1125)***. It is established in the onland record that arc volcanism in Northland, the earliest predecessor of the Hikurangi subduction margin, commenced in the late Oligocene at ~25 Ma. Through the Neogene, the volcanic alignment migrated successively eastward to the CVZ and TVZ, the latter being Earth's most productive Quaternary rhyolitic volcanic center. The Leg 181 record of 134 tephra, individually up to 92 cm thick, provides a new and detailed history of major explosive eruptions from the CVZ and TVZ since 12 Ma. Through the late Miocene and Pliocene, macroscopic tephra layers occur grouped into intervals with concentrated ash fall separated by intervals of several hundred thousand years of quiescence or lesser activity. From ~1.6 Ma onward, explosive activity was centered in the TVZ and large eruptions were more frequent than previously known. Ash dispersal from North Island volcanoes is overwhelmingly eastward, under the influence of westerly stratospheric winds. Most tephra accumulated during glacial periods, consistent with increased eruption (unloaded magma chambers) and increased windiness (northward wind-belt migration) then.
10. ***Micropaleontological Results (Sites 1119–1125 [all])***. Leg 181 drilling yielded a wealth of new material for micropaleontological studies, especially from periods of continuous accumulation in the Pliocene–Pleistocene at Site 1119 (SAMW/AIW), early Miocene–Holocene at Site 1123 (middle CDW), late Oligocene–early Miocene at Site 1124 (lower CDW), and middle–late Paleocene at Site 1121 (lower CDW). Uniquely in the World Ocean, Site 1123 retrieved an essentially complete and richly microfossiliferous Miocene–Quaternary record of high sedimentation rate (5–30 cm/k.y.), which has been astronomically tuned and which may contain every magnetic reversal since Chron C6r at 20.5 Ma.

This stratigraphic treasure trove has already yielded major insights into the evolution and distribution of deepwater benthic foraminifers, including the first detailed delineation of the *Stilostomella* extinction crisis in the middle Pleistocene; the biochronology and cold climate implications of bolboformids and their late Miocene planktonic foraminifer companions; the phytoplankton stratigraphy of the late Quaternary and of pre-Marshall Paraconformity nannofossil chalks of late Eocene (39–37 Ma) age; short-period climatic fluctuations and water mass changes of late Miocene and younger age, based on census counts of planktonic foraminifers and MAT paleotemperature reconstructions; and the first demonstration from palynological studies of cyclic changes in terrestrial vegetation that occur almost exactly in phase with marine climatic signals.

Finally, the high-resolution stratigraphic studies accomplished using Leg 181 materials and a wide variety of techniques have contributed to a quantum improvement in the accuracy of correlation among southwest Pacific drill sites. An especially important result of this is an improved integration

between the regional New Zealand stage classification and global events and timescales. Much of the valuable information contained in publications on New Zealand geology has previously been obscured behind a screen of arcane terminology. Leg 181 results will help greatly to bring this important regional stratigraphic archive within the reach of a wider geologic public and particularly so for information regarding the post-Eocene linkages between the ENZOSS and the evolution of the global ocean circulation system.

## FUTURE INVESTIGATIONS

Drilling in the southwest Pacific Ocean remains in a state of reconnaissance. Even after the completion of Leg 181 there are still only 10 drill sites with significant sediment recovery in a region that extends from 35° to 60°S. This region is comparable in size to the North American Basin of the Atlantic, where there are >100 cored sites. Further drilling is essential for improving our state of knowledge of the history of the Southern Ocean water masses, fronts, and currents that are part of the planet's ocean circulation system. The completion of Leg 181 has made it much easier to recognize high-priority targets for future attention. We identify five such targets:

1. Cores through the ~82- to 34-Ma-old postrift sediments of the circum-New Zealand sediment apron, especially at sites around the edges of the Campbell and Hikurangi Plateaus. Our knowledge of the oceanography of the southwestern proto-Pacific Ocean remains extremely limited and at present is essentially based on only three adventitious cores (Sites 1121, 1123, and 1124).
2. The coring of complete, and preferably expanded, Oligocene–early Miocene successions (34–20 Ma). In most places, sediments of this age have been removed by erosion at the Marshall Paraconformity and the location of sections suitable for high-resolution coring studies will probably require new seismic surveys in areas of likely sediment accumulation. One suitable area is in the axis of the Great South Basin (Carter, R., 1988a, fig. 5), a now-filled tributary rift to the Bounty Trough, where an apparently continuous Oligocene biopelagic section was penetrated by petroleum exploration drilling. Related to drilling such Oligocene targets, the coring of more successions through the Marshall Paraconformity will provide important information regarding the nature of the global Eocene–Oligocene ocean reorganization.
3. “Dipstick” coring through the DWBC drifts, especially the Chatham Drift, the record of which since 20.5 Ma has been so successfully deciphered at Site 1123. Shallower core sites may avoid the diagenesis problem encountered in the lower Miocene at Site 1123. A knowledge of the changing patterns of circulation and chemistry within the different CDW levels of the DWBC requires a depth transect of both shallower and deeper sites, which could be located on existing seismic profiles. In addition, coring the Hikurangi Fan-drift would provide a high-resolution century-scale record of sediment supply/DWBC interactions throughout the Pleistocene.

4. Coring the main body of the large intermediate–water depth drifts along the Canterbury slope in the head of the Bounty Trough. Results from Site 1119 indicate that the deeper parts of these Canterbury Drifts will yield an outstanding record of the history of the STF and of the AAIW water mass and its predecessors, including the likelihood of penetrating the Marshall Paraconformity, which is known from seismic imagery to lie beneath the drifts.
5. Coring “patch drifts” (Carter, L., and McCave, 1994) on the Hikurangi Plateau, close to the volcanic sources, will allow construction of the best available record of the pulsatory magmatic activity at the North Island convergent plate boundary.

## ACKNOWLEDGMENTS

We acknowledge warmly the members of the ODP panels and particularly leg “watchdog” Larry Petersen, who in the early 1990s nurtured Drilling Proposal 441 to the point that it became Leg 181. We thank also the ship’s crew, drilling crew, and technical and scientific members of the party aboard *JOIDES Resolution* who worked so hard and expertly, often in trying and dangerous conditions, to make the cruise a success. Faced as we were with the task of summarizing the science results of the cruise, we thank our scientific colleagues for making their results so readily available to us and especially those who allowed us the privilege of reading and citing work that is still in the final stages of preparation for publication. We also thank the ODP-TAMU (Texas A&M University) editorial team, and especially Lorri Peters and Gigi Delgado for their patient help and support, and Dr. Detlef Warnke for his constructive criticisms of the draft manuscript. In addition to the shipboard science party, a number of shore-based scientists made a very significant contribution to the results of the cruise, and we thank Drs. Martin Crundwell, Ian Graham, Chris Hollis, Dallas Mildenhall, George Scott (all New Zealand Institute of Geological and Nuclear Sciences; IGNS), and Helen Neill (National Institute of Water and Atmosphere; NIWA) in this regard, and also Rupert Sutherland (IGNS) for providing the base-maps for Figure F23 and Philip Maxwell for advice on Paleocene mollusks. We thank IGNS and NIWA management for supporting the participation of their research staff and for contributing to the cost of the color plates for this volume. We are grateful also for the major support given by NIWA by their underwriting of several research cruises, including site surveys, through which Leg 181 became possible. This research used samples and data provided by the Ocean Drilling Program (ODP). The ODP is sponsored by the U.S. National Science Foundation (NSF) and participating countries under management of Joint Oceanographic Institutions (JOI), Inc. Financial support for participation in the cruise and for the research undertaken by the three authors was provided by the Australian Research Council (Grant A-39805139; R.M. Carter), the National Environment Research Council (McCave), and NIWA (L. Carter), for which we express our appreciation.

## REFERENCES

- Abbott, S.T., and Carter, R.M., 1994. The sequence architecture of mid-Pleistocene (0.35–0.95 Ma) cyclothem from New Zealand: facies development during a period of known orbital control on sea-level cyclicity. *In* de Boer, P.L., and Smith, D.G. (Eds.), *Orbital Forcing and Cyclic Sequences*, Spec. Publ. Int. Assoc. Sedimentol., 19:367–394.
- Adams, C.G., Lee, D.E., and Rosen, B.R., 1990. Conflicting isotopic and biotic evidence for tropical sea-surface temperatures during the Tertiary. *Palaeogeogr., Palaeoclimatol., Palaeoecol.*, 77:289–313.
- Adams, C.J., Graham, I.J., Seward, D., and Skinner, D.N.B., 1994. Geochronological and geochemical evolution of late Cenozoic volcanism in the Coromandel Peninsula, New Zealand. *N. Z. J. Geol. Geophys.*, 37:359–379.
- Adams, J., 1980. Contemporary uplift and erosion of the Southern Alps, New Zealand. *Geol. Soc. Am. Bull.*, 91:1–114.
- Adkins, J.F., McIntyre, K., and Schrag, D.P., 2002. The salinity, temperature and  $\delta^{18}\text{O}$  of the glacial deep ocean. *Science*, 298:1769–1773.
- Aguirre, E., and Pasini, G., 1985. The Pliocene–Pleistocene boundary. *Episodes*, 8:11–120.
- Anastas, A.S., Dalrymple, R.W., James, N.P., and Nelson, C.S., 1997. Cross-stratified calcarenites from New Zealand: subaqueous dunes in a cool-water, Oligo–Miocene seaway. *Sedimentology*, 44:869–891.
- Andersson, C., 1997. Transfer function vs. modern analog technique for estimating Pliocene sea-surface temperatures based on planktonic foraminiferal data, western equatorial Pacific Ocean. *J. Foraminiferal Res.*, 27:123–132.
- Andrews, P.B., 1973. Late Quaternary continental shelf sediments off Otago Peninsula, New Zealand. *N. Z. J. Geol. Geophys.*, 16:793–830.
- , 1977. Depositional facies and the early phase of ocean basin evolution in the circum-Antarctic region. *Mar. Geol.*, 25:1–13.
- Ayress, M., Neil, H., Passlow, V., and Swanson, K., 1997. Benthonic ostracods and deep watermasses: a qualitative comparison of southwest Pacific, Southern and Atlantic Oceans. *Palaeogeogr., Palaeoclimatol., Palaeoecol.*, 131:287–302.
- Bains, S., Norris, R.D., Corfield, R.M., and Faul, K.L., 2000. Termination of global warmth at the Palaeocene/Eocene boundary through productivity feedback. *Nature*, 407:171–174.
- Ballance, P.F. (Ed.), 1993a. *South Pacific Sedimentary Basins*, Sedimentary Basins of the World (Vol. 2): Amsterdam (Elsevier).
- Ballance, P.F., 1976. Evolution of the Upper Cenozoic magmatic arc and plate boundary in northern New Zealand. *Earth Planet. Sci. Lett.*, 28:356–370.
- , 1993b. The paleo-Pacific, post-subduction, passive margin thermal relaxation sequence (Late Cretaceous–Paleogene) of the drifting New Zealand continent. *In* Ballance, P.F. (Ed.), *South Pacific Sedimentary Basins*, Sedimentary Basins of the World (Vol. 2): Amsterdam (Elsevier), 93–110.
- Ballance, P.F., Hayward, B.W., and Brook, F.J., 1985. Matters arising: subduction regression of volcanism in New Zealand. *Nature*, 313:820.
- Ballance, P.F., and Sporli, K.B., 1979. Northland Allochthon. *J. R. Soc. N. Z.*, 9:259–275.
- Balsam, W.L., Deaton, B.C., and Damuth, J.E., 1999. Evaluating optical lightness as a proxy for carbonate content in marine sediment cores. *Mar. Geol.*, 161:141–153.
- Barker, P.F., 2001. Scotia Sea regional tectonic evolution: implications for mantle flow and palaeocirculation. *Earth Sci. Rev.*, 55:1–39.
- Barker, P.F., and Burrell, J., 1977. The opening of the Drake Passage. *Mar. Geol.*, 25:15–34.

- , 1982. The influence upon Southern Ocean circulation, sedimentation, and climate of the opening of the Drake Passage. In Craddock, C. (Ed.), *Antarctic Geoscience*: Madison (Univ. of Wisconsin), 377–385.
- Barnes, P.M., 1994. Pliocene–Pleistocene depositional units on the continental slope off central New Zealand: control by slope currents and global current cycles. *Mar. Geol.*, 117:155–175.
- Barnes, P.M., and Lewis, K.B., 1991. Sheet slides and rotational failures on a convergent margin: the Kidnappers Slide, New Zealand. *Sedimentology*, 38:205–221.
- Barrett, P.J., 1996. Antarctic paleoenvironment through Cenozoic times: a review. *Terra Antart.*, 3:103–119.
- Barron, E.J., and Peterson, W.H., 1991. The Cenozoic ocean circulation based on ocean General Circulation Model results. *Palaeogeogr., Palaeoclimatol., Palaeoecol.*, 83:1–28.
- Barron, J., Larsen, B., et al., 1989. *Proc. ODP, Init. Repts.*, 119: College Station, TX (Ocean Drilling Program).
- Barrows, S.T., Juggins, S., De Deckker, P., Thiede, J., and Martinez, J.I., 2000. Sea-surface temperatures of the southwest Pacific Ocean during the Last Glacial Maximum. *Paleoceanography*, 15:95–109.
- Batt, G.E., Braun, J., Kohn, B.P., and McDougall, I., 2000. Thermochronological analysis of the dynamics of the Southern Alps, New Zealand. *Geol. Soc. Am. Bull.*, 112:250–266.
- Begg, A.C., and Begg, N.C., 1969. *James Cook and New Zealand*: Wellington, N.Z. (Government Printer).
- Belkin, I.M., and Gordon, A.L., 1996. Southern Ocean fronts from the Greenwich meridian to Tasmania. *J. Geophys. Res.*, 101:3675–3696.
- Benson, R., 1975. The origin of the psychrosphere as recorded in changes of deep-sea ostracode assemblages. *Lethaia*, 8:69–83.
- Benson, W.N., 1969. *Geological map of Dunedin district, explanatory notes [1:50,000]*: Wellington (New Zealand DSIR).
- Berggren, W.A., and Aubry, M.-P., 1995. A revised Cenozoic calcareous plankton magnetobiochronology and chronostratigraphy. *Eos, Trans. Am. Geophys. Union*, 76:S97.
- Berggren, W.A., and Hollister, C.D., 1977. Plate tectonics and paleocirculation: commotion in the ocean. *Tectonophysics*, 38:11–48.
- Berggren, W.A., Kent, D.V., Swisher, C.C., III, and Aubry, M.-P., 1995. A revised Cenozoic geochronology and chronostratigraphy. In Berggren, W.A., Kent, D.V., Aubry, M.-P., and Hardenbol, J. (Eds.), *Geochronology, Time Scales and Global Stratigraphic Correlation*. Spec. Publ.—SEPM, 54:129–212.
- Beu, A.G., and Edwards, A.R., 1984. New Zealand Pleistocene and late Pliocene glacio-eustatic cycles. *Palaeogeogr., Palaeoclimatol., Palaeoecol.*, 46:119–142.
- Beu, A.G., and Maxwell, P.A., 1990. Cenozoic Mollusca of New Zealand. *N. Z. Geol. Surv. Bull.*, Vol. 58.
- Bishop, D.G., and Laird, M.G., 1976. Stratigraphy and depositional environment of the Kyeburn Formation (Cretaceous), a wedge of coarse terrestrial sediments in Central Otago. *J. R. Soc. N. Z.*, 6:55–71.
- Bishop, D.G., and Turnbull, I.M., 1996. *Geology of the Dunedin Area [1:250,000]*. Lower Hutt, New Zealand (Inst. Geol. Nucl. Sci.).
- Boersma, A., and Shackleton, N., 1977. Tertiary oxygen and carbon isotope stratigraphy, Site 357 (mid-latitude South Atlantic). In Supko, P.R., Perch-Nielsen, K., et al., *Init. Repts. DSDP*, 39: Washington (U.S. Govt. Printing Office), 911–924.
- Boltovskoy, E., 1980. The age of the Drake Passage. *Alcheringa*, 4:289–297.
- Böttcher, M.E., Khim, B.-K., Suzuki, A., Gehre, M., Wortmann, U.G., and Brumsack, H.-J., in press. Microbial sulfate reduction in deep sediments of the southwest Pacific (ODP Leg 181: Sites 1119–1125): evidence from stable sulfur isotope fractionation and pore water modeling. *Mar. Geol.*
- Boyle, E., 2002. Oceanic salt switch. *Science*, 298:1724–1725.

- Brodie, J.W., and Dawson, E.W., 1971. Antarctic icebergs near New Zealand. *N. Z. J. Mar. Freshwater Res.*, 5:80–85.
- Bryant, W.R., Wetzel, A., Taylor, E., and Sweet, W., 1986. Shear strength, consolidation, porosity, and permeability in oceanic sediments. In Emiliani C. (Ed.), *The Sea* (Vol. 7): New York (Wiley), 1555–1616.
- Buening, N., Carlson, S.J., Spero, H.J., and Lee, D.E., 1998. Evidence for the early Oligocene formation of a proto-subtropical convergence from oxygen isotope records of New Zealand Paleogene brachiopods. *Palaeogeogr., Palaeoclimatol., Palaeoecol.*, 138:43–68.
- Burns, D.A., 1977. Major features of oceanographic development of the southeast Indian and southwest Pacific Oceans interpreted from microfossil evidence. *Mar. Geol.*, 25:35–39.
- Burns, D.A., and Nelson, C.S., 1981. Oxygen isotope paleotemperatures across the Runangan-Whaingaroan (Eocene–Oligocene) boundary in a New Zealand shelf sequence. *N. Z. J. Geol. Geophys.*, 24:529–538.
- Burns, R.E., Andrews, J.E., et al., 1973. *Init. Repts. DSDP*, 21: Washington (U.S. Govt. Printing Office).
- Cande, S.C., and Kent, D.V., 1995. Revised calibration of the geomagnetic polarity timescale for the Late Cretaceous and Cenozoic. *J. Geophys. Res.*, 100:6093–6095.
- Cande, S.C., Raymond, C.A., Stock, J., and Haxby, W.F., 1995. Geophysics of the Pitman Fracture Zone and Pacific-Antarctic plate motions during the Cenozoic. *Science*, 270:947–953.
- Cande, S.C., Stock, J.M., Muller, R.D., and Ishihara, T., 2000. Cenozoic motion between East and West Antarctica. *Nature*, 404:145–150.
- Carter, A.N., 1978. Contrasts between oceanic and continental ‘unconformities’ in the Oligocene of the Australian region. *Nature*, 274:152–154.
- Carter, L., 1975. Sedimentation on the continental terrace around New Zealand: a review. *Mar. Geol.*, 19:209–237.
- , 1989. New occurrences of manganese nodules in the South-western Pacific Basin, east of New Zealand. *N. Z. J. Mar. Freshwater Res.*, 23:247–253.
- , 2001. A large submarine debris flow in the path of the Pacific deep western boundary current off New Zealand. *Geo-Mar. Lett.*, 21:42–40.
- Carter, L., Alloway, B.V., Shane, P., and Westgate, J., in press a. Deep ocean records of major rhyolitic eruptions and dispersal from the Coromandel and Taupo Volcanic Zones of New Zealand. *N. Z. J. Geol. Geophys.*, 46.
- Carter, L., and Carter, R.M., 1986. Holocene evolution of the nearshore sand wedge, South Otago continental shelf, New Zealand. *N. Z. J. Geol. Geophys.*, 29:413–424.
- , 1988. Late Quaternary development of left bank dominant levees in the Bounty Trough, New Zealand. *Mar. Geol.*, 78:185–197.
- , 1990. Lacustrine sediment traps and their effect on continental shelf sedimentation - South Island, New Zealand. *Geo-Mar. Lett.*, 10:93–100.
- , 1993. Sedimentary evolution of the Bounty Trough: a Cretaceous rift basin, southwestern Pacific Ocean. In Ballance, P.F. (Ed.), *South Pacific Sedimentary Basins, Sedimentary Basins of the World* (Vol. 2): Amsterdam (Elsevier), 51–67.
- Carter, L., Carter, R.M., and Griggs, G.B., 1982. Sedimentation in the Conway Trough, a deep near-shore basin at the junction of the Alpine transform and Hikurangi subduction plate boundary, New Zealand. *Sedimentology*, 29:475–497.
- Carter, L., Carter, R.M., and McCave, I.N., in press b. Evolution of the sedimentary system beneath the deep Pacific inflow off eastern New Zealand. *Mar. Geol.*
- Carter, L., Carter, R.M., McCave, I.N., and Gamble, J., 1996. Regional sediment recycling in the abyssal Southwest Pacific Ocean. *Geology*, 24:735–738.
- Carter, L., Carter, R.M., McCave, I.N., and the Shipboard Scientific Party, 1999. You don’t know what’s there until you drill: initial results from Leg 181—SW Pacific Gateway. *Water Atmos.*, 7:14–16.

- , 2002. Case studies 101–103, eastern New Zealand drifts: Miocene to Recent. In Stow, D., Pudsey, C.J., Howe, J.A., Faugeres, J.C., and Viana, A.R. (Eds.), *Atlas of Deep Water Contourite Systems*. Geol. Soc. Spec. Publ., 22:385–408.
- Carter, L., Carter, R.M., Nelson, C.S., Fulthorpe, C.S., and Neil, H.L., 1990. Evolution of Pliocene to Recent abyssal sediment waves on Bounty Channel levees, New Zealand. *Mar. Geol.*, 95:97–109.
- Carter, L., and Herzer, R.H., 1979. The hydraulic regime and its potential to transport sediment on the Canterbury continental shelf. *Mem.— N. Z. Oceanogr. Inst.*, 83:1–33.
- Carter, L., Manighetti, B., Elliot, M., Trustrum, N., and Gomez, B., 2002a. Source, sea level and circulation effects on the sediment flux to the deep ocean over the past 15 ka off eastern New Zealand. *Global Planet. Change*, 33:339–355.
- Carter, L., and McCave, I.N., 1994. Development of sediment drifts approaching an active plate margin under the SW Pacific deep western boundary current. *Paleoceanography*, 9:1061–1085.
- , 1997. The sedimentary regime beneath the deep western boundary current inflow to the Southwest Pacific Ocean. *J. Sediment. Res.*, 67:1005–1017.
- Carter, L., and Mitchell, J.S., 1987. Late Quaternary sediment pathways through the deep ocean, east of New Zealand. *Paleoceanography*, 2:409–422.
- Carter, L., Neil, H.L., and McCave, I.N., 2000. Glacial to interglacial changes in non-carbonate and carbonate accumulation in the SW Pacific Ocean, New Zealand. *Palaeogeogr., Palaeoclimatol., Palaeoecol.*, 162:333–356.
- Carter, L., Neil, H.L., and Northcote, L., 2002b. Late Quaternary ice rafting events in the SW Pacific Ocean, off eastern New Zealand. *Mar. Geol.*, 191:19–35.
- Carter, L., Nelson, C.S., Neil, H.L., and Froggatt, P.C., 1995. Correlation, dispersal, and preservation of the Kawakawa Tephra and other late Quaternary tephra layers in the Southwest Pacific Ocean. *N. Z. J. Geol. Geophys.*, 38:29–46.
- Carter, L., Shane, P., Alloway, B., Hall, I.R., and Harris, S., 2003. Demise of one volcanic zone and birth of another—a 12 Ma deep-ocean record of major rhyolitic eruptions from New Zealand. *Geology*, 31:493–496.
- Carter, L., and Wilkin, J., 1999. Abyssal circulation around New Zealand—a comparison between observations and a global circulation model. *Mar. Geol.*, 159:221–239.
- Carter, R.M., 1985. The mid-Oligocene Marshall Paraconformity, New Zealand: coincidence with global eustatic sea-level fall or rise? *J. Geol.*, 93:359–371.
- , 1988a. Plate boundary tectonics, global sea-level changes and the development of the Eastern South Island Continental Margin, New Zealand, Southwest Pacific. *Mar. Pet. Geol.*, 5:90–107.
- , 1988b. Post-breakup stratigraphy of the Kaikoura Synthem (Cretaceous–Cenozoic), continental margin, southeastern New Zealand. *N. Z. J. Geol. Geophys.*, 31:405–429.
- Carter, R.M., Abbott, S.T., Fulthorpe, C.S., Haywick, D.W., and Henderson, R.A., 1991. Application of global sea-level and sequence stratigraphic models in Southern Hemisphere Neogene strata from New Zealand. In McDonald, D.I.M. (Ed.), *Sedimentation, Tectonics and Eustasy*. Spec. Publ. Int. Assoc. Sedimentol., 12:41–65.
- Carter, R.M., and Carter, L., 1987. The Bounty Channel system: a 55-million-year-old sediment conduit to the deep sea, Southwest Pacific Ocean. *Geo-Mar. Lett.*, 7:183–190.
- , 1992. Seismic imaging of Pleistocene deep-sea cyclothem: implications for sequence stratigraphy. *Terra Nova*, 4:682–692.
- , 1996. The abyssal Bounty Fan and lower Bounty Channel: evolution of a rifted-margin sedimentary system. *Mar. Geol.*, 130:182–202.
- Carter, R.M., Carter, L., and Davy, B., 1994. Geologic and stratigraphic history of the Bounty Trough, southwestern Pacific Ocean. *Mar. Petrol. Geol.*, 11:79–93.
- Carter, R.M., Carter, L., and McCave, I.N., 1996. Current controlled sediment deposition from the shelf to the deep ocean: the Cenozoic evolution of circulation through the SW Pacific gateway. *Geol. Rundsch.*, 85:438–451.

- Carter, R.M., Carter, L., Williams, J.J., and Landis, C.A., 1985. Modern and relict sedimentation on the South Otago continental shelf, New Zealand. *Mem. N. Z. Oceanogr. Inst.*, 93.
- Carter, R.M., Fulthorpe, C.S., and Naish, T.R., 1998. Sequence concepts at seismic and outcrop scale: the distinction between physical and conceptual stratigraphic surfaces. In Carter, R.M., Naish, T.R., Ito, M., and Pillans, B.J. (Eds.), *Sequence Stratigraphy in the Plio–Pleistocene: An Evaluation*. *Sediment. Geol., Spec. Issue*, 122:165–179.
- Carter, R.M., Gammon, P.R., and Millwood, L., in press. Glacial–interglacial (MIS 1–10) migrations of the Subtropical Front across ODP Site 1119, Canterbury Bight, southwest Pacific Ocean. *Mar. Geol.*
- Carter, R.M., and Landis, C.A., 1972. Correlative Oligocene unconformities in southern Australasia. *Nature*, 237:12–13.
- Carter, R.M., Landis, C.A., Norris, R.J., and Bishop, D.G., 1974. Suggestions towards a high-level nomenclature for New Zealand rocks. *J. R. Soc. N. Z.*, 4:5–18.
- Carter, R.M., Linquist, J.K., and Norris, R.J., 1982. Oligocene unconformities and nodular phosphate hard ground horizons in western Southland and northern West coast. *J. R. Soc. N. Z.*, 12:11–46.
- Carter, R.M., McCave, I.N., Richter, C., Carter, L., et al., 1999. *Proc. ODP, Init. Repts.*, 181 [CD-ROM]. Available from: Ocean Drilling Program, Texas A&M University, College Station, TX 77845-9547, U.S.A.
- Carter, R.M., and Naish, T.R., 1998. Have local stages outlived their usefulness for the New Zealand Pliocene–Pleistocene? *N. Z. J. Geol. Geophys.*, 41:271–279.
- Carter, R.M., and Norris, R.J., 1976. Cainozoic history of southern New Zealand: an accord between geological observations and plate-tectonic predictions. *Earth Planet. Sci. Lett.*, 31:85–94.
- Chang, K.H., 1975. Unconformity-bounded stratigraphic units. *Geol. Soc. Am. Bull.*, 86:1544–1552.
- Chiswell, S.M., 1994. Variability in sea surface temperature around New Zealand from AVHRR images. *N. Z. J. Mar. Freshwater Res.*, 28:179–192.
- Ciesielski, P.F., and Wise, S.W., 1977. Geologic history of the Maurice Ewing Bank of the Falkland Plateau (southwest Atlantic sector of the Southern Ocean) based on piston and drill cores. *Mar. Geol.*, 25:175–207.
- Cifelli, R., 1969. Radiation of Cenozoic planktonic foraminifera. *Syst. Zool.*, 18:154–168.
- Cita, M.B., 1975. The Miocene/Pliocene boundary: history and definition. In Saito, T., and Burckle, L.H. (Eds.), *Late Neogene Epoch Boundaries*. *Spec. Publ.—Micropaleontol.*, 1–30.
- Clement, A.C., Cane, M.A., and Seager, R., 2001. An orbitally driven tropical source for abrupt climate change. *J. Clim.*, 14:2369–2375.
- Collins, L.S., Coates, A.G., Berggren, W.A., Aubry, M.-P., and Zhang, J., 1996. The late Miocene Panama isthmian strait. *Geology*, 24:687–690.
- Collot, J.-Y., Lewis, K., Lamarache, G., and Lallemand, S., 2001. The giant Ruatoria debris avalanche on the northern Hikurangi margin, New Zealand; result of oblique seamount subduction. *J. Geophys. Res.*, 106:19271–19297.
- Cooke, P.J., Nelson, C.S., Crundwell, M.P., and Spiegler, D., 2002. *Bolboforma* as monitors of Cenozoic palaeoceanographic changes in the Southern Ocean. *Palaeogeogr., Palaeoclimatol., Palaeoecol.*, 188:73–100.
- Cotton, C.A., 1954. Notocenoic: the New Zealand Cretaceous–Tertiary. *N. Z. Sci. Rev.*, 12:105–112.
- , 1955. Review of the Notocenoic, or Cretaceous–Tertiary of New Zealand. *Trans. R. Soc. N. Z.*, 82:1071–1122.
- Crouch, E.M., Heilmann-Clausen, C., Brinkhuis, H., Morgans, H.E.G., Rogers, K.M., Egger, H., and Schmitz, B., 2001. Global dinoflagellate event associated with the Late Paleocene Thermal Maximum. *Geology*, 29:315–318.
- Crowell, J.C., and Frakes, L.A., 1970. Phanerozoic glaciation and the causes of ice ages. *Am. J. Sci.*, 268:193–224.

- Crundwell, M.P., in press. A magnetostratigraphically constrained chronology for late Miocene bolboforms and planktic foraminifers in the temperate southwest Pacific. *Micropaleontology*.
- Cullen, D.J., 1965. Autochthonous rocks from the Chatham Rise, east of New Zealand. *N. Z. J. Geol. Geophys.*, 8:465–474.
- , 1980. Distribution, composition and age of submarine phosphorites on Chatham Rise, east of New Zealand. *Spec. Publ.—Soc. Econ. Paleontol. Mineral.*, 29:139–148.
- Cutten, H.N.C., 1979. Rappahannock Group: late Cenozoic sedimentation and tectonics contemporaneous with Alpine Fault movement. *N. Z. J. Geol. Geophys.*, 22:535–553.
- Davey, B.W., 1993. The Bounty Trough—basement structure influences on sedimentary basin evolution. In Ballance, P.F. (Ed.), *South Pacific Sedimentary Basins, Sedimentary Basins of the World (Vol. 2)*: Amsterdam (Elsevier), 69–92.
- Davey, F.J., 1977. Marine seismic measurements in the New Zealand region. *N. Z. J. Geol. Geophys.*, 20:719–777.
- DeConto, R.M., and Pollard, D., 2003. Rapid Cenozoic glaciation of Antarctica induced by declining atmospheric CO<sub>2</sub>. *Nature*, 421:245–249.
- Delteil, J., Morgans, H.E.G., Raine, J.I., Field, B.D., and Cutten, H.N.C., 1996. Early Miocene thin-skinned tectonics and wrench faulting in the Pongaroa district, Hikurangi margin, North Island, New Zealand. *N. Z. J. Geol. Geophys.*, 39:271–282.
- Dersch, M., and Stein, R., 1991. Paläoklima und paläoozeanische Verhältnisse im SW-Pazifik während der letzten 6 Mill. Jahre (DSDP-Site 594, Chatham Rücken, Östlich Neuseeland). *Geol. Rundsch.*, 80:535–556.
- Devereux, I., 1967. Oxygen isotope palaeotemperatures on New Zealand Tertiary fossils. *N. Z. J. Sci.*, 10:988–1011.
- Dickens, G.R., and Owen, R.M., 1999. The latest Miocene–early Pliocene biogenic bloom: a revised Indian Ocean perspective. *Mar. Geol.*, 161:75–91.
- Diester-Haass, L., Robert, C., and Chamley, H., 1993. Paleooceanographic and paleoclimatic evolution of the Wedell Sea (Antarctica) during the middle Eocene–late Oligocene, from coarse sediment fraction and clay mineral data (ODP Site 689). *Mar. Geol.*, 114:233–250.
- Diester-Haass, L., and Zahn, R., 1996. Eocene–Oligocene transition in the Southern Ocean: history of water mass circulation and biological productivity. *Geology*, 24:163–166.
- Dowsett, H.J., Barron, J., and Poore, R., 1996. Middle Pliocene sea surface temperatures: a global reconstruction. *Mar. Micropaleontol.*, 27:13–15.
- Dudley, W.C., and Nelson, C.S., 1988. The  $\delta^{13}\text{C}$  content of calcareous nannofossils as an indicator of Quaternary productivity in the southwest Pacific region (Note). *N. Z. J. Geol. Geophys.*, 31:111–116.
- Dudley, W.C., and Nelson, C.S., 1989. Quaternary surface-water stable isotope signal from calcareous nannofossils at DSDP Site 593, southern Tasman Sea. *Mar. Micropaleontol.*, 13:353–373.
- Eagles, G., and Livermore, R.A., 2002. Opening history of Powell Basin, Antarctic Peninsula. *Mar. Geol.*, 185:195–205.
- Edwards, A.R., 1973. Southwest Pacific regional unconformities encountered during Leg 21. In Burns, R.E., Andrews, J.E., et al., *Init. Repts. DSDP*, 21: Washington (U.S. Govt. Printing Office), 701–720.
- , 1991. *The Oamaru Diatomite*. N. Z. Geol. Surv. Paleontol. Bull.
- Ewing, M., Houtz, R., and Ewing, J., 1969. South Pacific sediment distribution. *J. Geophys. Res.*, 74:2477–2493.
- Exon, N., Kennett, J., Malone, M., Brinkhuis, H., Chaproniere, G., Ennyu, A., Fothergill, P., Fuller, M., Grauer, M., Hill, P., Janecek, T., Kelly, C., Latimer, J., McGonigal, K., Nees, S., Ninnemann, U., Nuernberg, D., Pekar, S., Pellaton, C., Pfuhl, H., Robert, C., Röhl, U., Schellenberg, S., Shevenell, A., Stickley, C., Suzuki, N., Touchard, Y., Wei, W., and White, T., 2002. Drilling reveals climatic conse-

- quences of Tasmanian Gateway opening. *Eos, Trans. Am. Geophys. Union*, 83:253, 258–259.
- Exon, N.F., Kennett, J.P., Malone, M., et al., 2001. *Proc. ODP, Init. Repts.*, 189 [CD-ROM]. Available from: Ocean Drilling Program, Texas A&M University, College Station TX 77845-9547, USA.
- Fenner, J., Carter, L., and Stewart, R., 1992. Late Quaternary paleoclimatic and paleoceanographic change over northern Chatham Rise, New Zealand. *Mar. Geol.*, 108:383–404.
- Fenner, J., and Di Stefano, A., in press. Oceanic fronts along Chatham Rise indicated by phytoplankton assemblages and refined calcareous nannofossil stratigraphy of the mid-latitude SW Pacific. *Mar. Geol.*
- Field, B.D., and Browne, G.H., 1989. *Cretaceous and Cenozoic Sedimentary Basins and Geological Evolution of Canterbury Region, South Island, New Zealand*. N. Z. Geol. Surv., Basin Stud., 2.
- Field, B.D., Uruski, C.I., Bey, A., Browne, G., Crampton, J., Funnell, R., Killips, S., Laird, M., Mazengarb, C., Morgans, H., Rait, G., Smale, D., and Strong, P., 1997. *Cretaceous–Cenozoic Geology and Petroleum Systems of the East Coast Region, New Zealand*. Inst. Geol. Nucl. Sci., Geol. Monogr., Vol. 19.
- Findlay, C.S., and Giraudeau, J., 2002. Movement of oceanic fronts south of Australia during the last 10 ka: interpretation of calcareous nannoplankton in surface sediments from the Southern Ocean. *Mar. Micropaleontol.*, 893:1–14.
- Finlay, H.J., 1925. Some modern conceptions applied to the study of the Cainozoic Mollusca of New Zealand. *Verh. K. Ned. Geol. Mijnbouwkd. Genoot., Geol. Ser.*, VIII:161–172.
- , 1953. The geology of the Geraldine Subdivision, S102 sheet district, Appendix II—Foraminifera. *N. Z. Geol. Surv. Bull.*, 50:47–51.
- Finlay, H.J., and Marwick, J., 1940. The divisions of the Upper Cretaceous and Tertiary of New Zealand. *Trans. R. Soc. N. Z.*, 70:77–135.
- Fleming, C.A., 1953. The geology of the Wanganui Subdivision, Waverley and Wanganui sheet districts (N137 and N138). *N. Z. Geol. Surv. Bull.*, 52:1–362.
- , 1962. New Zealand biogeography: a paleontologist's approach. *Tuatara*, 10:53–108.
- , 1975. The geological history of New Zealand and its biota. In Kuschel, G. (Ed.), *Biogeography and Ecology in New Zealand: The Hague* (W. Junk), 1–86.
- Flower, B.P., and Kennett, J.P., 1993. Middle Miocene ocean/climate transition: high-resolution oxygen and carbon isotopic records from DSDP Site 588A, Southwest Pacific. *Paleoceanography*, 8:811–843.
- , 1994. The middle Miocene climatic transition: East Antarctic Ice Sheet development, deep ocean circulation, and global carbon cycling. *Palaeogeogr., Palaeoclimatol., Palaeoecol.*, 108:537–555.
- , 1995. Middle Miocene deepwater paleoceanography in the southwest Pacific: relations with East Antarctic Ice Sheet development. *Paleoceanography*, 10:1095–1112.
- Fordyce, R.E., 1977. The development of the circum-Antarctic current and the evolution of the Mysticeti (Mammalia: Cetacea). *Palaeogeogr., Palaeoclimatol., Palaeoecol.*, 21:265–271.
- , 1981. Whale evolution and Oligocene Southern Ocean environments. *Palaeogeogr., Palaeoclimatol., Palaeoecol.*, 31:319–336.
- Foster, G., and Carter, L., 1997. Mud sedimentation on the continental shelf at an accretionary margin—Poverty Bay, New Zealand. *N. Z. J. Geol. Geophys.*, 40:157–173.
- Foster, R.J., 1974. Eocene echinoids and the Drake Passage. *Nature*, 249:75.
- Frakes, L.A., 1979. *Climate throughout Geological Time*: New York (Elsevier).
- Froggatt, P.C., Nelson, C.S., Carter, L., Griggs, G., and Black, K.P., 1986. An exceptionally large late Quaternary eruption from New Zealand. *Nature*, 319:578–582.
- Fulthorpe, C.S., and Carter, R.M., 1991. Continental-shelf progradation by sediment-drift accretion. *Geol. Soc. Am. Bull.*, 103:300–309.

- Fulthorpe, C.S., Carter, R.M., Miller, K.G., and Wilson, J. 1996. The Marshall Paraconformity: a mid-Oligocene record of inception of the Antarctic circumpolar current and coeval glacio-eustatic lowstand. *Mar. Pet. Geol.*, 13:61–77.
- Gair, H.S., 1959. The Tertiary geology of the Pareora district, south Canterbury. *N. Z. J. Geol. Geophys.*, 2:265–296.
- Gardner, J.V., Nelson, C.S., and Baker, P.A., 1986. Distribution and character of pale green laminae in sediment from Lord Howe Rise: a probable late Neogene and Quaternary tephrostratigraphic record. In Kennett, J.P., von der Borch, C.C., et al., *Init. Repts. DSDP*, 90 (Pt. 2): Washington (U.S. Govt. Printing Office), 1145–1159.
- Gibb, J.G., 1979. Aspects of beach sediments and their transport along the New Zealand coast. *Workshop on Physical Aspects of Coastal Problems*, Ministry of Works and Development, Hamilton, Oct. 11–12.
- Gibb, J.G., and Adams, J., 1982. A sediment budget for the east coast between Oamaru and Banks Peninsula, South Island, New Zealand. *N. Z. J. Geol. Geophys.*, 25:335–352.
- Gill, A.E., and Bryan, K., 1971. Effects of geometry on the circulation of a three-dimensional Southern Hemisphere ocean model. *Deep-Sea Res.*, 18:685–721.
- Glasby, G.P., 1990. *Antarctic Sector of the Pacific*: Amsterdam (Elsevier).
- Graham, I.J., Carter, R.M., Ditchburn, R.G., and Zondervan, A., in press. Chronostratigraphy of ODP 181, Site 1121 sediment core (SW Pacific Ocean) using  $^{10}\text{Be}/^{9}\text{Be}$  dating of entrapped ferromanganese nodules. *Mar. Geol.*
- Graham, I.J., Morgans, H.E., Waghorn, D.B., Trotter, J.A., and Whitford, D.A., 2000. Strontium isotope stratigraphy of the Oligocene–Miocene Otekaike Limestone (Trig Z section) in southern New Zealand: age of the Duntroonian/Waitakian boundary. *N. Z. J. Geol. Geophys.*, 43:335–347.
- Grant, K.M., and Dickens, G.R., 2003. Coupled productivity and carbon isotope records in the southwest Pacific Ocean during the late Miocene–early Pliocene bloom. *Palaeogeogr., Palaeoclimatol., Palaeoecol.*, 187:61–82.
- Griffiths, G.A., and Glasby, G.P., 1985. Input of river-derived sediment to the New Zealand continental shelf: I. *Mass. Estuar. Coast. Shelf Sci.*, 21:773–787.
- Griggs, G.B., Carter, L., Kennett, J.P., and Carter, R.M., 1983. Late Quaternary marine stratigraphy southeast of New Zealand. *Geol. Soc. Am. Bull.*, 94:791–797.
- Grindley, G.W., Harrington, H.J., and Wood, B.L., 1959. The geological map of New Zealand [1:2,000,000]. *N. Z. Geol. Surv. Bull.*, 66.
- Gupta, A.K., 1993. Biostratigraphic vs. paleoceanographic importance of *Stilostomella lepidula* (Schwager) in the Indian Ocean. *Micropaleontology*, 39:47–51.
- Hall, I.R., Carter, L., and Harris, S., 2002. Major depositional events under the deep Pacific inflow. *Geology*, 30:487–490.
- Hall, I.R., McCave, I.N., Shackleton, N.J., Weedon, G.P., and Harris, S.E., 2001. Intensified deep Pacific inflow and ventilation in Pleistocene glacial times. *Nature*, 412:809–812.
- Hall, I.R., McCave, I., Zahn, N., Carter, R., Knutz, L., and Weedon, G.P., 2003. Palaeo-current reconstruction of the deep Pacific inflow during the middle Miocene: reflections of East Antarctic Ice Sheet growth. *Paleoceanography*, 18:10.1029/200PA000817.
- Hancock, H.J.L., Dickens, G.R., Strong, C.P., Hollis, C.J., and Field, B.F., 2003. Foraminiferal and carbon isotope stratigraphy through the Paleocene–Eocene transition at Dee Stream, Marlborough, New Zealand. *N. Z. J. Geol. Geophys.*, 46:1–19.
- Handwerker, D.A., and Jarrard, R.D., in press. Neogene changes in Southern Ocean sedimentation based on mass accumulation rates at four continental margins. *Paleoceanography*.
- Haq, B.U., Hardenbol, J., and Vail, P.R., 1987. Chronology of fluctuating sea levels since the Triassic. *Science*, 235:1156–1167.
- Haq, B.U., Worsley, T.R., Burckle, L.H., Douglas, R.G., Keigwin, L.D., Jr., Opdyke, N.D., Savin, S.M., Sommer, M.A., II, Vincent, E., and Woodruff, F., 1980. Late Mio-

- cene marine carbon-isotopic shift and synchronicity of some phytoplanktonic biostratigraphic events. *Geology*, 8:427–431.
- Haug, G.H., and Tiedemann, R., 1998. Effect of the formation of the Isthmus of Panama on Atlantic Ocean thermohaline circulation. *Nature*, 393:673–676.
- Haug, G.H., Tiedemann, R., Zahn, R., and Ravelo, A.C., 2001. Role of Panama uplift on oceanic freshwater balance. *Geology*, 29:207–210.
- Hayes, D., and Ringis, J., 1973. Seafloor spreading in the Tasman Sea. *Nature*, 243:454–458.
- Hayes, D.E., and Pitman, W.C., 1972. Review of marine geophysical observations in the Southern Ocean. In Adie, R.J. (Ed.), *Antarctic Geology and Geophysics*: Oslo (Universitetsforlaget), 725–732.
- Hayward, B.C., Carter, R., Grenfell, H.R., and Hayward, J.J., 2001. Depth distribution of Recent deep-sea benthic foraminifera east of New Zealand, and their potential for improving paleobathymetric assessments of Neogene microfaunas. *N. Z. J. Geol. Geophys.*, 44:555–587.
- Hayward, B.W., 1993. The tempestuous 10 million year life of a double arc and intra-arc basin—New Zealand's Northland Basin in the early Miocene. In Ballance, P.F. (Ed.), *South Pacific Sedimentary Basins*, Sedimentary Basins of the World (Vol. 2): Amsterdam (Elsevier), 13–142.
- Hayward, B.W., 2001. Global deep-sea extinctions during the Pleistocene ice-ages. *Geology*, 29:599–602.
- , 2002. Late Pliocene to middle Pleistocene extinctions of deep-sea benthic foraminifera (“*Stilostomella* extinction”) in the Southwest Pacific. *J. Foramin. Res.*, 32:274–306.
- Hayward, B.W., Grenfell, H.R., Carter, R., and Hayward, J., in press. Benthic foraminiferal proxy evidence for the Neogene paleoceanographic history of the southwest Pacific, east of New Zealand. *Mar. Geol.*
- Hayward, B.W., Neil, H., Carter, R., Grenfell, H.R., and Hayward, J.J., 2002. Factors influencing the distribution patterns of Recent deep-sea benthic foraminifera, east of New Zealand, southwest Pacific Ocean. *Mar. Micropaleontol.*, 46:139–176.
- Haywick, D.W., Carter, R.M., and Henderson, R.A., 1992. Sedimentology of 40,000 year Milankovitch-controlled cyclothem from central Hawke's Bay, New Zealand. *Sedimentology*, 39:675–696.
- Head, P.S., and Nelson, C.S., 1994. A high-resolution oxygen isotope record for the past 6.4 million years at DSDP Site 593, Challenger Plateau, southern Tasman Sea. In van der Lingen, G.J., Swanson, K.M., and Muir, R.J. (Eds.), *Evolution of the Tasman Sea Basin*: Rotterdam (A.A. Balkema), 159–179.
- Heath, R.A., 1985. A review of the physical oceanography of the seas around New Zealand—1982. *N. Z. J. Mar. Freshwater Res.*, 19:70–124.
- Hellstrom, J., McCulloch, M., and Stone, J., 1998. A detailed 31,000-year record of climate and vegetation change, from the isotope geochemistry of two New Zealand speleothems. *Quat. Res.*, 50:167–178.
- Herzer, R.H., 1979. Submarine slides and submarine canyons on the continental slope off Canterbury, New Zealand. *N. Z. J. Geol. Geophys.*, 22:391–406.
- , 1981. Late Quaternary stratigraphy and sedimentation of the Canterbury continental shelf, New Zealand. *N. Z. Oceanogr. Inst. Mem.*, 89:1–71.
- Hesse, P.P., 1994. The record of continental dust from Australia in Tasman Sea sediments. *Quat. Sci. Rev.*, 13:257–272.
- Heusser, L.E., and Morley, J.J., 1996. Pliocene climate of Japan and environs between 4.8 and 2.8 Ma: a joint pollen and marine faunal study. *Mar. Micropaleontol.*, 27:85–106.
- Heusser, L.E., and Van de Geer, G., 1994. Direct correlation of terrestrial and marine paleoclimate records from four glacial–interglacial cycles; DSDP Site 594, Southwest Pacific. In Murray-Wallace, C.V. (Ed.), *Quaternary Marine and Terrestrial Records in Australasia: Do They Agree?* Quat. Sci. Rev., 13:273–282.

- Hiramatsu, C., and De Deckker, P., 1997. The calcareous nannoplankton assemblages of surface sediments in the Tasman and Coral Seas. *Palaeogeogr., Palaeoclimatol., Palaeoecol.*, 131:257–285.
- Hodell, D.A., and Kennett, J.P., 1986. Late Miocene–Early Pliocene stratigraphy and paleoceanography of the South Atlantic and southwest Pacific Oceans: a synthesis. *Paleoceanography*, 1:285–311.
- Hollis, C.J., 2002. Biostratigraphy and paleoceanographic significance of Paleocene radiolarians from offshore eastern New Zealand. *Mar. Micropaleontol.*, 46:265–316.
- Hollis, C.J. (Ed.), 2003. Profiling mass extinction—the Cretaceous/Tertiary boundary event in New Zealand from swamp to deep ocean. *N. Z. J. Geol. Geophys.*, 46:153–321.
- Hollis, C.J., Rodgers, K.A., and Parker, R.J., 1995. Siliceous plankton bloom in the earliest Tertiary of Marlborough, New Zealand. *Geology*, 23:835–838.
- Hornibrook, N. de B., 1966. The stratigraphy of Landon (or Boundary) Creek, Oamaru. *N. Z. J. Geol. Geophys.*, 9:458–470.
- , 1980. Correlation of Pliocene biostratigraphy, magnetostratigraphy and O<sup>18</sup> fluctuations in New Zealand and DSDP Site 284. *Newslett. Stratig.*, 9:114–120.
- , 1981. *Globorotalia* (planktic Foraminiferida) in the Late Pliocene and early Pleistocene of New Zealand, *N. Z. J. Geol. Geophys.*, 24:263–292.
- , 1982. Late Miocene to Pleistocene *Globorotalia* (Foraminiferida) from DSDP Leg 29, Site 284, southwest Pacific. *N. Z. J. Geol. Geophys.*, 25:83–99.
- , 1984. *Globorotalia* (planktic foraminifera) at the Miocene/Pliocene boundary in New Zealand., *Palaeogeogr., Palaeoclimatol., Palaeoecol.*, 46:107–117.
- , 1992. New Zealand Cenozoic marine paleoclimates: a review based on the distribution of some shallow water and terrestrial biota. In Tsuchi, R., and Ingle, J.C., Jr. (Eds.), *Pacific Neogene: Environment, Evolution, and Events*: Tokyo (Univ. of Tokyo Press), 83–106.
- Houtz, R., Ewing, J., Ewing, M., and Lonardi, A.G., 1967. Seismic reflection profiles of the New Zealand Plateau. *J. Geophys. Res.*, 72:4713–4729.
- Howard, W.R., and Prell, W.L., 1992. Late Quaternary surface circulation of the southern Indian Ocean and its relationship to orbital variations. *Paleoceanography*, 7:79–117.
- Isaac, M.J., Moore, P.R., and Joass, Y.J., 1991. Tahora Formation: the basal facies of a Late Cretaceous transgressive sequence, northeastern New Zealand. *N. Z. J. Geol. Geophys.*, 34:227–236.
- Isacks, B., Oliver, J., and Sykes, L.R., 1968. Seismology and the new global tectonics. *J. Geophys. Res.*, 73:5855–5899.
- Jenkins, D.G., 1974. Initiation of the ProtoCircum-Antarctic Current. *Nature*, 252:371–373.
- , 1993. The evolution of the Cenozoic Southern high- and mid-latitude planktonic foraminiferal faunas. In Kennett, J.P., and Warnke, D.A. (Eds.), *The Antarctic Paleoenvironment: a Perspective of Global Change*. Antarct. Res. Ser., 60:175–194.
- Joseph, L.H., Rea, D.K., and van der Pluijm, B.A., 1998. Use of grain-size and magnetic fabric analyses to distinguish among depositional environments. *Paleoceanography*, 13:291–501.
- , in press. Neogene history of the Deep Western Boundary Undercurrent at Rekohu Sediment Drift, southwest Pacific (ODP Site 1124). *Mar. Geol.*
- Journeaux, T.D., Kamp, P.J.J., and Naish, T., 1996. Middle Pliocene cyclothems, Mangaweka region, Wanganui Basin, New Zealand: a lithostratigraphic framework. *N. Z. J. Geol. Geophys.*, 39:135–149.
- Kaiho, K., Arinobu, T., Ishiwatar, R., Morgans, H.E.G., Okada, H., Takeda, N., Tazaki, K., Zhou, G., Kajiwar, Y., Matsumoto, R., Hirai, A., Niitsuma, N., and Wada, H., 1996. Latest Paleocene benthic foraminiferal extinction and environmental changes at Tawanui, New Zealand. *Paleoceanography*, 11:447–465.

- Kamp, P.J.J., Waghorn, D.B., and Nelson, C.S., 1990. Late Eocene–early Oligocene integrated isotope stratigraphy and biostratigraphy for paleoshelf sequences in southern Australia. *Palaeogeogr., Palaeoclimatol., Palaeoecol.*, 80:311–323.
- Kaneps, A.G., 1975. Cenozoic planktonic foraminifers from Antarctic deep-sea sediments, Leg 28, DSDP. In Hayes, D.E., Frakes, L.A., et al., *Init. Repts. DSDP*, 28: Washington (U.S. Govt. Printing Office), 573–584.
- Katz, H.R., 1968. Potential oil formations in New Zealand and their stratigraphic position as related to basin evolution. *N. Z. J. Geol. Geophys.*, 11:1077–1133.
- Katz, M.E., and Miller, K.G., 1991. Early Paleogene benthic foraminiferal assemblages and stable isotopes in the Southern Ocean. In Ciesielski, P.F., Kristoffersen, Y., et al., *Proc. ODP, Sci. Results*, 114: College Station, TX (Ocean Drilling Program), 481–512.
- Katz, M.E., Pak, D.K., Dickens, G.R., and Miller, K.G., 1999. The source and fate of massive carbon input during the Latest Paleocene Thermal Maximum. *Science*, 286:1531–1533.
- Kawahata, H., 2002. Shifts in oceanic and atmospheric boundaries in the Tasman Sea (southwest Pacific) during the late Pleistocene: evidence from organic carbon and lithogenic fluxes. *Palaeogeogr., Palaeoclimatol., Palaeoecol.*, 184:225–249.
- Kear, D., and Waterhouse, B.C., 1967. Onerahi Chaos-Breccia of Northland. *N. Z. J. Geol. Geophys.*, 10:629–646.
- Keigwin, L.D., 1980. Palaeoceanographic change in the Pacific at the Eocene–Oligocene boundary. *Nature*, 287:722–725.
- Kennett, J.P., 1968. Paleo-oceanographic aspects of the foraminiferal zonation in the upper Miocene–lower Pliocene of New Zealand. *G. Geol.*, XXXV:143–156.
- , 1977. Cenozoic evolution of Antarctic glaciation, the circum-Antarctic Ocean, and their impact on global paleoceanography. *J. Geophys. Res.*, 82:3843–3860.
- , 1978. The development of planktonic biogeography in the Southern Ocean during the Cenozoic. *Mar. Micropaleontol.*, 3:301–345.
- Kennett, J.P., Burns, R.E., Andrews, J.E., Churkin, M., Jr., Davies, T.A., Dumitrica, P., Edwards, A.R., Galehouse, J.S., Packham, G.H., and van der Lingen, G.J., 1972. Australian–Antarctic continental drift, paleo-circulation change and Oligocene deep-sea erosion. *Nature*, 239:51–55.
- Kennett, J.P., Houtz, R.E., et al., 1975. *Init. Repts. DSDP*, 29. Washington (U.S. Govt. Printing Office).
- Kennett, J.P., Houtz, R.E., Andrews, P.B., Edwards, A.R., Gostin, V.A., Hajos, M., Hampton, M.A., Jenkins, D.G., Margolis, S.V., Ovenshine, A.T., and Perch-Nielsen, K., 1974. Development of the Circum-Antarctic Current. *Science*, 186:144–147.
- , 1975. Cenozoic paleoceanography in the southwest Pacific Ocean, Antarctic glaciation, and the development of the Circum-Antarctic Current. In Kennett, J.P., Houtz, R.E., et al., *Init. Repts. DSDP*, 29: Washington (U.S. Govt. Printing Office), 1155–1169.
- Kennett, J.P., Keller, G., and Srinivasan, M.S., 1985. Miocene planktonic foraminiferal biogeography and paleoceanographic development of the Indo-Pacific region. In Kennett, J.P. (Ed.), *The Miocene Ocean: Paleoceanography and Biogeography*. Mem.—Geol. Soc. Am., 163:197–236.
- Kennett, J.P., Shackleton, N.J., Margolis, S.V., Goodney, D.E., Dudley, W.C., and Kroopnick, P.M., 1979. Late Cenozoic oxygen and carbon isotopic history and volcanic ash stratigraphy: DSDP Site 284, South Pacific. *Am. J. Sci.*, 279:52–69.
- Kennett, J.P., and Stott, L.D., 1991. Abrupt deep-sea warming, paleoceanographic changes and benthic extinctions at the end of the Palaeocene. *Nature*, 353:225–229.
- Kennett, J.P., and von der Borch, C.C., 1986. Southwest Pacific Cenozoic paleoceanography. In Kennett, J.P., von der Borch, C.C., et al., *Init. Repts. DSDP*, 90 (Pt. 2): Washington (U.S. Govt. Printing Office), 1493–1517.
- Kennett, J.P., von der Borch, C.C., et al., 1986. *Init. Repts. DSDP*, 90: Washington (U.S. Govt. Printing Office).

- Killops, S.D., Hollis, C.J., Morgans, H.E.G., Sutherland, R., Field, B.D., and Leckie, D.A., 2000. Paleooceanographic significance of late Paleocene dysaerobia at the shelf/slope break around New Zealand. *Palaeogeogr., Palaeoclimatol., Palaeoecol.*, 156:51–70.
- Kim, J., Lee, Y.-D.E., Bryant, W.R., and Tieh, T.T., 2001. The effects of laboratory consolidation on petrophysical properties of fine-grained marine sediments: electron microscopic observations. *Mar. Georesour. Geotechnol.*, 18:347–360.
- King, A.L., and Howard, W.R., 2000. Middle Pleistocene sea-surface temperature change in the southwest Pacific on orbital and suborbital time scales. *Geology*, 28:659–662.
- King, P.R., 2000. Tectonic reconstructions of New Zealand: 40 Ma to the present. *N. Z. J. Geol. Geophys.*, 43:611–638.
- Koons, P.O., 1989. The topographic evolution of collisional mountain belts: a numerical look at the Southern Alps, New Zealand. *Am. J. Sci.*, 289:1041–1069
- Kowalski, E.A., and Meyers, P.A., 1997. Glacial–interglacial variations in Quaternary production of marine organic matter at DSDP Site 594, Chatham Rise, southeastern New Zealand margin. *Mar. Geol.*, 140:249–263.
- Laird, M.G., 1993. Cretaceous continental rifts: New Zealand region. In Ballance, P.F. (Ed.), *South Pacific Sedimentary Basins*, Sedimentary Basins of the World (Vol. 2): Amsterdam (Elsevier), 37–49.
- , in press. *From Gondwana to Ice Age—The Cretaceous–Cenozoic Sedimentary Basins of New Zealand: Canterbury*, New Zealand (Canterbury Univ. Press).
- Lawver, L.A., and Gahagan, L.M., 1998. Opening of Drake Passage and its impact on Cenozoic ocean circulation. In Crowley, T.J., and Burke, K.C. (Eds.), *Tectonic Boundary Conditions for Climate Reconstructions*. Oxford Monogr. Geol. Geophys.: Oxford, UK (Oxford Univ. Press), 39:212–223.
- Lawver, L.A., Gahagan, L.M., and Coffin, M.F., 1992. The development of paleoseaways around Antarctica. In Kennett, J.P., and Warnke, D.A. (Eds.), *The Antarctic Paleoenvironment: A Perspective on Global Change (Pt. 1)*. Am. Geophys. Union, Antarct. Res. Ser., 56:7–30.
- Lawver, L.A., Williams, T., and Sloan, B.J., 1994. Seismic stratigraphy and heat flow of Powell Basin. *Terra Antart.*, 1:309–310.
- Lazarus, D., and Caulet, J.-P., 1993. Cenozoic Southern Ocean reconstructions from sedimentologic, radiolarian and other microfossil data. In Kennett, J.P., and Warnke, D.A. (Eds.), *The Antarctic Paleoenvironment: A Perspective on Global Change*. Antarct. Res. Ser., 60:145–174.
- Lazarus, D., Spencer-Cervato, C., Pianka-Biolzi, M., Beckmann, J.P., von Salis, K., Hilbrecht, H., and Thierstein, H., 1995. Revised Chronology of Neogene DSDP Holes from the World. *ODP Tech. Note*, 24.
- Le Pichon, X., 1968. Sea-floor spreading and continental drift. *J. Geophys. Res.*, 73:3661–3697.
- Lean, C.M.B., and McCave, I.N., 1998. Glacial to interglacial mineral magnetic and palaeoceanographic changes at Chatham Rise, SW Pacific Ocean. *Earth Planet. Sci. Lett.*, 163:247–260.
- Lear, C.H., Elderfield, H., and Wilson, P.A., 2000. Cenozoic deep-sea temperatures and global ice volumes from Mg/Ca in benthic foraminiferal calcite. *Science*, 287:269–272.
- Lear, C.H., Rosenthal, Y., and Wright, J.D., 2003. The closing of a seaway: ocean water masses and global climate change. *Earth Planet. Sci. Lett.*, 210:425–436.
- Leckie, D.A., 1994. Canterbury Plains, New Zealand—implications for sequence stratigraphic models. *AAPG Bull.*, 78:1240–1256.
- Lewis, D.W., Laird, M.G., and Powell, R.D., 1980. Debris flow deposits of early Miocene age, Deadman Stream, Marlborough. *Sediment. Geol.*, 27:83–118.
- Lewis, K.B., 1971. Slumping on a continental slope inclined at 1–4°. *Sedimentology*, 16:97–110.

- , 1973. Sediments on the continental shelf and slope between Napier and Castlepoint, New Zealand. *N. Z. J. Geol. Geophys.*, 7:183–208.
- , 1994. The 1500-km long Hikurangi Channel: trench-axis channel that escapes its trench, crosses a plateau, and feeds a fan-drift. *Geo-Mar. Lett.*, 14:19–28.
- Lewis, K.B., and Barnes, P.M., 1999. Kaikoura Canyon, New Zealand: active conduit from nearshore sediment zones to trench-axis channel. *Mar. Geol.*, 162:39–69.
- Lewis, K.B., Bennett, D.J., Herzer, R.H., and von der Borch, C.C., 1985. Seismic stratigraphy and structure adjacent to an evolving plate boundary, western Chatham Rise, New Zealand. In Kennett, J.P., von der Borch, C.C., et al., *Init. Repts. DSDP*, 90: Washington (U.S. Govt. Printing Office), 1325–1337.
- Lewis, K.B., Collott, J.-Y., and Lallemand, S.E., 1998. The dammed Hikurangi Trough: a channel-fed trench blocked by subducting seamounts and their wake avalanches (New Zealand–France GeodyNZ Project). *Basin Res.*, 10:441–468.
- Lewis, K.B., and Kohn, B.P., 1973. Ashes, turbidites and rates of sedimentation on the continental slope off Hawkes Bay. *N. Z. J. Geol. Geophys.*, 16:439–454.
- Lewis, K.B., and Pettinga, J.G., 1993. The emerging frontal wedge of the Hikurangi margin. In Ballance, P.F. (Ed.), *South Pacific Sedimentary Basins*, Sedimentary Basins of the World (Vol. 2): Amsterdam (Elsevier), 225–250.
- Lillie, A.R., 1953. The geology of the Dannevirke subdivision. *N. Z. Geol. Surv. Bull.*, Vol. 46.
- Lourens, L.J., Antonarakou, A., Hilgen, F.J., Van Hoof, A.A.M., Vergnaud-Grazzini, C., and Zachariasse, W.J., 1996. Evaluation of the Plio-Pleistocene astronomical time-scale. *Paleoceanography*, 11:391–413.
- Lu, H., Fulthorpe, C.S., and Mann, P., 2003. Three-dimensional architecture of shelf-building sediment drifts in the offshore Canterbury Basin, New Zealand. *Mar. Geol.*, 193:19–47.
- Lutze, G.F., 1979. Benthic foraminifers at Site 397: fluctuations and ranges in the Quaternary. In von Rad, U., Ryan, W.B.F., et al., *Init. Repts. DSDP*, 47 (Pt. 1): Washington (U.S. Govt. Printing Office), 419–431.
- Macleod, N., Ortiz, N., Fefferman, N., Clyde, W., Schuller, C., and Maclean, J., 2000. Phenotypic response of foraminifera to episodes of global environmental change. In Culver, S.J., and Rawson, P.F. (Eds.), *Biotic Response to Global Change, the Last 145 Million Years*: Cambridge (Cambridge Univ. Press), 51–78.
- MacPherson, E.O., 1949. The upper Senonian transgression in New Zealand. *N. Z. J. Sci. Technol., Sect. B*, 29:280–296.
- Marcantonio, F., Anderson, R.F., Higgins, S., Stute, M., Schlosser, P., and Kubik, P., 2001. Sediment focusing in the central equatorial Pacific Ocean. *Paleoceanography*, 16:260–267.
- Marples, B.J., 1952. Early Tertiary penguins of New Zealand. *N. Z. Geol. Surv. Bull.*, Vol. 20.
- Marshall, P., 1912. New Zealand and adjacent islands. In Steinmann, G., and Wilckens, O. (Eds.), *Handb. Reg. Geol.*, VII:1–78. (Abstract)
- Martinez, J.I., 1994. Late Pleistocene palaeoceanography of the Tasman Sea: implications for the dynamics of the warm pool in the western Pacific. *Palaeogeogr., Palaeoclimatol., Palaeoecol.*, 112:19–62.
- Martinson, D.G., Pisias, N.G., Hays, J.D., Imbrie, J., Moore, T.C., Jr., and Shackleton, N.J., 1987. Age dating and the orbital theory of the ice ages: development of a high-resolution 0 to 300,000-year chronostratigraphy. *Quat. Res.*, 27:1–29.
- McCave, I.N., 2002. Sedimentary settings on continental margins—an overview. In Wefer, G., Billett, D., Hebbeln, D., Jørgensen, B.B., Schlueter, M., and Van Weering, T.C.E. (Eds.), *Ocean Margin Systems*: Berlin (Springer-Verlag), 1–14.
- McCave, I.N., and Carter, L., 1997. Recent sedimentation beneath the deep western boundary current off northern New Zealand. *Deep-Sea Res.*, 44:1203–1237.
- McCave, I.N., Carter, L., Carter, R.M., and Hayward, B.W., in press. The southwest Pacific Gateway; ODP Leg 181: introduction. *Mar. Geol.*

- McCave, I.N., Manighetti, B., and Beveridge, N.A.S., 1995. Circulation in the glacial North Atlantic inferred from grain-size measurements. *Nature*, 374:149–151.
- McGlone, M.S., 2001. A late Quaternary pollen record from marine core P69, south-eastern North Island, New Zealand. *N. Z. J. Geol. Geophys.*, 44:69–77.
- McKinney, M.L., 1987. Taxonomic selectivity and continuous variation in mass and background extinctions of marine taxa. *Nature*, 325:143–145.
- McLennan, J.M., and Bradshaw, J.D., 1984. Angular unconformity between Oligocene and older rocks at Avoca, Canterbury. *N. Z. J. Geol. Geophys.*, 27:299–303.
- McLernon, C.R., 1972. Oil prospecting wells drilled in New Zealand 1865–1970. *Inf. Ser.—N. Z. Dept. Sci. Ind. Res.*, Vol. 88.
- McMillan, S.G., and Wilson, G.J., 1997. Allostratigraphy of coastal south and east Otago: a stratigraphic framework for interpretation of the Great South Basin, New Zealand. *N. Z. J. Geol. Geophys.*, 40:91–108.
- McMinn, A., Howard, W.R., and Roberts, D., 2001. Late Pliocene dinoflagellate cyst and diatom analysis from a high resolution sequence in DSDP Site 594, Chatham Rise, southwest Pacific. *Mar. Micropaleontol.*, 43:207–221.
- Menard, H.W., 1955. Deep-sea channels, topography and sedimentation. *AAPG Bull.*, 39:236–255.
- Mikolajewicz, U., Maier-Reimer, E., Crowley, T.J., and Kim, K.-Y., 1993. Effect of Drake and Panamanian gateways on the circulation of an ocean model. *Paleoceanography*, 8:409–426.
- Mildenhall, D.C., 2003. Deep sea record of Pliocene and Pleistocene terrestrial palynomorphs from offshore eastern New Zealand (ODP Site 1123, Leg 181). *N. Z. J. Geol. Geophys.*, 46:341–358.
- Mildenhall, D.C., Hollis, C.J., and Naish, T.R., in press. Orbitally-influenced vegetation record of the mid-Pleistocene climate transition, offshore eastern New Zealand (ODP Leg 181, Site 1123). *Mar. Geol.*
- Miller, K.G., 1992. Middle Eocene to Oligocene stable isotopes, climate, and deep-water history: the Terminal Eocene Event? In Prothero, D., and Berggren, W.A. (Eds.), *Eocene–Oligocene Climatic and Biotic Evolution*: Princeton, NJ (Princeton Univ. Press), 160–177.
- Miller, K.G., Mountain, G.S., and Tucholke, B.E., 1985. Oligocene glacio-eustasy and erosion on the margins of the North Atlantic. *Geology*, 13:10–13.
- Miller, K.G., Wright, J.D., and Fairbanks, R.G., 1991. Unlocking the Ice House: Oligocene–Miocene oxygen isotopes, eustasy, and margin erosion. *J. Geophys. Res.*, 96:6829–6848.
- Molnar, P., Atwater, T., Mammerickx, J., and Smith, S., 1975. Magnetic anomalies, bathymetry and the tectonic evolution of the South Pacific since the Late Cretaceous. *Geophys. J. R. Astron. Soc.*, 40:383–420.
- Moore, P.R., and Morgans, H.E.H., 1987. Two new reference sections for the Wanstead Formation (Paleocene–Eocene) in southern Hawkes Bay. *N. Z. Geol. Surv. Bull.*, 20:81–87.
- Moore, T.C., Jr., van Andel, T.H., Sancetta, C., and Pisias, N., 1978. Cenozoic hiatuses in the pelagic sediments. *Micropaleontology*, 24:113–138.
- Morgans, H.E.G., Edwards, A.R., Scott, G.H., Graham, I.J., Kamp, P.J.J., Mumme, T.C., Wilson, G.J., and Wilson, G.S., 1999. Integrated biostratigraphy of the Waitakian–Otaian boundary stratotype, early Miocene, New Zealand. *N. Z. J. Geol. Geophys.*, 42:581–614.
- Morgans, H.E.G., Scott, G.H., Beu, A.G., Graham, I.J., Mumme, T.C., George, W.St., and Strong, C.P., 1996. New Zealand Cenozoic time scale (version 11/96). *Rep.—Inst. Geol. Nucl. Sci.*, 96/38:1–12.
- Morgans, H.E.G., Scott, G.H., Edwards, A.R., Graham, I.J., Mumme, T.C., Waghorn, D.B., and Wilson, G.S., 2002. Integrated stratigraphy of the lower Altonian (early Miocene) sequence at Tangakaka Stream, East Cape, New Zealand. *N. Z. J. Geol. Geophys.*, 45:145–173.

- Morris, M., Stanton, B., and Neil, H., 2001. Subantarctic oceanography around New Zealand: preliminary results from an ongoing survey. *N. Z. J. Mar. Freshwater Res.*, 35:499–519.
- Mortimer, N., Sutherland, R., and Nathan, S., 2001. Torlesse greywacke and Haast schist source for Pliocene conglomerates near Reefton, New Zealand. *N. Z. J. Geol. Geophys.*, 44:105–111.
- Murphy, M.G., and Kennett, J.P., 1986. Development of latitudinal thermal gradients during the Oligocene: oxygen-isotope evidence from the southwest Pacific. In Kennett, J.P., von der Borch, C.C., et al., *Init. Repts. DSDP*, 90: Washington (U.S. Govt. Printing Office), 1347–1360.
- Naish, T.R., and Kamp, P.J.J., 1995. Pliocene–Pleistocene marine cyclothem, Wanganui Basin, New Zealand: a lithostratigraphic framework. *N. Z. J. Geol. Geophys.*, 38:223–243.
- Nelson, C.S., 1986. Lithostratigraphy of Deep Sea Drilling Project Leg 90 drill sites in the Southwest Pacific: an overview. In Kennett, J.P., von der Borch, C.C., et al., *Init. Repts. DSDP*, 90: Washington (U.S. Govt. Printing Office), 1471–1491.
- Nelson, C.S., and Cooke, P.J., 2001. History of oceanic front development in the New Zealand sector of the Southern Ocean during the Cenozoic—a synthesis. *N. Z. J. Geol. Geophys.*, 44:535–553.
- Nelson, C.S., Cooke, P.J., Hendy, C.H., and Cuthbertson, A.M., 1993. Oceanographic and climatic changes over the past 160,000 years at Deep Sea Drilling Project Site 594 off southeastern New Zealand, southwest Pacific Ocean. *Paleoceanography*, 8:435–458.
- Nelson, C.S., Froggatt, P.C., and Gosson, G.J., 1986b. Nature, chemistry, and origin of late Cenozoic megascopic tephra in Leg 90 cores from the southwestern Pacific. In Kennett, J.P., von der Borch, C.C., et al. (Eds.), *Init. Repts. DSDP*, 90: Washington (U.S. Govt. Printing Office), 1161–1173.
- Nelson, C.S., Hancock, G.E., and Kamp, P.J.J., 1981. Shelf to basin, temperate skeletal carbonate sediments, Three Kings Plateau, New Zealand. *J. Sediment. Petrol.*, 52:717–732.
- Nelson, C.S., Hendy, C.H., Cuthbertson, A.M., and Jarrett, G.R., 1986a. Late Quaternary carbonate and isotope stratigraphy, subantarctic Site 594, Southwest Pacific. In Kennett, J.P., von der Borch, C.C., et al., *Init. Repts. DSDP*, 90: Washington (U.S. Govt. Printing Office), 1425–1436.
- Nelson, C.S., Hendy, C.H., Jarrett, G.R., and Cuthbertson, A.M., 1985. Near-synchronicity of New Zealand alpine glaciations and Northern Hemisphere continental glaciations during the past 750 kyr. *Nature*, 318:361–363.
- Nelson, C.S., Hendy, I.L., Neil, H.L., Hendy, C.H., and Weaver, P.P.E., 2000. Last glacial jetting of cold waters through the Subtropical Convergence zone in the Southwest Pacific off eastern New Zealand. *Palaeogeogr., Palaeoclimatol., Palaeoecol.*, 156:103–121.
- Ness, G.E., and Kulm, L.D., 1973. Origin and development of Surveyor Deep-sea Channel. *Geol. Soc. Am. Bull.*, 84:3339–3354.
- Ninkovich, D., 1968. Pleistocene volcanic eruptions in New Zealand recorded in deep-sea sediments. *Earth Planet. Sci. Lett.*, 4:89–102.
- Norris, R.M., and Grant-Taylor, T.L., 1989. Late Quaternary shellbeds, western shelf, New Zealand. *N. Z. J. Geol. Geophys.*, 32:343–356.
- Orpin, A.R., Gammon, P.R., Naish, T.R., and Carter, R.M., 1998. Modern and ancient *Zygochlamys delicatula* shellbeds in New Zealand, and their sequence stratigraphic implications. *Sed. Geol.*, 122:267–284.
- Orsi, A.H., Whitworth, III, T., and Nowlin, Jr., W.D., 1995. On the meridional extent and fronts of the Antarctic Circumpolar Current. *Deep-Sea Res. Part I*, 42:641–673.
- Pantin, H.M., 1966. Sedimentation in Hawke Bay. *N. Z. Oceanogr. Inst. Mem.*, Vol. 28.
- Paterne, M., Labreyrie, J., Guichard, F., Mazaud, A., and Maitre, F., 1990. Fluctuations of the Campanian explosive volcanic activity (South Italy) during the past 190,000

- years, as determined by marine tephrochronology. *Earth Planet. Sci. Lett.*, 98:166–174.
- Pearson, P.N., and Palmer, M.R., 2000. Atmospheric carbon dioxide concentrations over the past 60 million years. *Nature*, 406:695–699.
- Petit, J.R., Jouzel, J., Raynaud, D., Barkov, N.I., Barnola, J.-M., Basile, I., Bender, M., Chappellaz, J., Davis, M., Delaygue, G., Delmotte, M., Kotlyakov, M., Legrand, M., Lipenkov, Y., Lorius, C., Pepin, L., Ritz, C., Saltzman, E., and Stievenard, M., 1999. Climate and atmospheric history of the past 420,000 years from the Vostok ice core, Antarctica. *Nature*, 399:429–436.
- Pfuhl, H.A., and McCave, I.N., 2003. Integrated age models for early Oligocene to early Miocene of Sites 1168 and 1170–1172. In Exon, N.F., Kennett, J.P., and Malone, M.J. (Eds.), *Proc. ODP, Sci. Results*, 189, 1–21 [Online]. Available from: Ocean Drilling Program, Texas A&M University, College Station TX 77845-9547.
- Pillans, B., and Wright, I., 1992. Late Quaternary tephrostratigraphy from the southern Havre Trough—Bay of Plenty, northeast New Zealand. *N. Z. J. Geol. Geophys.*, 35:129–143.
- Pillans, B.J., Kohn, B.P., Berger, G., Froggatt, P., Duller, G., Alloway, B.V., and Hesse, P., 1996. Multi-method dating comparison for mid-Pleistocene Rangitawa Tephra, New Zealand. *Quat. Sci. Rev.*, 15:641–653.
- Powell, A.W.B., 1950. Mollusca from the Continental Shelf, Eastern Otago. *Rec. Auckland Inst. Mus.*, 4:73–81.
- Proctor, R., and Carter, L., 1989. Tidal and sedimentary response to the late Quaternary closure and opening of Cook Strait, New Zealand: results from numerical modelling. *Paleoceanography*, 4:167–180.
- Prothero, D., Ivany, L., and Nesbitt, E., 2000. Penrose Conference report: the marine Eocene–Oligocene transition. *GSA Today*, 10:10–11.
- Pyle, D.M., 1989. The thickness, volume and grain size of tephra fall deposits. *Bull. Volcanol.*, 51:1–15.
- Rack, F.R., 1993. A geologic perspective on the Miocene evolution of the Antarctic Circumpolar Current system. *Tectonophysics*, 222:397–415.
- Raymo, M.E., 1994. The initiation of Northern Hemisphere glaciation. *Annu. Rev. Earth Planet. Sci.*, 22:353–383.
- Reay, M.B., and Strong, C.P., 1992. The Branch Sandstone, Clarence Valley, and implications for latest Cretaceous paleoenvironments and geological history of central Marlborough. *N. Z. Geol. Surv. Bull.*, 44:43–49.
- Robert, C., Diester-Haas, L., and Chamley, H., 2002. Late Eocene–Oligocene oceanographic development at southern high latitudes, from terrigenous and biogenic particles: a comparison of Kerguelen Plateau and Maud Rise, ODP Sites 744 and 689. *Mar. Geol.*, 191:37–54.
- Rogers, K.M., Morgans, H.E., and Wilson, G.S., 2001. Identification of a Waipawa Formation equivalent in the upper Te Uri Member of the Whangai Formation—implications for depositional history and age. *N. Z. J. Geol. Geophys.*, 44:347–354.
- Royer, J.-Y., and Rollet, N., 1997. Plate-tectonic setting of the Tasmanian region. In Exon, N.F., and Crawford, A.J. (Eds.), *West Tasmanian Margin and Offshore Plateaus: Geology, Tectonic and Climatic History, and Resource Potential*. Aust. J. Earth Sci., 44:543–560.
- Sabaa, A.T., Sikes, E.L., Hayward, B.W., and Howard, W.R., in press. Pliocene sea surface temperature changes in ODP Site 1125 Chatham Rise, east of New Zealand. *Mar. Geol.*
- Saul, G., Naish, T.R., Abbott, S.T., and Carter, R.M., 1999. Sedimentary cyclicity in the marine Pliocene–Pleistocene of the Wanganui Basin (New Zealand): sequence stratigraphic motifs characteristic of the last 2.5 m.y. *Geol. Soc. Am. Bull.*, 111:524–537.
- Schmitz, W.J., 1995. On the interbasin-scale thermohaline circulation. *Rev. Geophys.*, 33:151–173.
- Schneider, J.-L., Ruyet, A.L., Chanier, F., Buret, C., Ferriere, J., Proust, J.-N., and Rosseel, J.-B., 2001. Primary or secondary distal volcanoclastic turbidites: how to make

- the distinction? An example from the Miocene of New Zealand (Mahia Peninsula, North Island). *Sediment. Geol.*, 145:1–22.
- Schonfeld, J., 1996. The “*Stilostomella* extinction”: structure and dynamics of the last turn-over in deep-sea benthic foraminiferal assemblages. In Moguilevsky, E.A., and Whatley, R. (Eds.), *Microfossils and Oceanic Environments: Aberystwyth* (Univ. Wales), 27–37.
- Schonfeld, J., and Spiegler, D., 1995. Benthic foraminiferal biostratigraphy of ODP Site 141-861 (Chile triple junction, southeastern Pacific). In Lewis, S.D., Behrmann, J.H., Musgrave, R.J., and Cande, S.C. (Eds.), *Proc. ODP, Sci. Results*, 141: College Station, TX (Ocean Drilling Program), 213–224.
- Schuur, C.L., Coffin, M.F., Frohlich, C., Mann, P., Massell, C.G., Karner, G.D., Ramsay, D., and Caress, D.W., 1998. Sedimentary regimes at the Macquarie Ridge Complex: interaction of Southern Ocean circulation and plate boundary bathymetry. *Paleoceanography*, 13:646–670.
- Scott, G.H., 1992. Planktonic foraminiferal biostratigraphy (Altonian–Tongaporutuan Stages, Miocene) at DSDP Site 593, Challenger Plateau, Tasman Sea. *N. Z. J. Geol. Geophys.*, 35:501–513.
- , 1995. Coiling excursions in *Globorotalia miotumida*: high resolution bio-events at the middle–upper Miocene boundary in southern temperate water masses? *Inst. Geol. Nucl. Sci.*, 443:299–308.
- Scott, G.H., and Hall, I., in press. Planktonic foraminiferal evidence on late Pliocene–Quaternary surface water masses at ODP Site 1123B, northern Chatham Rise, east of New Zealand. *Mar. Geol.*
- Semtner, A.J., and Chervin, R.M., 1992. Ocean general circulation from a global eddy-resolving model. *J. Geophys. Res.*, 97:5493–5550.
- Shackleton, N.J., 2000. The 100,000-year ice-age cycle identified and found to lag temperature, carbon dioxide, and orbital eccentricity. *Science*, 289:1897–1902.
- Shackleton, N.J., Berger, A., and Peltier, W.A., 1990. An alternative astronomical calibration of the lower Pleistocene timescale based on ODP Site 677. *Trans. R. Soc. Edinburgh: Earth Sci.*, 81:251–261.
- Shackleton, N.J., Hall, M.A., Raffi, I., Tauxe, L., and Zachos, J., 2000. Astronomical calibration age for the Oligocene–Miocene boundary. *Geology*, 28:447–450.
- Shackleton, N.J., and Kennett, J.P., 1975. Paleotemperature history of the Cenozoic and the initiation of Antarctic glaciation: oxygen and carbon isotope analyses in DSDP Sites 277, 279, and 281. In Kennett, J.P., Houtz, R.E., et al., *Init. Repts. DSDP*, 29: Washington (U.S. Govt. Printing Office), 743–755.
- Shane, P., 2000. Tephrochronology: a New Zealand case study. *Earth Sci. Rev.*, 49:223–259.
- Shane, P.A.R., and Froggatt, P.C., 1992. Composition of widespread volcanic glass in deep-sea sediments of the Southern Pacific Ocean, an Antarctic source inferred. *Bull. Volcanol. (Heidelberg)*, 54:595–601.
- Sikes, E.L., Howard, W.R., Neil, H.L., and Volkman, J.K., 2002. Glacial–interglacial sea surface temperatures across the subtropical front east of New Zealand based on alkenone unsaturation ratios and foraminiferal assemblages. *Paleoceanography*, 17:1–12.
- Sikes, E.L., Samson, C., Guilderson, T.P., and Howard, W.R., 2000. Old radiocarbon ages in the southwest Pacific Ocean during the last glacial period and deglaciation. *Nature*, 405:555–559.
- Sloss, L.L., 1963. Sequences in the cratonic interior of North America. *Geol. Soc. Am. Bull.*, 74:93–114.
- Stanton, B.R., and Morris, M.Y., in press. Direct velocity measurements in the Sub-Antarctic Front and over Campbell Plateau, southeast of New Zealand. *J. Geophys. Res.*
- Stewart, R.B., and Neall, V.E., 1984. Chronology of palaeoclimatic change at the end of the last glaciation. *Nature*, 311:47–48.

- Stickley, C.E., Carter, L., McCave, I.N., and Weaver, P.P.E., 2001. Lower Circumpolar Deep Water flow through the SW Pacific Gateway for the last 190 ky: evidence from Antarctic diatoms. *In* Seidov, D., Haupt, B.J., and Maslin, M. (Eds.), *The Oceans and Rapid Climate Change*, Geophys. Monogr., 126:101–116.
- Stonely, R., 1968. A lower Tertiary decollement on the east coast, North Island, New Zealand. *N. Z. J. Geol. Geophys.*, 11:128–156.
- Stramma, L., Peterson, R.G., and Tomczak, M., 1995. The South Pacific Current. *J. Phys. Oceanogr.*, 25:77–91.
- Strong, C.P., Hollis, C.J., and Wilson, G.J., 1995. Foraminiferal, radiolarian, and dinoflagellate biostratigraphy of Late Cretaceous to middle Eocene pelagic sediments (Muzzle Group), Mead Stream, Marlborough, New Zealand. *N. Z. J. Geol. Geophys.*, 38:171–209.
- Suggate, R.P., Stevens, G.R., and Te Punga, M.T., 1978. *The Geology of New Zealand*: Wellington (New Zealand Govt. Printer).
- Sutherland, R., 1995. The Australia–Pacific boundary and Cenozoic plate motions in the SW Pacific: some constraints from Geosat data. *Tectonics*, 14:819–831.
- , 1996. Transpressional development of the Australia–Pacific boundary through southern New Zealand: constraints from Miocene–Pliocene sediments, Waiho-1 borehole, South Westland. *N. Z. J. Geol. Geophys.*, 39:251–264.
- Swanson, K., and van der Lingen, G., 1997. Late Quaternary ostracod and planktonic foraminiferal dissolution signals from the eastern Tasman Sea—palaeoenvironmental implications. *Palaeogeogr., Palaeoclimatol., Palaeoecol.*, 131:303–314.
- Thiede, J., 1979. Wind regimes over the late Quaternary southwest Pacific Ocean. *Geology*, 7:259–262.
- Thiede, J., Nees, S., Schulz, H., and De Deckker, P., 1997. Oceanic surface conditions recorded on the sea floor of the southwest Pacific Ocean through the distribution of foraminifers and biogenic silica. *Palaeogeogr., Palaeoclimatol., Palaeoecol.*, 131:207–239.
- Thomas, E., 1987. Late Oligocene to Recent deep-sea benthic foraminifers from the central equatorial Pacific Ocean. *In* Ruddiman, W.F., Kidd, R.B., Thomas, E., et al., *Init. Repts. DSDP*, 94: Washington (U.S. Govt. Printing Office), 213–224.
- Thompson, R.-M., 1994. *The First Forty Years: New Zealand Oceanographic Institute*: Wellington (4th Jubilee Comm.).
- Tippett, J.M., and Kamp, P.J.J., 1993. Fission track analysis of the late Cenozoic vertical kinematics of continental Pacific crust, South Island, New Zealand. *J. Geophys. Res.*, 98:16119–16148.
- Tiedemann, R., Sarnthein, M., and Shackleton, N.J., 1994. Astronomical timescale for the Pliocene Atlantic  $\delta^{18}\text{O}$  and dust flux records of Ocean Drilling Program Site 659. *Paleoceanography*, 9:619–638.
- Toggweiler, J.R., and Samuels, B., 1993. Is the magnitude of the deep outflow from the Atlantic Ocean actually governed by Southern Hemisphere winds? *In* Heimann, M. (Ed.), *The Global Carbon Cycle*: Berlin (Springer-Verlag), 303–331.
- , 1995. Effect of Drake Passage on the global thermohaline circulation. *Deep-Sea Res. Part I*, 42:477–500.
- Tomczak, M., and Godfrey, J.S., 1994. *Regional Oceanography: An Introduction*: New York (Pergamon Press).
- Trenberth, K.E., 1992. Global analyses from ECMWF and atlas of 1000-10 mb circulation statistics. *Tech. Note 373*: Boulder, Colorado (Natl. Cent. Atmos. Res.).
- Tucholke, B.E., and Embley, R.W., 1984. Cenozoic regional erosion of the abyssal seafloor off South Africa. *In* Schlee, J.S. (Ed.), *Interregional Unconformities and Hydrocarbon Accumulation*. AAPG Mem., 36:145–164.
- Tucholke, B.E., Hollister, C.D., Weaver, F.M., and Vennum, W.R., 1976. Continental rise and abyssal plain sedimentation in the southeast Pacific basin—Leg 35 Deep Sea Drilling Project. *In* Hollister, C.D., Craddock, C., et al., *Init. Repts. DSDP*, 35: Washington (U.S. Govt. Printing Office), 359–400.

- Turnbull, I.M., 1991. Eocene olistostromes in Sandfly Formation, Franklin Mountains, Eastern Fiordland. *N. Z. Geol. Surv. Bull.*, 43:101–105.
- Turnbull, I.M., Uruski, C.I., et al., 1993. Cretaceous and Cenozoic sedimentary basins of western Southland, New Zealand. *Inst. Geol. Nucl. Sci.*, Monogr. 1.
- van Andel, T.H., 1975. Mesozoic/Cenozoic calcite compensation depth and the global distribution of calcareous sediments. *Earth Planet. Sci. Lett.*, 26:187–194.
- van Morkhoven, F.P.C.M., Berggren, W.A., and Edwards, A.S., 1986. *Cenozoic Cosmopolitan Deep-Water Benthic Foraminifera*. Bull. Cent. Rech. Explor.—Prod. Elf-Aquitaine, 11.
- Van der Lingen, G.J., Swanson, K.M., and Muir, R.J. (Eds.), 1994. *Evolution of the Tasman Sea Basin*: Rotterdam (Balkema).
- Veevers, J.J., and Li, Z.X., 1991. Review of seafloor spreading around Australia. II. Marine magnetic anomaly modelling. *Am. J. Earth Sci.*, 38:391–408.
- Vella, P., 1973. Ocean paleotemperatures and oscillations of the Subtropical Convergence Zone on the eastern side of New Zealand. In Fraser, R. (Ed.), *Oceanography of the South Pacific*: Wellington (N. Z. Natl. Comm. UNESCO), 315–318.
- Waghorn, D.B., 1981. New Zealand and southwest Pacific late Eocene and early Oligocene calcareous nannofossils. [Ph.D. Dissert.], Victoria Univ., Wellington, N. Z.
- Walcott, R.I., 1978. Present tectonics and late Cenozoic evolution of New Zealand. *Geophys. J. R. Astron. Soc.*, 52:137–164.
- , 1984. Reconstruction of the New Zealand region for the Neogene. *Palaeogeogr., Palaeoclimatol., Palaeoecol.*, 46:217–231.
- Walker, G.P.L., 1980. The Taupo pumice: product of the most powerful known (ultra-plinian) eruption? *J. Volcanol. Geotherm. Res.*, 8:69–94.
- Ward, D.M., and Lewis, D.W., 1975. Paleoenvironmental implications of storm-scoured ichnofossiliferous mid-Tertiary limestones, Waihao district, South Canterbury, New Zealand. *N. Z. J. Geol. Geophys.*, 18:881–908.
- Warren, B.A., 1981. Deep circulation in the world ocean. In Warren, B.A., and Wunsch, C. (Eds.), *Evolution of Physical Oceanography*: Cambridge (MIT Press), 6–42.
- , 1983. Why is no deep water formed in the North Pacific? *J. Marine Res.*, 41:327–347.
- Warren, G., and Speden, I., 1978. The Piripauan and Haumurian stratotypes (Mata Series, Upper Cretaceous) and correlative sequences in the Haumuri Bluff district, South Marlborough (S56). *N. Z. Geol. Surv. Bull.*, Vol. 92.
- Watkins, N.D., and Huang, T.C., 1977. Tephra in abyssal sediments east of the North Island, New Zealand; chronology, paleowind velocity, and paleoexplosivity. *N. Z. J. Geol. Geophys.*, 20:179–199.
- Watkins, N.D., and Kennett, J.P., 1971. Antarctic Bottom Water: major change in velocity during the late Cenozoic between Australia and Antarctica. *Science*, 173:813–818.
- Weaver, P.P.E., Carter, L., and Neil, H., 1998. Response of surface water masses and circulation to late Quaternary climate change, east of New Zealand. *Paleoceanography*, 13:70–83.
- Weaver, P.P.E., Neil, H., and Carter, L., 1997. Sea surface temperature estimates from the southwest Pacific based on planktonic foraminifera and oxygen isotopes. *Palaeogeogr., Palaeoclimatol., Palaeoecol.*, 131:241–256.
- Webb, P.N., 1973. A re-examination of the Wangaloan problem. *N. Z. J. Geol. Geophys.*, 16:158–169.
- Weedon, G.P., and Hall, I.R., in press. Neogene palaeoceanography of Chatham Rise (SW Pacific) based on sediment geochemistry. *Mar. Geol.*
- Wei, K.-Y., 1998. Southward shifting of the Tasman Front at 4.4 Ma (early Pliocene): paleobiogeographic and oxygen isotopic evidence. *J. Asian Earth Sci.*, 16:97–108.
- Wei, W., 1991. Evidence for an earliest Oligocene abrupt cooling in the surface waters of the Southern Ocean. *Geology*, 19:780–783.

- Weinholz, P., and Lutze, G.F., 1989. The *Stilostomella* extinction. In Ruddiman, W., Sarnthein, M., et al., *Proc. ODP, Sci. Results*, 108: College Station, TX (Ocean Drilling Program), 113–117.
- Weissel, J.K., and Hayes, D.E., 1977. Evolution of the Tasman Sea reappraised. *Earth Planet. Sci. Lett.*, 36:77–84.
- Weissel, J.K., Hayes, D.E., and Herron, E.M., 1977. Plate tectonics synthesis: the displacements between Australia, New Zealand, and Antarctica since the Late Cretaceous. *Mar. Geol.*, 25:231–277.
- Wellman, H.W., 1979. An uplift map for the South Island of New Zealand, and a model for the uplift of the Southern Alps. In Walcott, R.I., and Cresswell, M.M. (Eds.), *The Origin of the Southern Alps*, Bull.—R. Soc. N. Z., 18:13–20.
- Wells, P.E., and Connell, R., 1997. Movement of hydrological fronts and widespread erosional events in the southwestern Tasman Sea during the late Quaternary. *Aus. J. Earth Sci.*, 44:105–112.
- Wells, P.W., and Okada, H., 1997. Response of nannoplankton to major changes in sea-surface temperature and movements of hydrological fronts over Site DSDP 594 (south Chatham Rise, southeastern New Zealand), during the last 130 kyr. *Mar. Micropaleontol.*, 32:341–363.
- Whitworth, T., Warren, B.A., Nowlin, W.D., Pillsbury, R.D., and Moore, M.L., 1999. On the deep western-boundary current in the southwest Pacific Basin. *Prog. Oceanogr.*, 43:1–54.
- Willett, S.D., and Brandon, M.T., 2002. On steady states in mountain belts. *Geology*, 30:175–178.
- Wilson, C.J.N., 1994. Ash-fall deposits from large scale phreatomagmatic volcanism: limitations of available eruption column models. In Casadevall, T.J. (Ed.), *Proc. Int. Symp. Volcanic Ash Aircr. Saf., 1st, 1994*, U.S. Geol. Surv. Bull., 2047:93–99.
- Wilson, C.J.N., Houghton, B.F., Kamp, P.J.J., and Williams, M.O., 1995a. An exceptionally widespread ignimbrite with implications for pyroclastic flow emplacement. *Nature*, 378:605–607.
- Wilson, C.J.N., Houghton, B.F., Williams, M.O., Lanphere, M.A., Weaver, S.D., and Briggs, R.M., 1995b. Volcanic and structural evolution of Taupo Volcanic Zone, New Zealand: a review. *J. Volcanol. Geotherm. Res.*, 68:1–28.
- Wilson, D.D., 1956. The Late Cretaceous and early Tertiary transgression in South Island, New Zealand. *N. Z. J. Sci. Technol., Sect. B*, 37:610–622.
- Wilson, G.S., Hu, S., Richter, C., Howe, J., and Roberts, A.P., 2000a. Chronostratigraphy of turbidite-drift interactions at ODP Site 1122 on the Bounty Fan, offshore New Zealand. ODP Leg 181 Post Cruise Meeting (Mt. Cook), Abstracts, p. 57.
- Wilson, G.S., Hu, S., Richter, C., Howe, J., Roberts, A.P., Harris, S., Verosub, K.L., and Weedon, G.P., 2000b. Twenty-one million years of continuous late Neogene sedimentation beneath the Deep Western Boundary Current, ODP Site 1123, Chatham Rise, SW Pacific. ODP Leg 181 Post Cruise Meeting (Mt. Cook), Abstracts, p. 59.
- Woodburne, M.O., and Zinsmeister, W.J., 1982. Fossil land mammal from Antarctica. *Science*, 218:284–286.
- Woodruff, F., and Savin, S.M., 1989. Miocene deepwater oceanography. *Paleoceanography*, 4:87–140.
- , 1991. Mid-Miocene isotope stratigraphy in the deep-sea: high resolution correlations, paleoclimatic cycles, and sediment preservation. *Paleoceanography*, 6:755–806.
- Wright, I.C., McGlone, M.S., Nelson, C.S., and Pillans, B.J., 1995. An integrated latest quaternary (Stage 3 to present) paleoclimatic and paleoceanographic record from offshore northern New Zealand. *Quat. Res.*, 44:283–293.
- Wright, J.D., and Miller, K.G., 1993. Southern Ocean influences on late Eocene to Miocene deep-water circulation. In Kennett, J.P., and Warnke, D.A. (Eds.), *The Antarctic Paleoenvironment: A Perspective on Global Change*. Antarct. Res. Ser., 60:1–25.

- Wright, J.D., Miller, K.G., and Fairbanks, R.G., 1991. Evolution of modern deepwater circulation: evidence from the late Miocene Southern Ocean. *Paleoceanography*, 6:275–290.
- Yang, T.-N., Wei, K.-Y., Wang, G.-S., and Chen, Y.-G., 2002. Pliocene–Pleistocene foraminiferal oxygen and carbon isotopic records from Site 1125 of ODP 181, southwest Pacific. *Geol. Annu. Meet.*, Taipei, Taiwan, 35–38. (Abstract)
- Zachos, J., Pagani, M., Sloan, L., Thomas, E., and Billups, K., 2001. Trends, rhythms, and aberrations in global climate 65 Ma to present. *Science*, 292:686–693.
- Zachos, J.C., Breza, J.R., and Wise, S.W., 1992. Early Oligocene ice-sheet expansion on Antarctica: stable isotope and sedimentological evidence from Kerguelen Plateau, southern Indian Ocean. *Geology*, 20:569–573.
- Zhou, L., and Kyte, F.T., 1992. Sedimentation history of the south Pacific pelagic clay province over the last 85 million years inferred from the geochemistry of Deep Sea Drilling Project Hole 596. *Paleoceanography*, 7:441–465.

**Figure F1.** Model simulation of sea-surface height at 1/8 degree resolution for the Southwest Pacific Ocean, Tasman Sea, and adjoining Southern Ocean ([www7320.nrlssc.navy.mil/global\\_ncom](http://www7320.nrlssc.navy.mil/global_ncom)). To locate Leg 181 sites on this figure, see Figure F2, p. 84. The Subantarctic (SAF), Subtropical (STF), and Tasman (TF) fronts are well delineated, as indicated in the color key. The southern branch of the west-flowing South Equatorial Current impinges on the Queensland coast a little north of the latitude of New Caledonia, where its main flow is diverted southward in the East Australian Current (EAC) and then eastward again along the Tasman Front. Dynamic eddy activity occurs along all three fronts but is especially prominent along the EAC-TF and its continuation around northern New Zealand as the East Auckland and East Coast currents. The SAF and STF are well separated across the Campbell Plateau region, but east and the west from here lie in such close proximity as to form a single merged zone of intense frontal gradient. The clockwise circulation of cold subantarctic water within the Bounty Trough is well delineated.

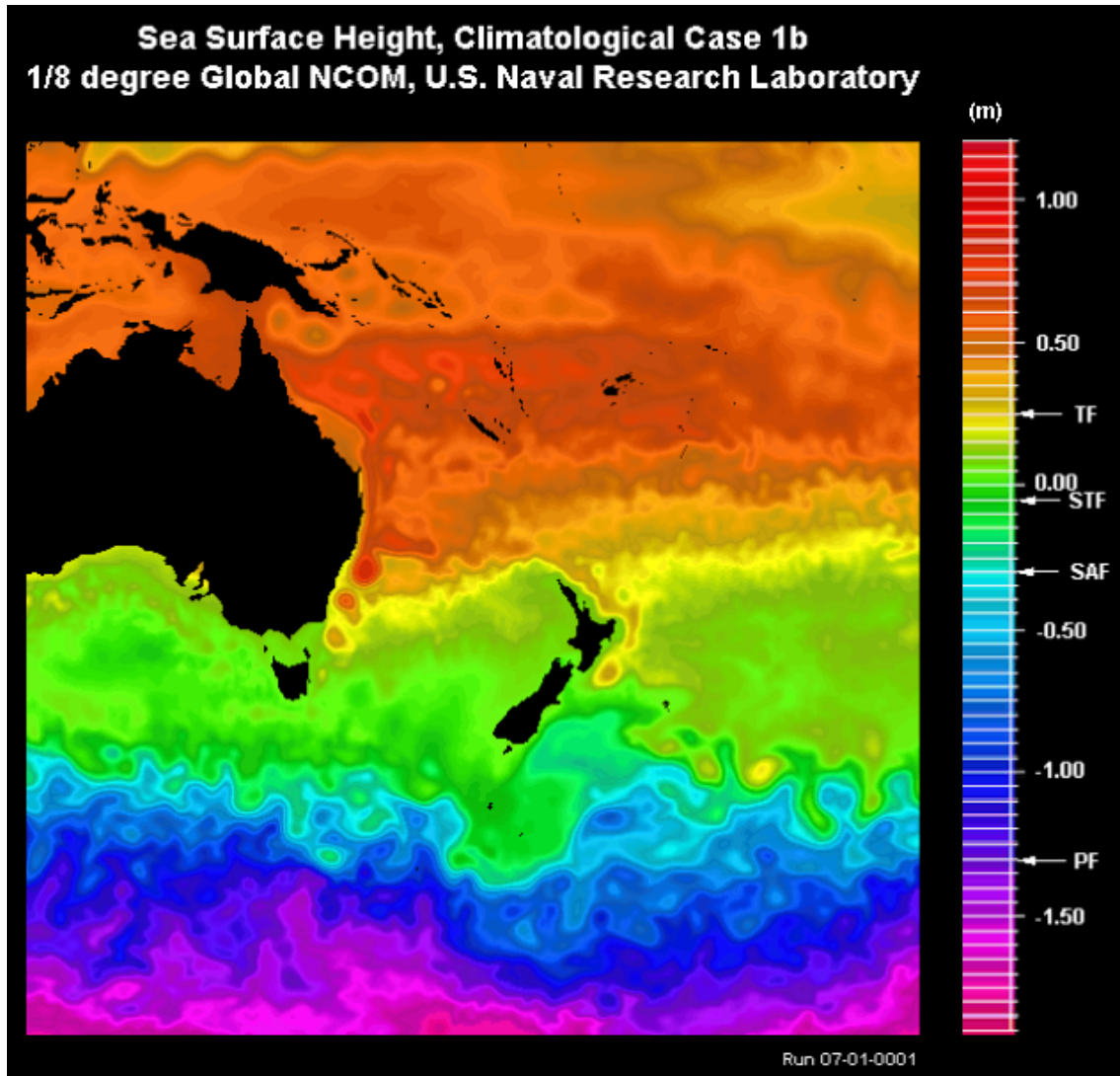


Figure F2. Location map for all ocean drilling sites in the Southwest Pacific region that have retrieved substantial sediment cores, including sites from DSDP Legs 29 and 90 and ODP Legs 181 and 189.

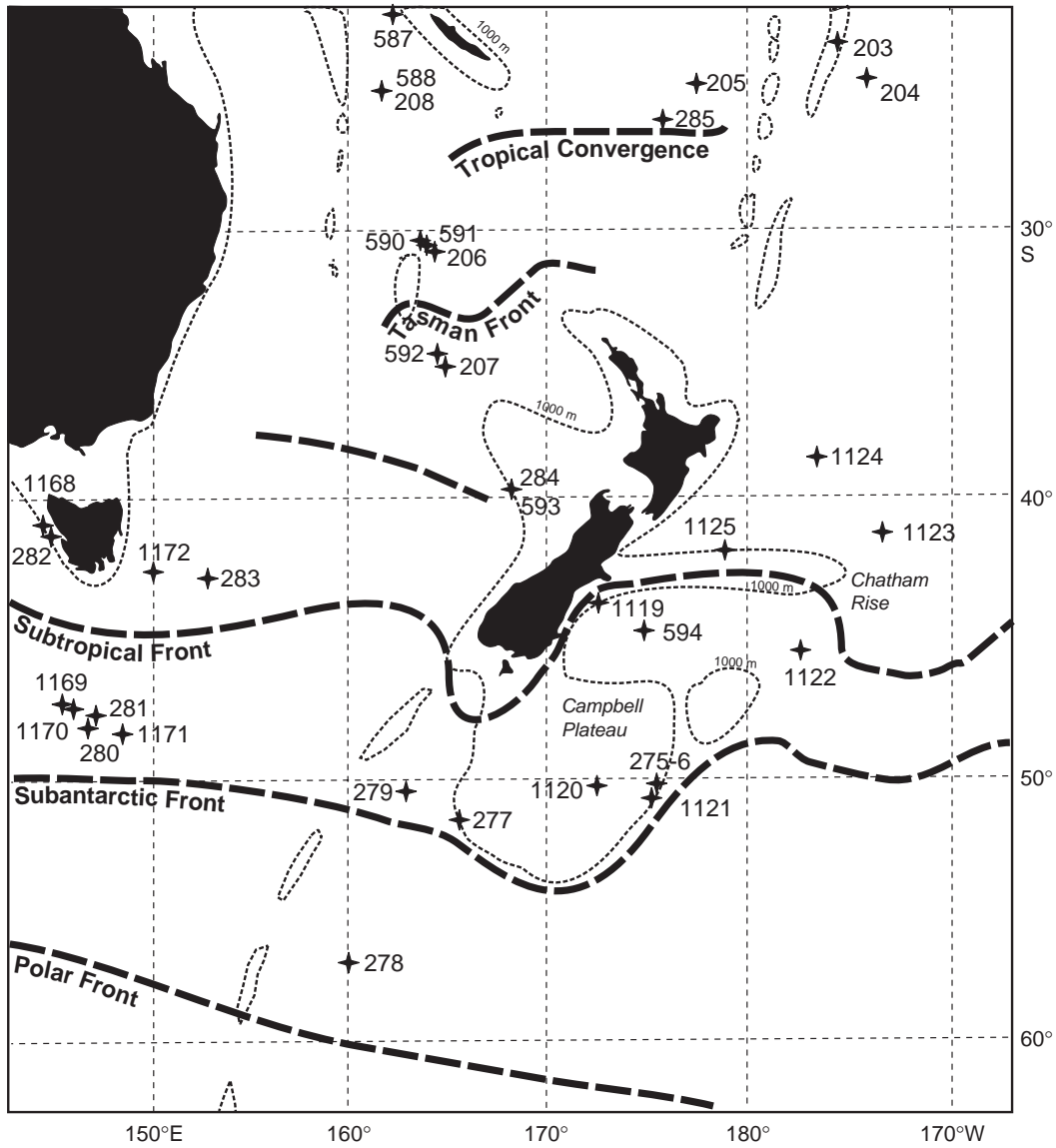


Figure F3. Summary diagram of the climatic history of the New Zealand region, based on the onland occurrence of stenothermal fossil flora and fauna (based on sources summarized in Hornibrook, 1992). Paleocene molluscan attributions at 45°S (Pentland Hills) are from Philip Maxell (pers. comm., 2003). See caption to Figure F6, p. 88, for key to New Zealand biostratigraphic stage abbreviations.

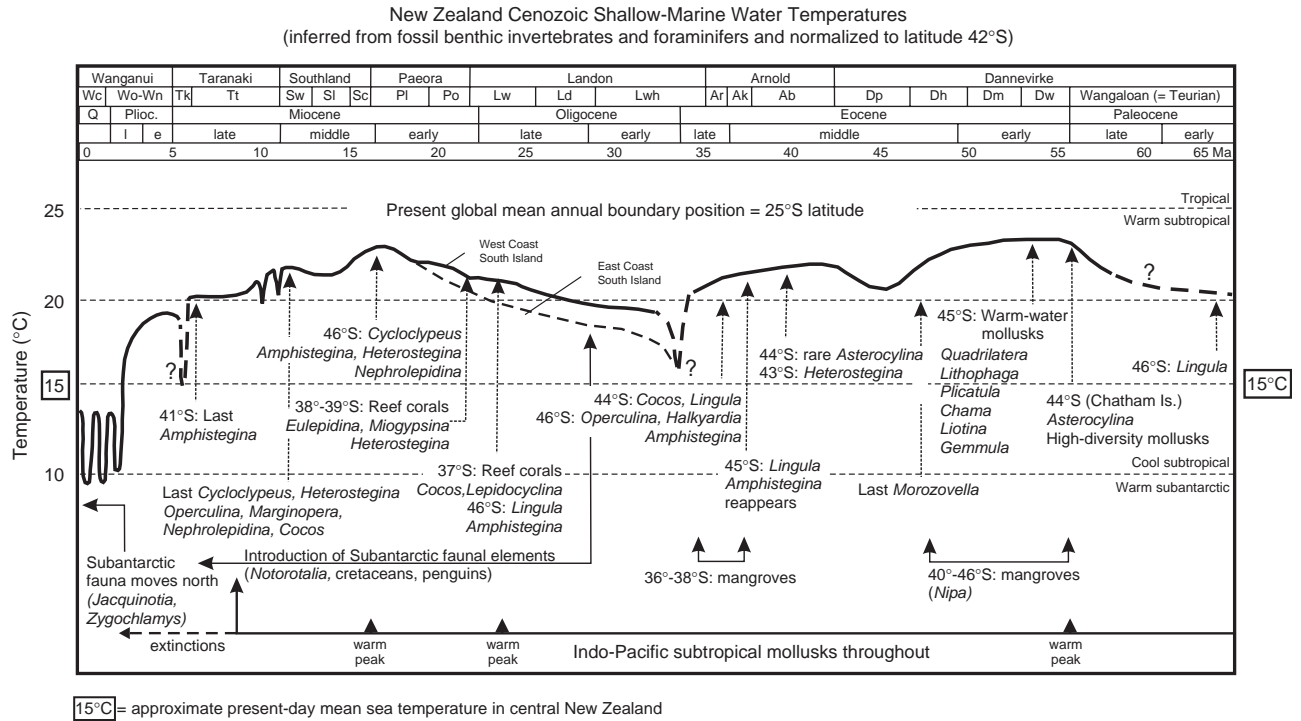
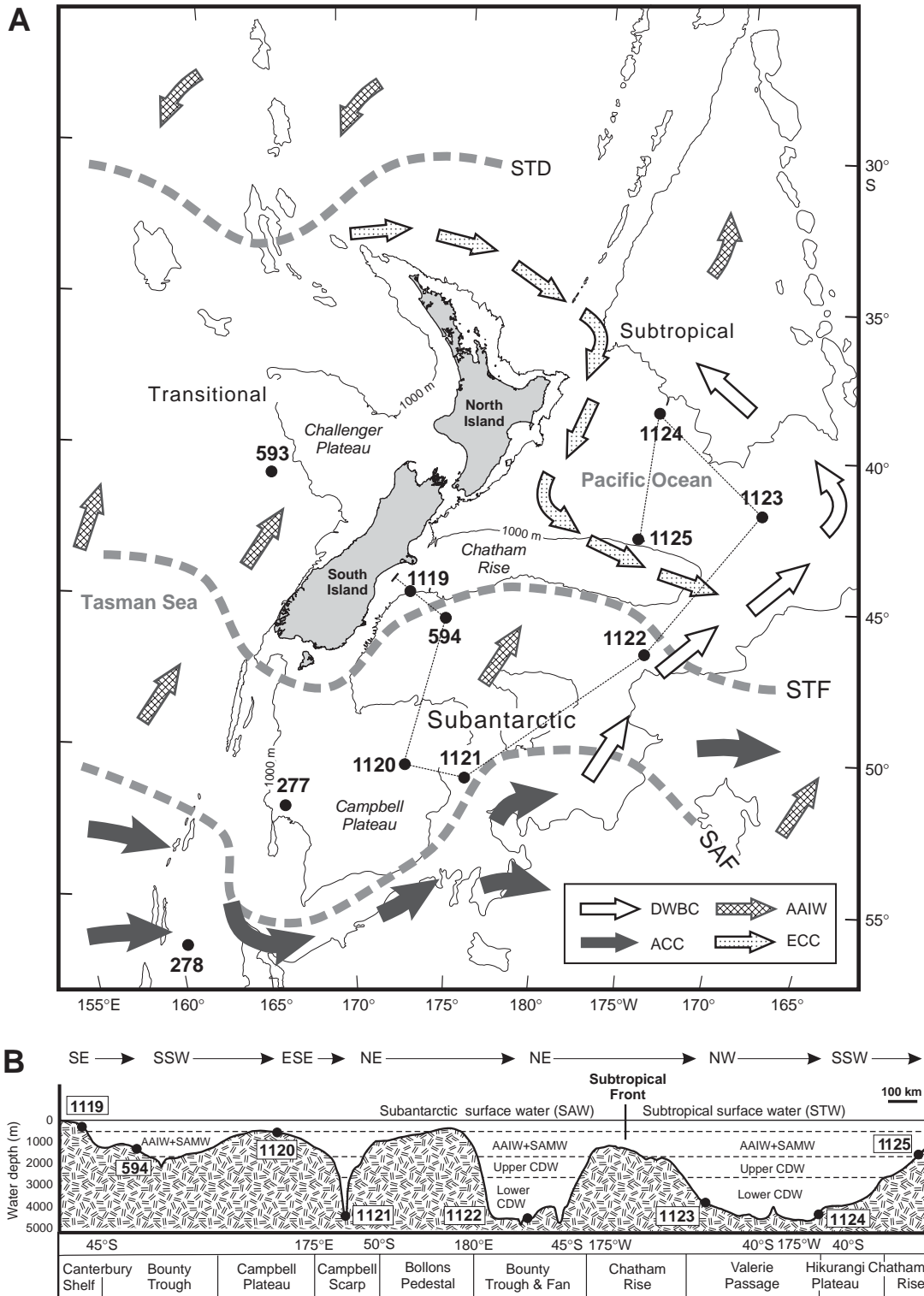
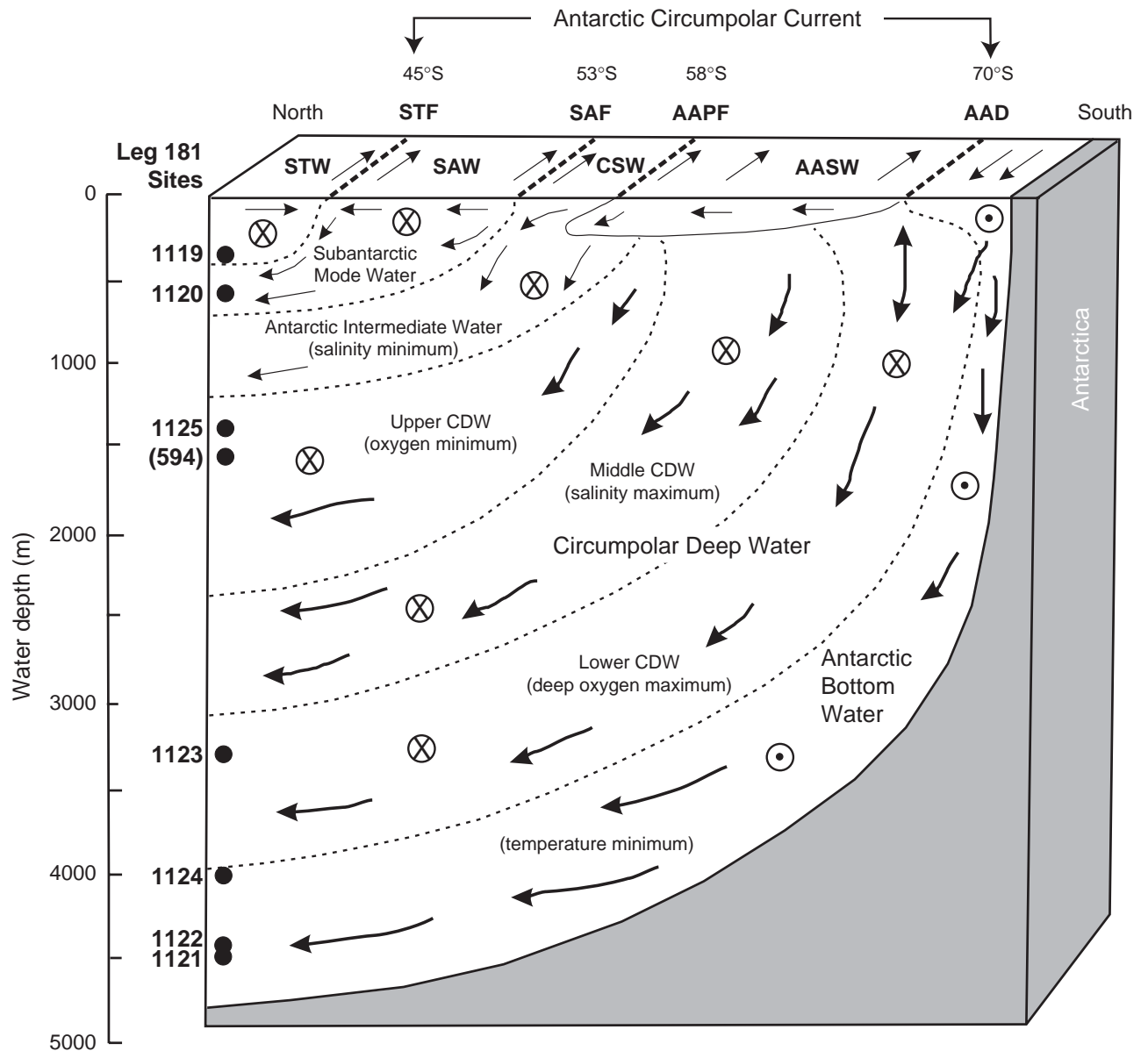


Figure F4. A. Oceanographic setting of the Leg 181 drill sites, showing position of the major ocean water masses, fronts, and current systems. B. Profile connecting all Leg 181 drill sites, showing their locations with respect to bathymetry and water mass. SAF = Subantarctic Front, STF = Subtropical Front, STD = Subtropical Divergence, DWBC = Deep Western Boundary Current, ACC = Antarctic Circumpolar Current, AAIW = Antarctic Intermediate Water, ECC = Equatorial Counter Current, SAMW= Subantarctic Mode Water, CDW = Circumpolar Deep Water.



**Figure F5.** Water masses, fronts, and circulation patterns that characterize the southwest Pacific section of the Southern Ocean (after Tomczak and Godfrey, 1994). STF = Subtropical Front, SAF = Subantarctic Front, AAPF = Antarctic Polar Front, AAD = Antarctic Divergence, CDW = Circumpolar Deep Water, STW = Subtropical Water, SAW = Subantarctic Water, CSW = Circumpolar Surface Water, AASW = Antarctic Surface Water.



**Figure F6.** Summary stratigraphic data for all available southwest Pacific and nearby Southern Ocean drill sites, DSDP Legs 29 and 90 and ODP Legs 181 and 189 (after Kennett, Houtz, et al., 1975; Kennett, von der Borch, et al., 1986; Carter, R., McCave, Richter, Carter, L., et al., 1999; Exon, Kennett, Malone, et al., 2001). Arranged in order from southwest (left) to northeast (right). Note that three different interpretations of the Eocene–Oligocene stratigraphy for Leg 189 sites have been published by Exon, Kennett, Malone, et al. (2001), Exon et al. (2002), and Pfuhl and McCave (2003). We follow mainly the last of these references, except that in addition to the early Oligocene breaks inferred by Pfuhl and McCave we recognize the presence of the Marshall Paraconformity at Site 1168 also. Our reasons for this are (1) the major facies change—marked by a decrease in total organic carbon and an increase in carbonate content—that occurs at 760 mbsf in the Site 1168 core and (2) otherwise, Site 1168 would be the only locality in the whole of southern Australasia, either offshore or onshore, at which the Marshall Paraconformity failed to manifest itself; this is an unlikely happenstance. Paleocene/Eocene boundary after Berggren et al. (1995), Eocene/Oligocene boundary after Berggren and Aubry (1995), Oligocene/Miocene boundary after Shackleton et al. (2000), Miocene/Pliocene boundary after Cita (1975), Pliocene/Pleistocene boundary after Aguirre and Pasini (1985). New Zealand stage abbreviations (4th column from the right), from older to younger—*Mata Series*: Mh = Haumurian; *Dannevirke Series*: Dg = Wangaloan (= Teurian), Dw = Waipawan, Dm = Mangaorapan, Dh = Heretaungan, Dp = Porangan; *Arnold Series*: Ab = Bortonian, Ak = Kaiatan, Ar = Runangan; *Landon Series*: Lwh = Whaingaroan, Ld = Duntroonian, Lw = Waitakian; *Pareora Series*: Po = Otaian, Pl = Altonian; *Southland Series*: Sc = Clifdenian, Sl = Lillburnian, Sw = Waiauian; *Taranaki Series*: Tt = Tongaporutuan, Tk = Kapitean; *Wanganui Series*: Wo = Opoitian; Ww = Waitoraran (Mangapanian and Waipipian substages), Wn = Nukumaruan (Hautawan and Marahauan substages), Wc = Castlecliffian (Okehuan and Putikian substages), Wh = Haweran. The Paleocene Wangaloan Stage (after Finlay and Marwick, 1940) is preferred to Teurian Stage because of its clear historical priority (cf. Webb, 1973). Wanganui Series stages and substages are after Carter, R., and Naish (1998).

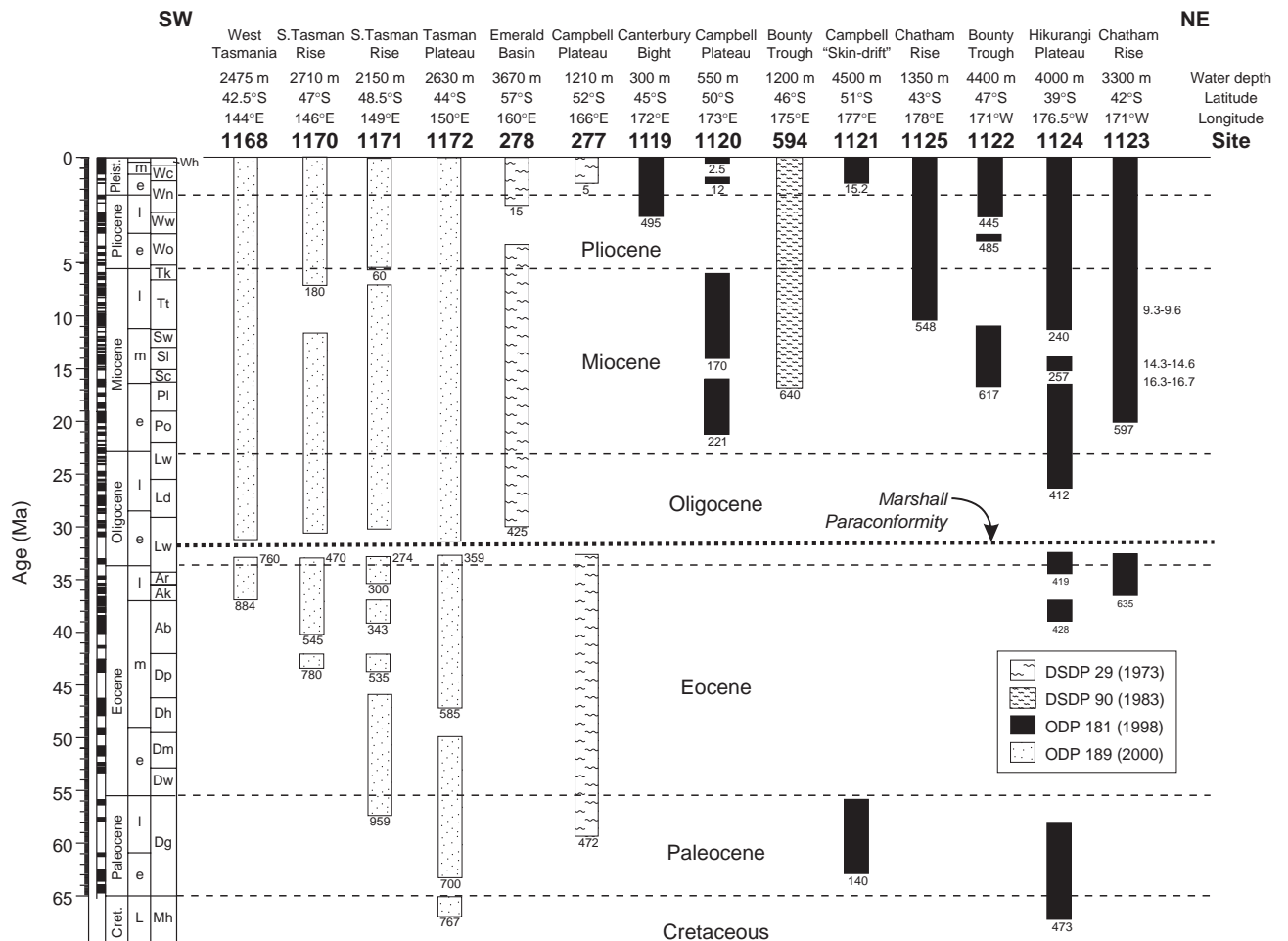


**Figure F7.** Climatic records from Site 1119 (water depth = 396 m), Canterbury upper slope (natural gamma ray [NGR] signal), and the Vostok ice core (deuterium isotope ratio), compared with the insolation curve for latitude 65°N (after Petit et al., 1999; Shackleton, 2000; Carter, R., et al., in press). Position of timescale control points (mapped from the Vostok core) indicated by black triangles along the base of the gamma ray record. Note the close correspondence of major climatic events as recorded in the widely separated temperate marine and polar ice cap records. Inset (top left of gamma ray record): proxy climate record for the last 30 k.y. for South Island, New Zealand, as indicated by oxygen isotope measurements on speleothems from Mt. Arthur, Southern Alps (Hellstrom et al., 1998).

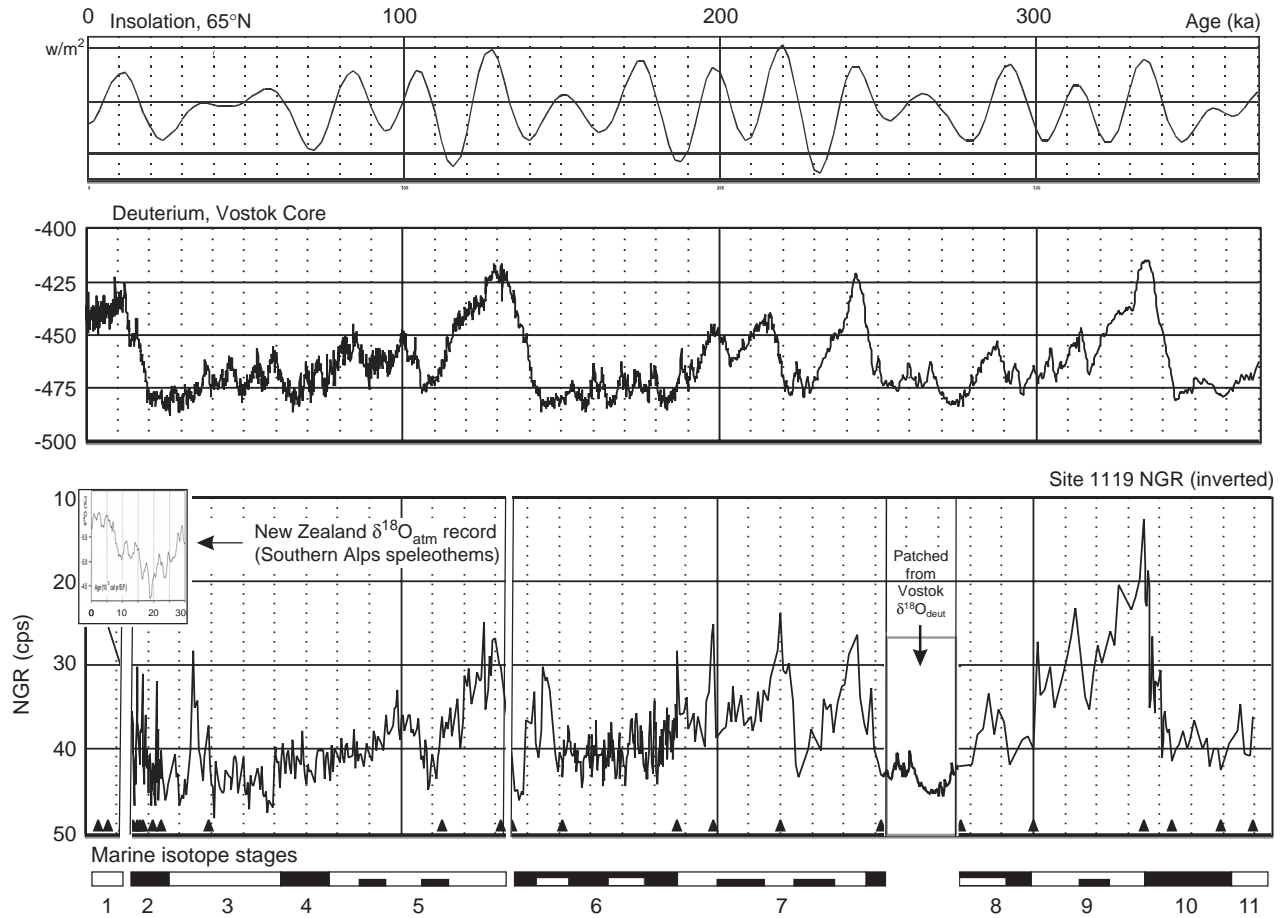


Figure F8. <sup>10</sup>Be stratigraphy and age profile for the upper 9 mbsf of Site 1121 (water depth = 4488 m; Campbell "skin drift") (after Graham et al., in press). SWPO = southwest Pacific Ocean.

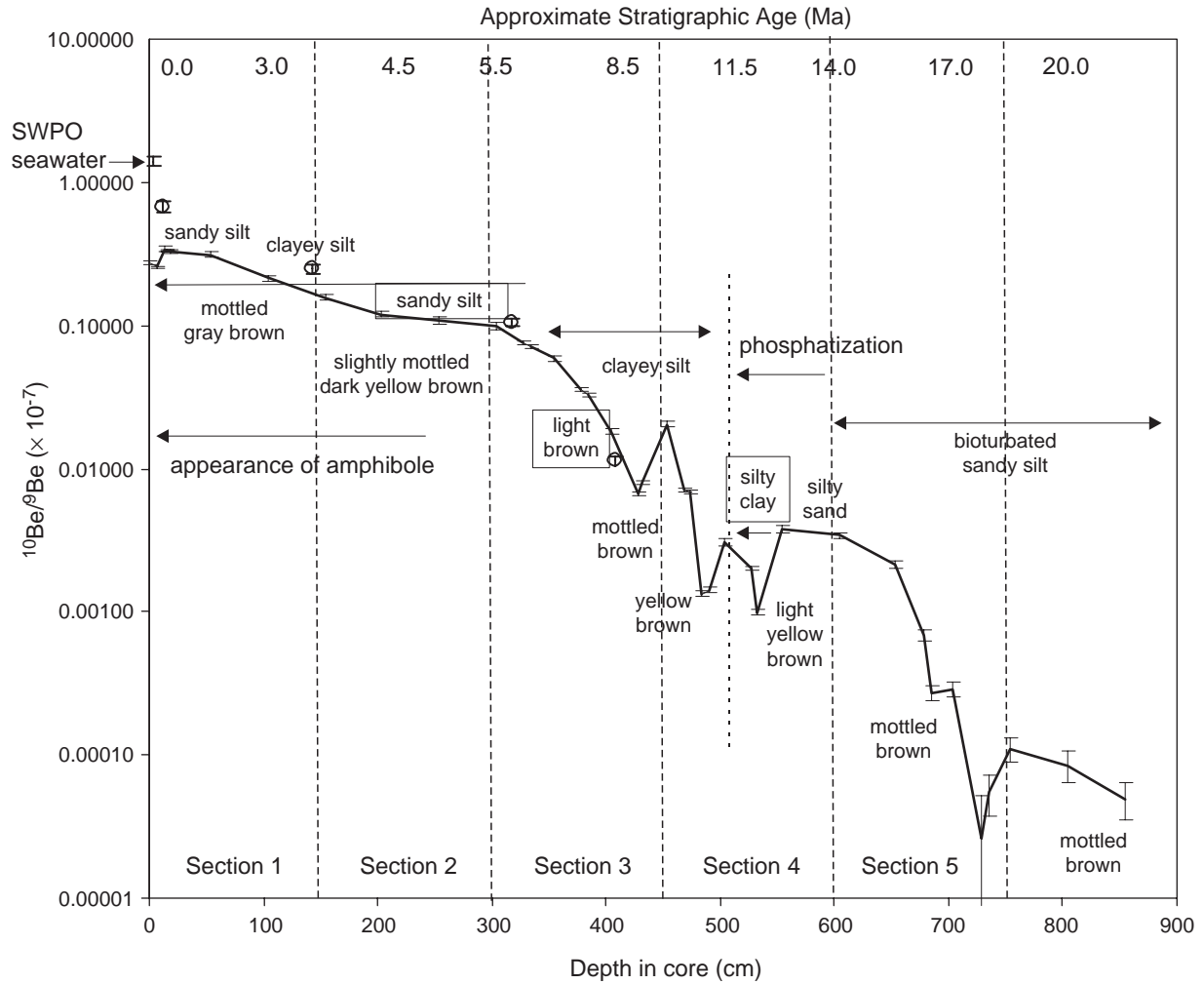




Figure F10. Revised age model for Site 1123 based on paleomagnetic and biostratigraphic indicators (after Wilson et al., 2003a). See caption to Figure F6, p. 88, for key to New Zealand biostratigraphic stage abbreviations.

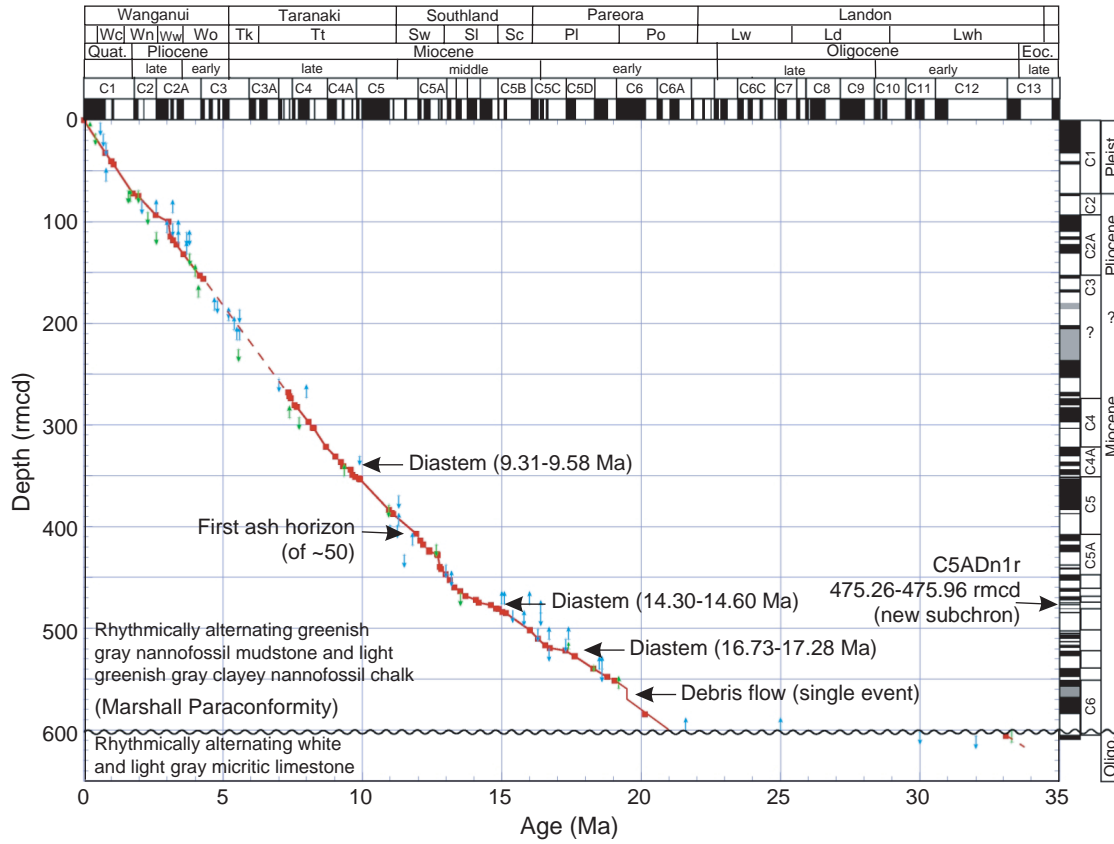
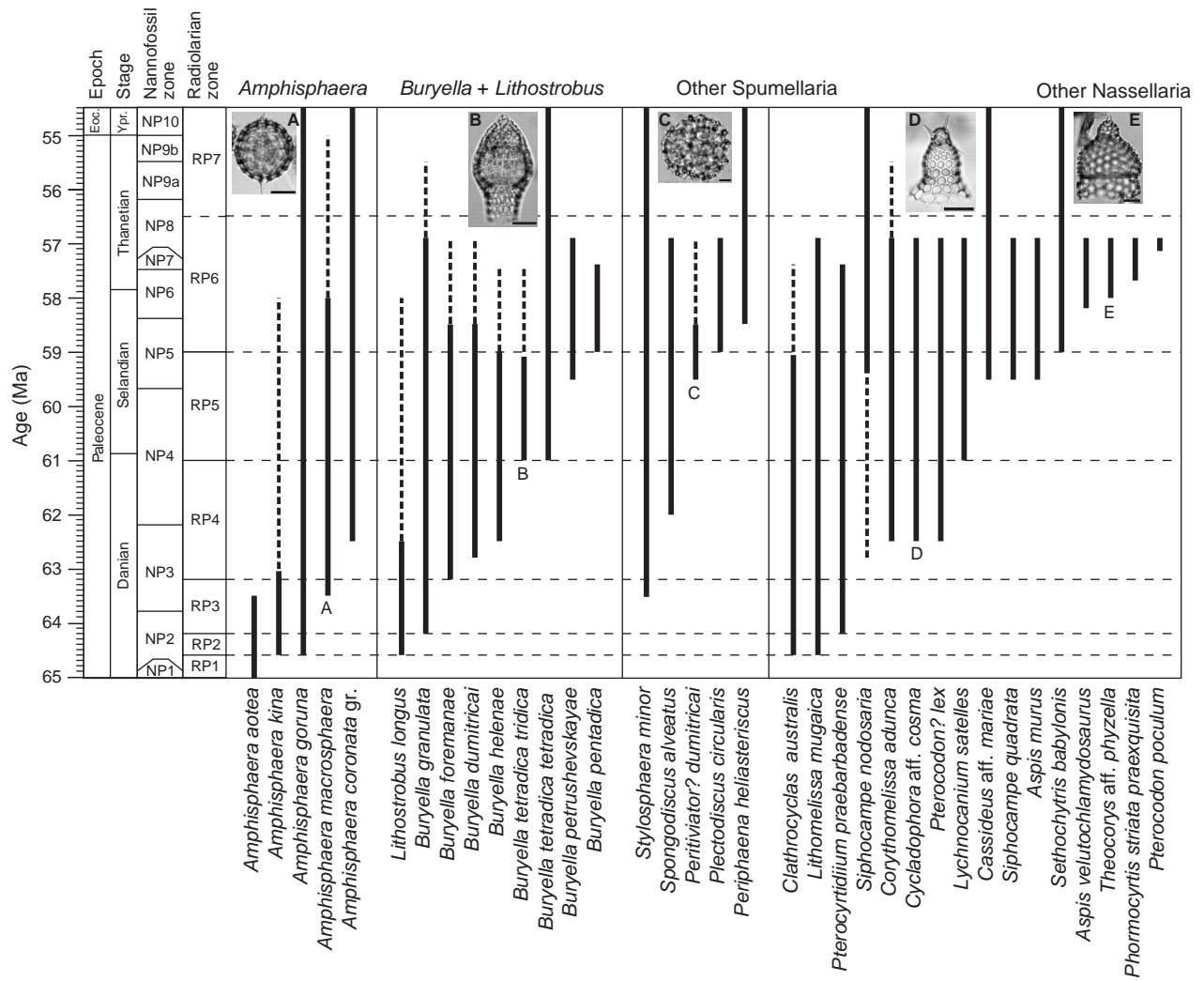


Figure F11. Age ranges of key radiolarian species in the southern Pacific based upon their ranges at ODP Site 1121 (water depth = 4488 m; Campbell Paleogene sediment apron), DSDP Leg 21 Site 208 (water depth = 1545 m; northern Lord Howe Rise), and onland in Marlborough, northeast South Island (after Hollis, 2002). Scale bars = 50  $\mu$ m.



**Figure F12.** Late Miocene bolboform and foraminiferal data from Site 1123 (water depth = 3290 m, North Chatham Drift) plotted against the paleomagnetic timescale of Wilson et al. (2003a). In benthic plot: light gray line = benthic foraminifer abundances; dark line = 11-point moving average; note that high benthic foraminifer abundances correspond to high dissolution (after Crundwell, in press). AAIW = Antarctic Intermediate Water. New Zealand (NZ) stage correlation after Morgans et al. (1996). TCZ = Tukemokihi Coiling Zone (after Crundwell, in press), KCZ = Kaiti Coiling Zone (after Scott, 1995).

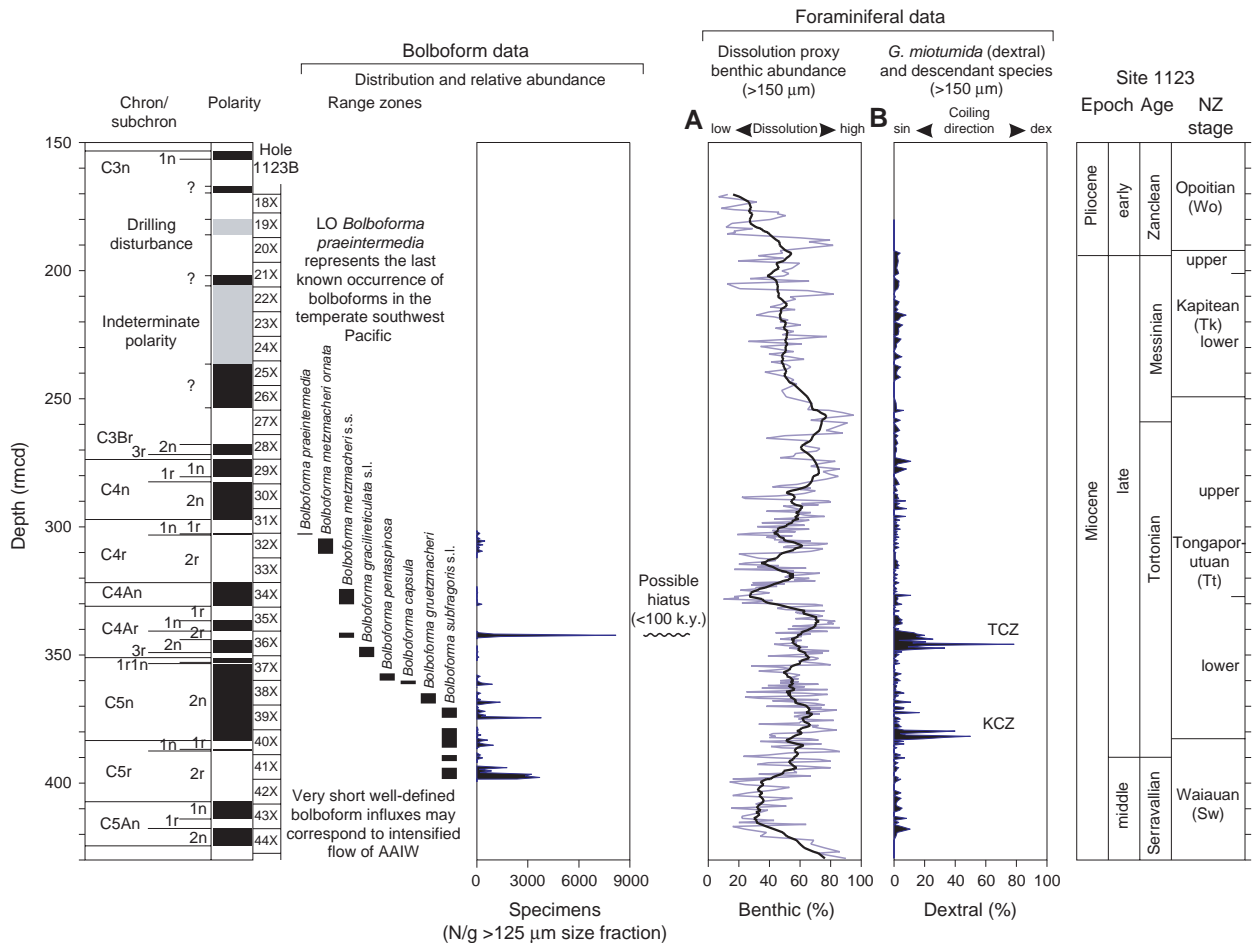
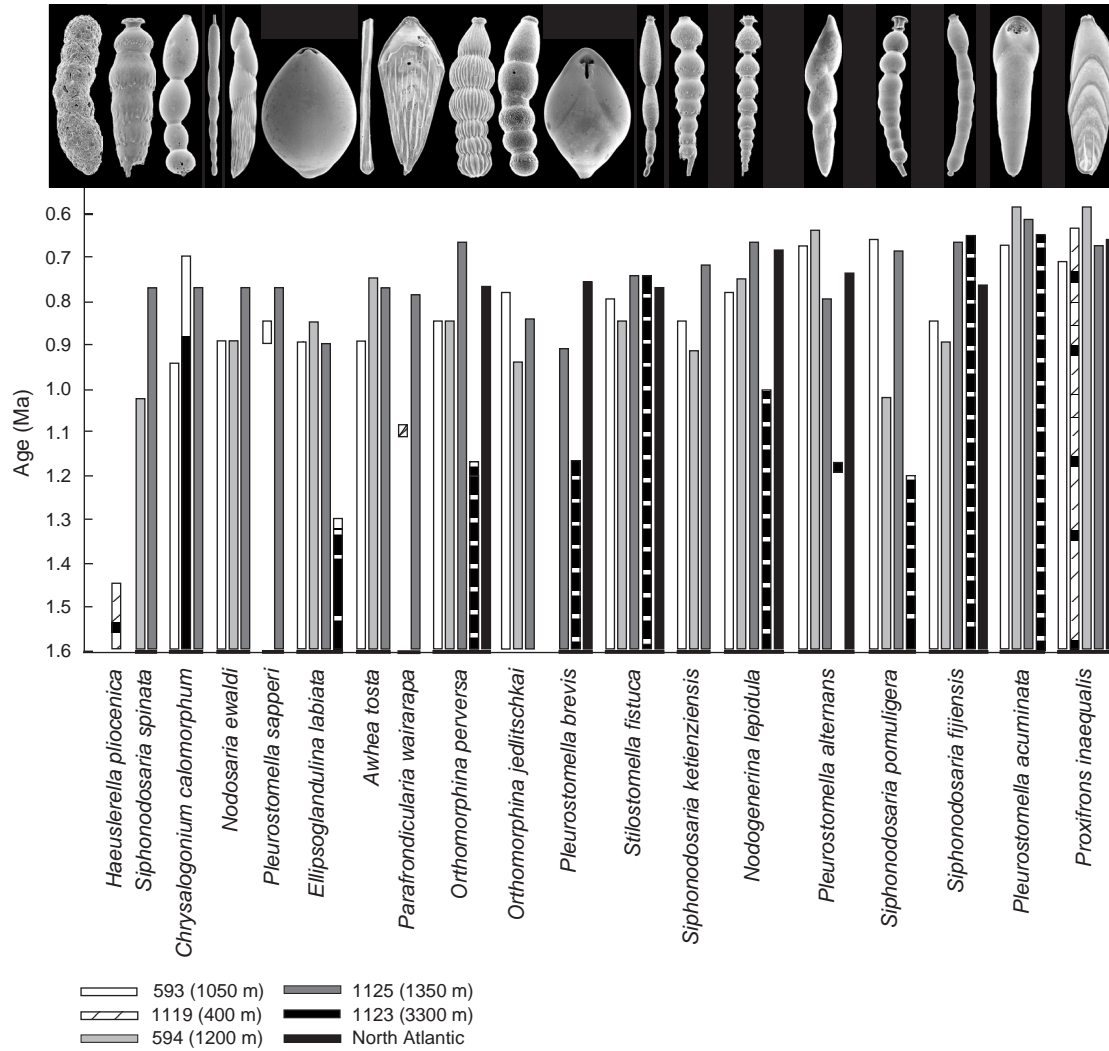
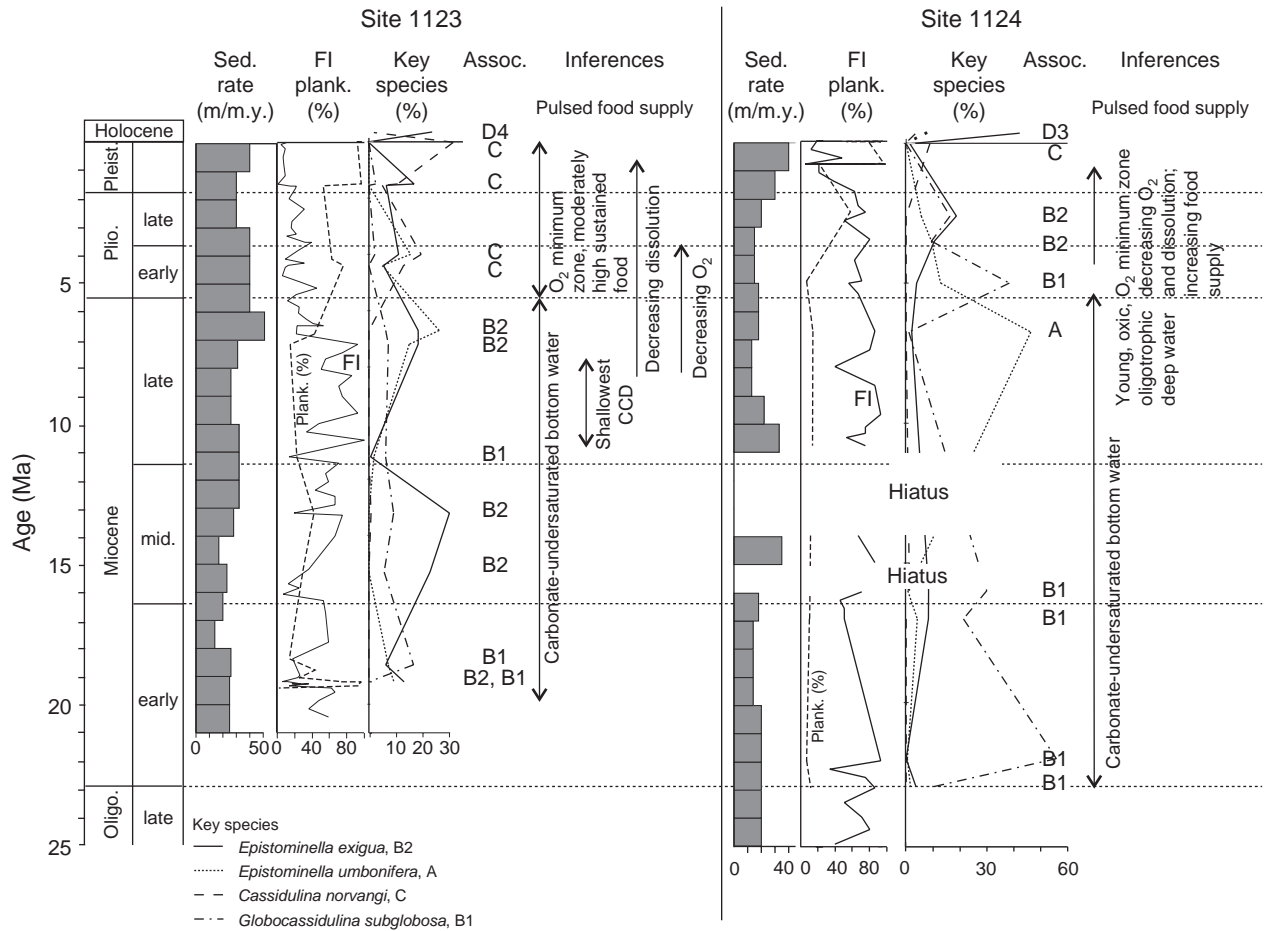


Figure F13. Comparison of the ranges between sites of nineteen selected deep-sea benthic foraminifers that became extinct during the middle Pleistocene “*Stilostomella* event” in the southwest Pacific. Age range for each species in the North Atlantic is also plotted (after Hayward, 2001).



**Figure F14.** Record of Neogene sedimentation rates, planktonic foraminiferal abundance and fragmentation index (FI), and benthic foraminiferal associations and key species from Sites 1123 (water depth = 3290 m; North Chatham Drift) and 1124 (water depth = 3967 m; Rekohu Drift). Major paleoceanographic interpretations are indicated (after Hayward et al., in press). CCD = calcite compensation depth.



**Figure F15.** Pollen and spore record for the upper 60 rncd (last 1.6 m.y.) of Site 1123 (water depth = 3290 m; North Chatham Drift). The data, which show obvious 41-k.y. Milankovitch cyclicality, are plotted against the color reflectance log (% carbonate proxy), the ODP Leg 111 Site 677 oxygen isotope record (Shackleton et al., 1990), and the paleomagnetic timescale (after Mildenhall, in press). The glacial vegetation (GV) index is based upon the proportion of cool-climate pollen present in each sample, expressed as (*Halocarpus* + *Phyllocladus* + *Nothofagus fusca* type + *Coprosma*)/(total pollen – *Prumnopitys/Podocarpus*). SSS = Standard Stratigraphic Scale.

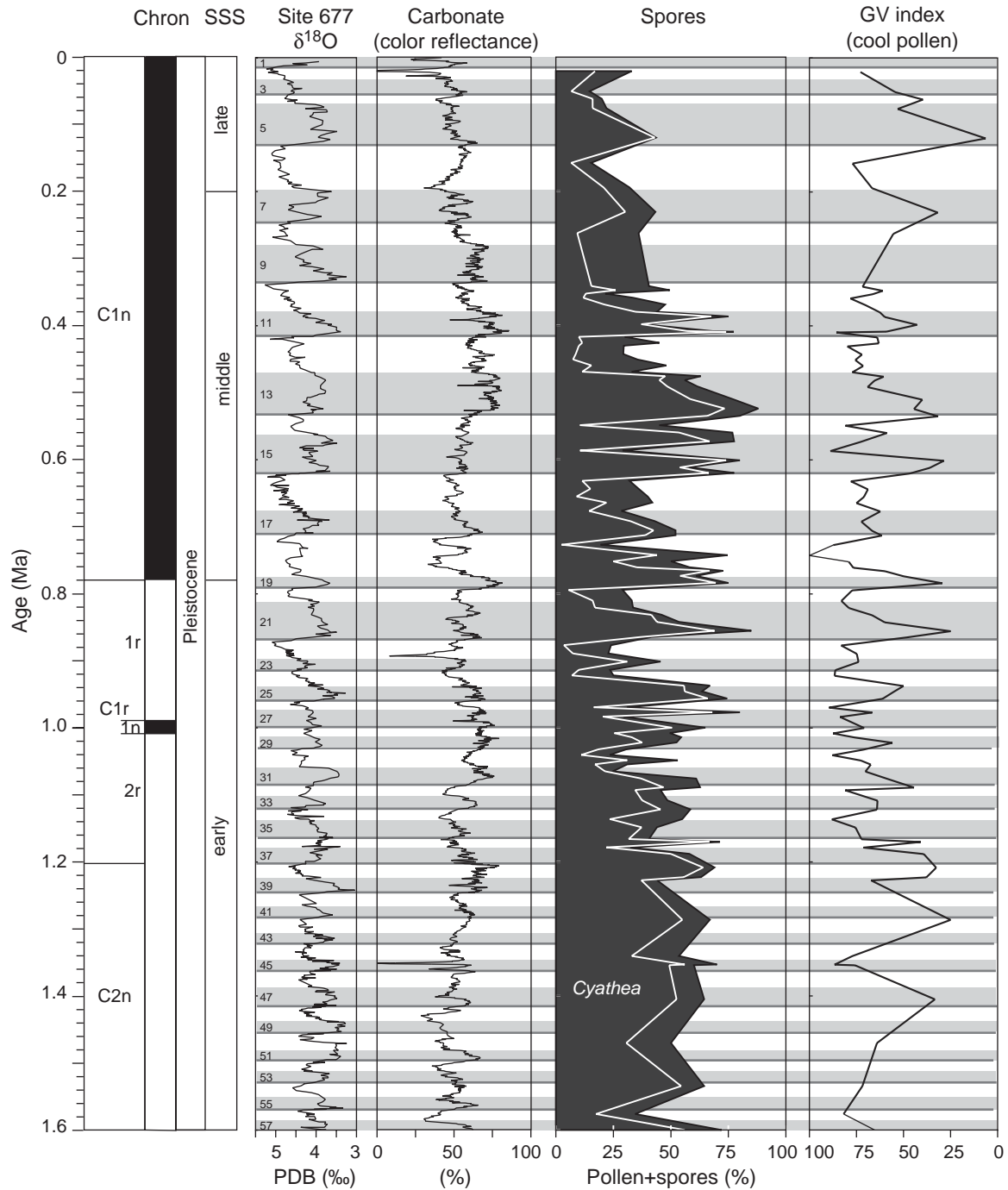
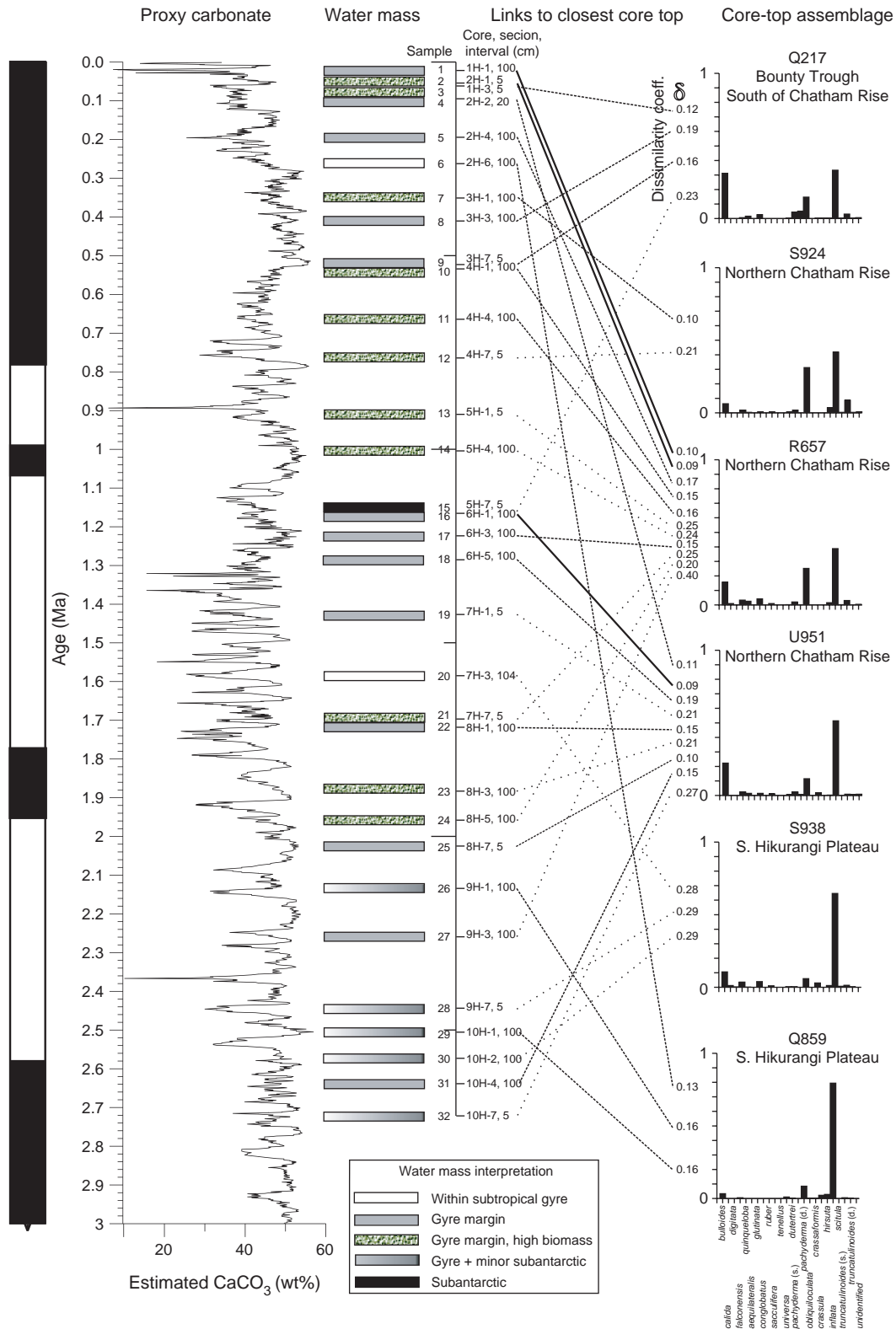
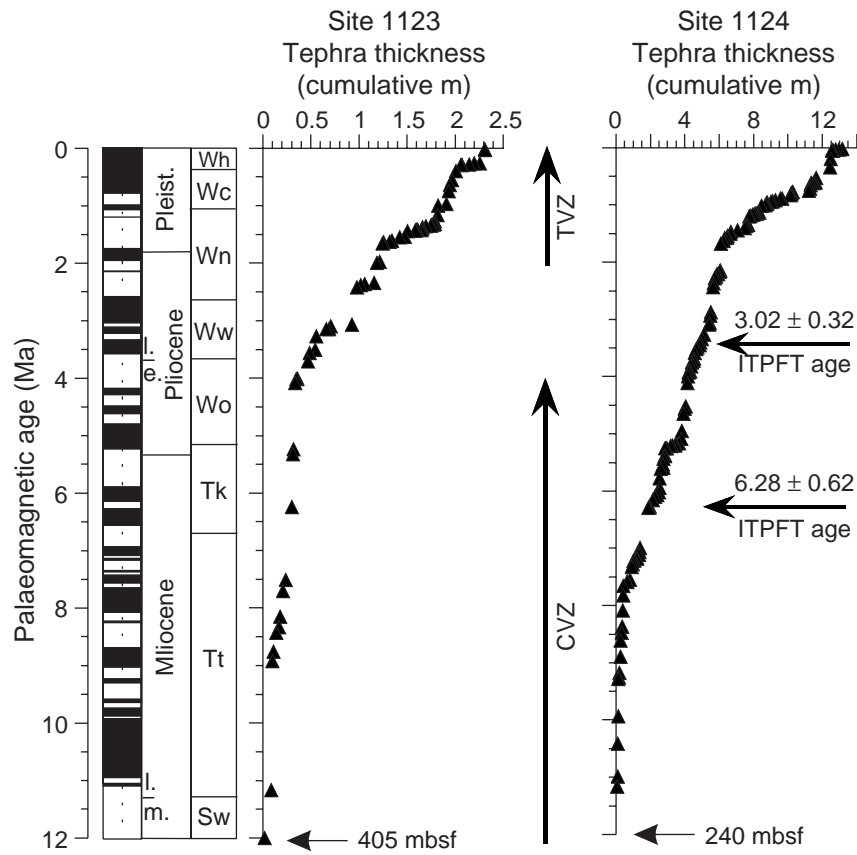


Figure F16. Planktonic foraminiferal census data from the upper ~110 mcd (last 3 m.y.) of Site 1123 (water depth = 3290 m; North Chatham Drift), compared with known core-top assemblages from the southwest Pacific and plotted against the color reflectance log (% carbonate proxy) and the paleomagnetic timescale (after Scott and Hall, in press).



**Figure F17.** Ash record, plotted as cumulative thickness through time, for Sites 1123 (water depth = 3290 m; North Chatham Drift) and 1124 (water depth = 3967 m; Rekohu Drift). The paleomagnetic age model is calibrated from the orbitally tuned benthic stable isotope record (Site 1123) and with isothermal plateau fission track (ITPFT) ages (Site 1124) (after Carter, L., et al., 2003). Note the inflection points, which indicate increases in the rate of ash supply at ~8 and 1.85 Ma. TVZ = Taupo Volcanic Zone; CVZ = Coromandel Volcanic Zone.



**Figure F18.** Quantitative comparison of clay mineral assemblages from DSDP Leg 90 Site 594 (water depth = 1204 m; northwest flank of Bounty Trough) and ODP Site 1123 (water depth = 3290; North Chatham Drift) (after Dersch and Stein, 1991; **Winkler and Dullo**, this volume). A compositional shift toward chlorite + illite-rich and smectite-poor clay assemblages starts under the DWBC at ~21 Ma (early Miocene) at Site 1123. Clover-leaf asterisks identify culminations in chlorite content that occur at ~18, 8.5, 5.3, and 1.2 Ma and are inferred to represent irregular pulses of uplift along the South Island alpine chain.

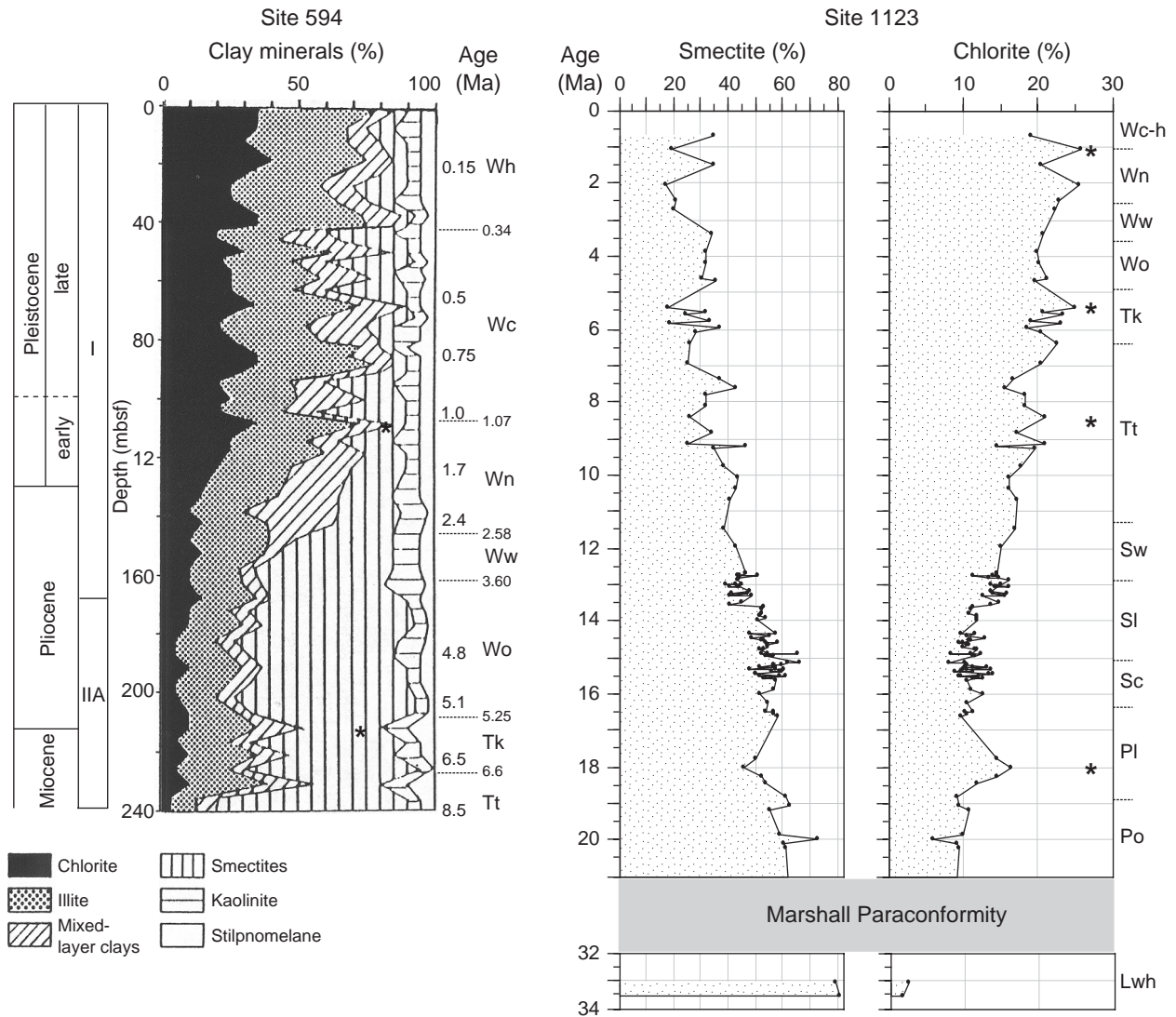
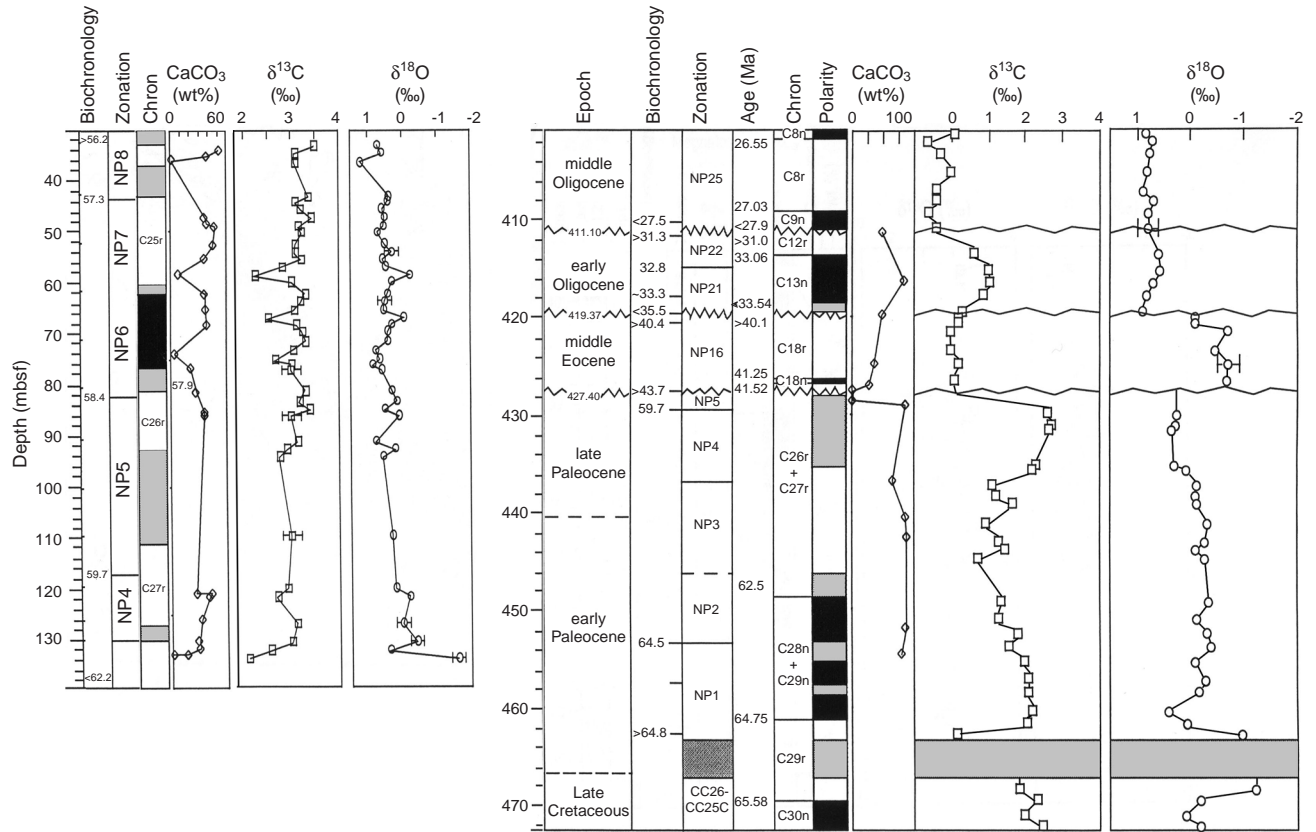
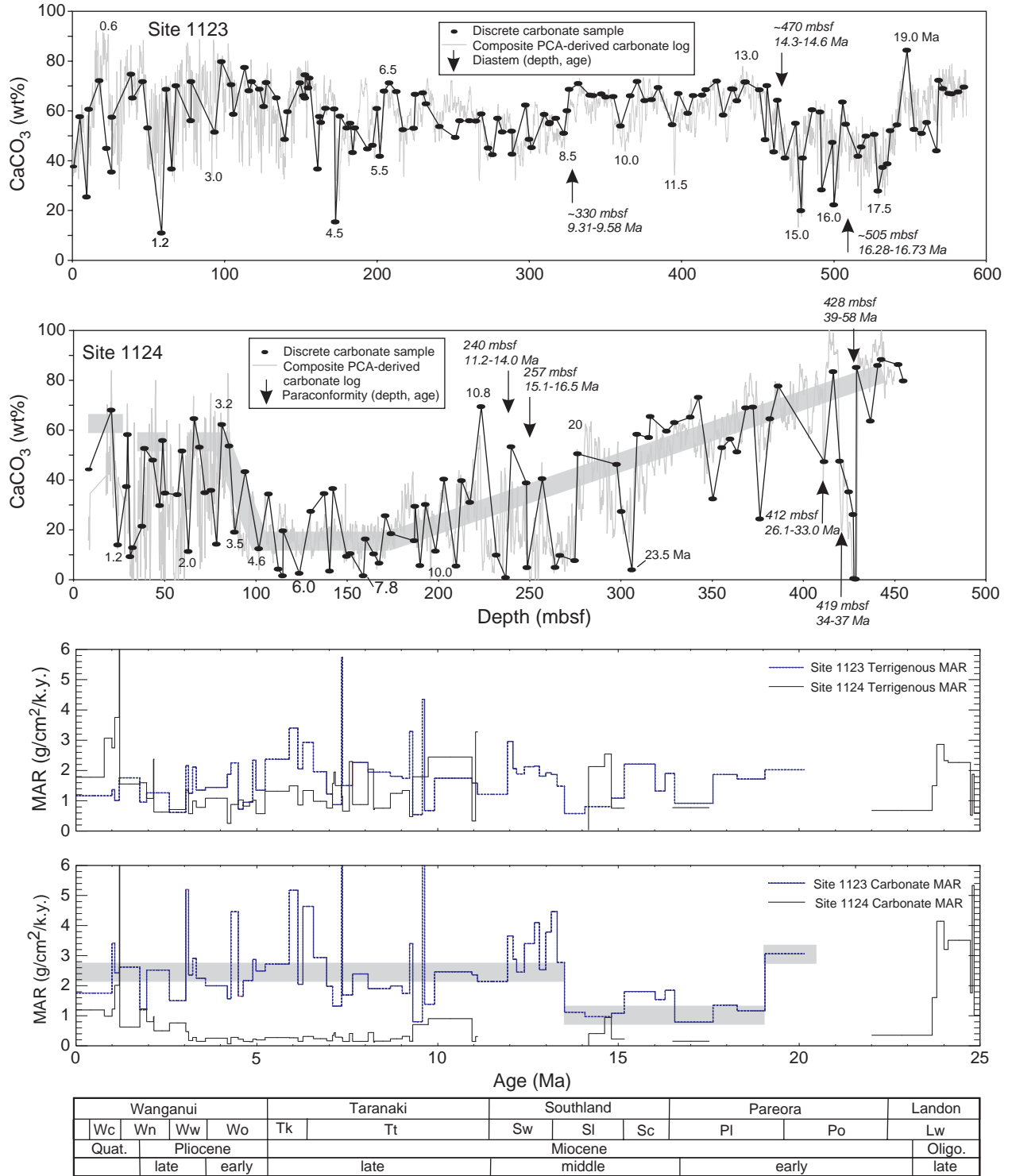


Figure F19. Carbon and oxygen isotope values for bulk sediment samples from Holes 1121B and 1124C. Error bars represent two standard deviations (after Wei et al., submitted [N2]).



**Figure F20.** Calcium carbonate rates and carbonate and terrigenous mass accumulation rates (MAR) for Sites 1123 (water depth = 3290 m; North Chatham Drift) and 1124 (water depth = 3967 m; Rekohu Drift), based upon downhole log profiles (after Handwerger and Jarrard, in press). PCA = principal component analysis. Position of paraconformities is indicated by vertical arrows and accompanying italic text (upper two diagrams). See caption to Figure F6, p. 88, for key to New Zealand biostratigraphic stage abbreviations. See text for detailed comments.



**Figure F21.** Selected time series records from Sites 1123 (water depth = 3290 m; North Chatham Drift) and 1124 (water depth = 3967 m; Rekohu Drift). **A.** Middle Miocene (12.5–15.5 Ma) sortable silt (SS) record from Site 1123 and its filtered 41-k.y. orbital obliquity component plotted against the geomagnetic polarity and Site 1123 timescales. The filter has a central frequency of 0.04065 cycles/k.y. and a bandwidth of 0.01046 cycles/k.y. (after Hall et al., 2003). Note the way that these two records vary in close sympathy with each other, with enhanced Deep Western Boundary Current flow (increased mean grain size of sortable silt) corresponding to obliquity maxima. **B.** Post-Pliocene (0–3.0 Ma) records of benthic  $\delta^{18}\text{O}$  for Site 1123 (above) and carbonate:terrigenous ratio for Sites 1123 (middle) and 1124 (below). Thick lines indicate a 50-point moving average, to better show the general similarity between the profiles through time (after Hall et al., 2002). Note the presence of enhanced terrigenous ratios and wider fluctuations in ratios from about 1.4 Ma onward, in correspondence with the enhanced amplitude then of the benthic oxygen isotope signal. **C.** Pleistocene (0–1.2 Ma) records from Site 1123 for benthic  $\delta^{18}\text{O}$  (above), benthic  $\delta^{13}\text{C}$  (middle), and mean grain size of sortable silt (SS) below (after Hall et al., 2001). Note the correspondence between glacial climates and enhanced Deep Western Boundary Current flow (DWBC). MIS = marine isotope stage.

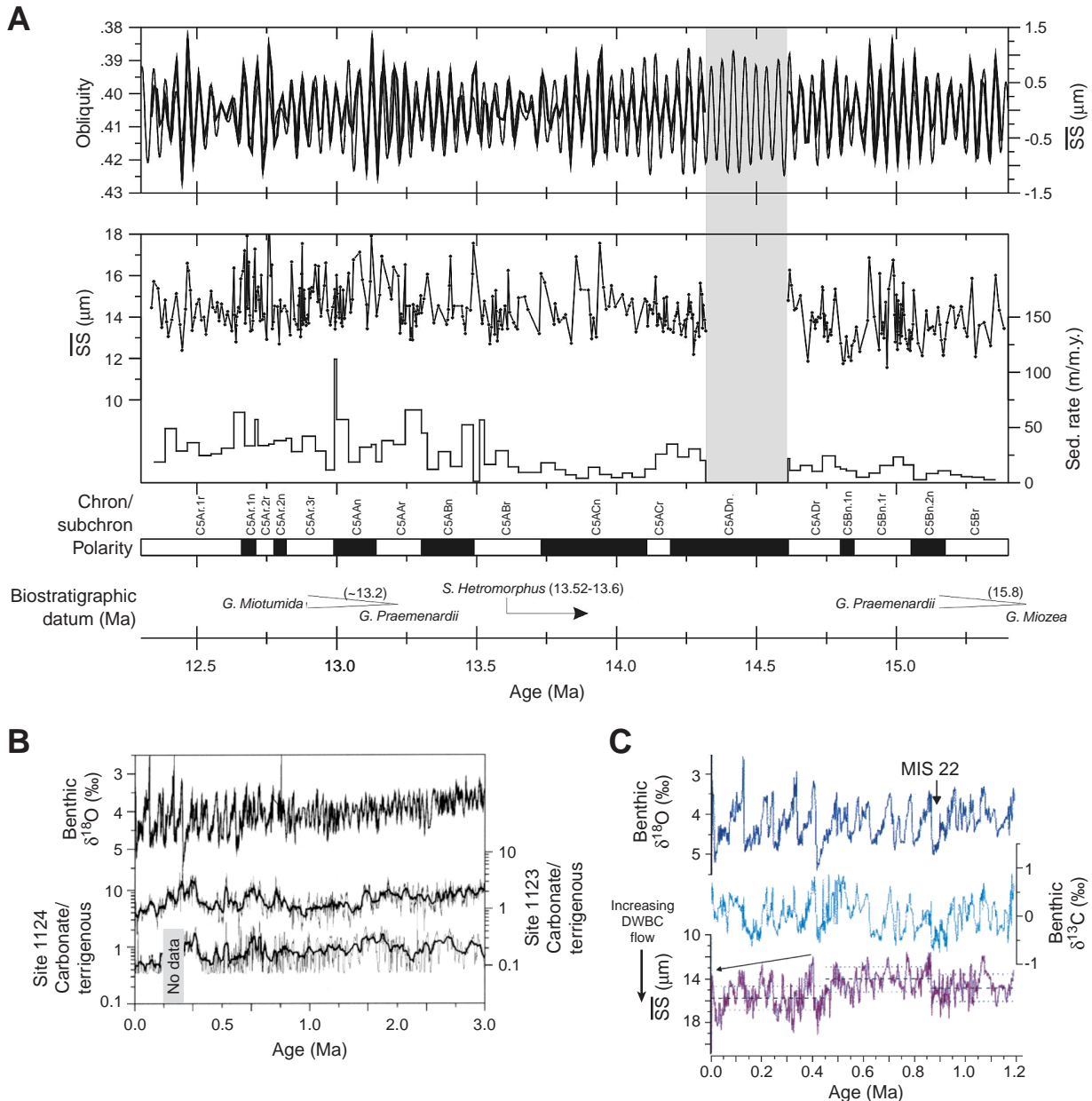
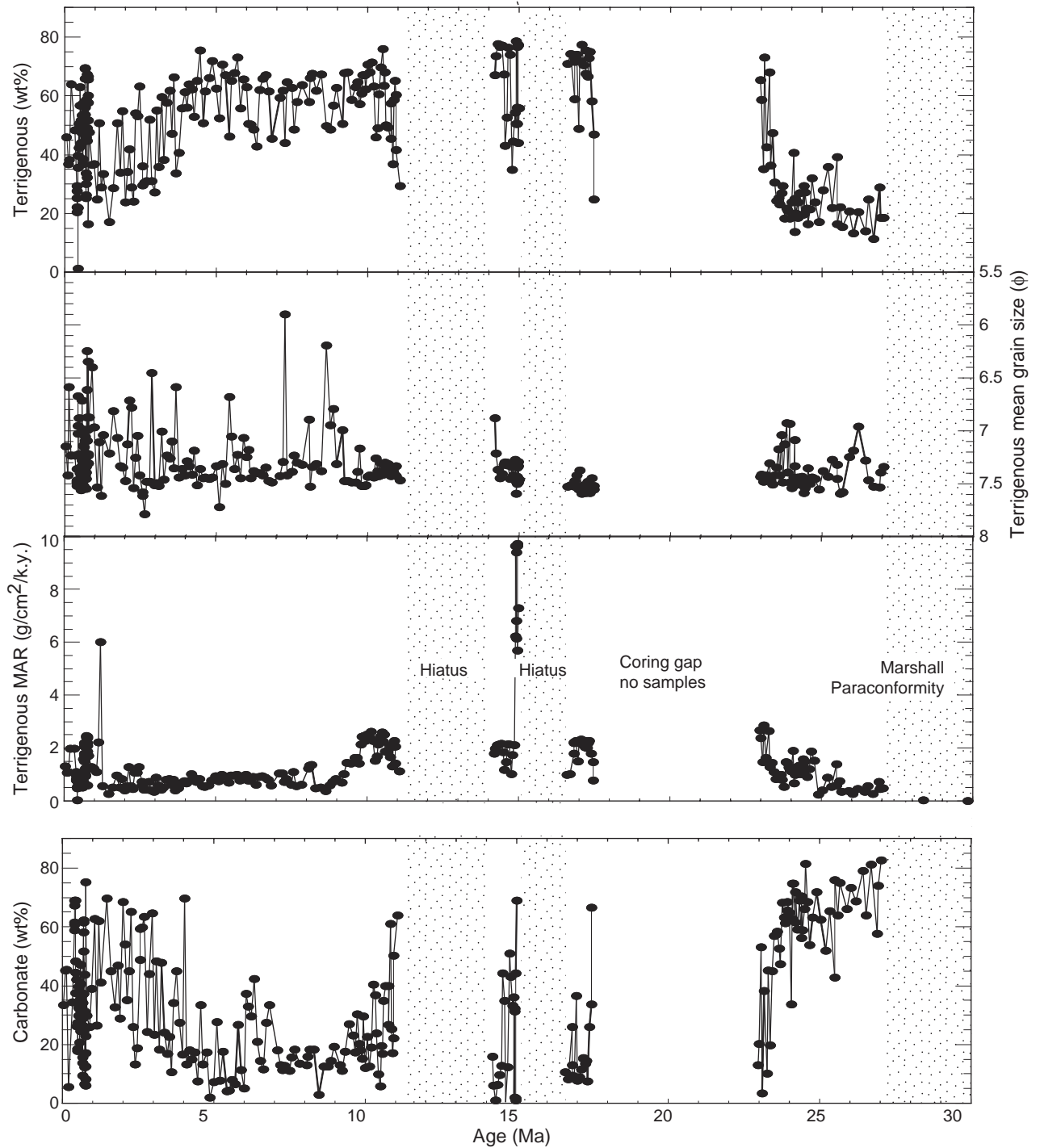
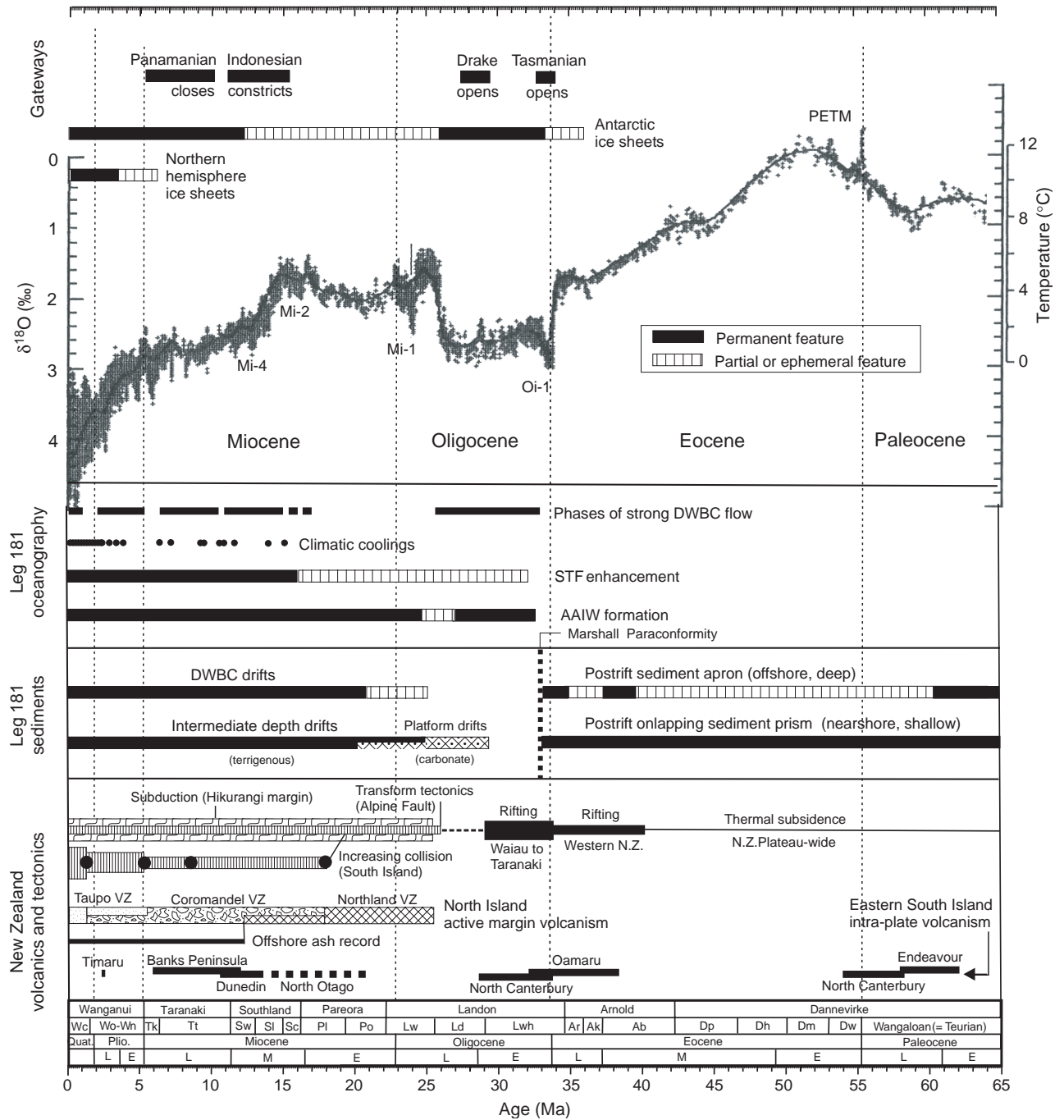


Figure F22. Sediment characterization at Site 1124 (water depth = 3967 m; Rekohu Drift) (after Joseph et al., in press). See caption to Figure F6, p. 88, for key to New Zealand biostratigraphic stage abbreviations. See text for detailed comments. MAR = mass accumulation rate.



Wanganui			Taranaki			Southland			Pareora		Landon		
Wc	Wn	Ww	Wo	Tk	Tt	Sw	Sl	Sc	Pl	Po	Lw	Ld	Lwh
Quat.		Pliocene					Miocene			Oligocene			
	late	early		late			middle			early		late	early

Figure F23. Major Leg 181 stratigraphic and climatic events plotted against the summary global ocean benthic foraminifer oxygen isotope curve of Zachos et al. (2001). The temperature scale (right) is scaled to an ice-free ocean, and therefore only applies for the period 35–65 Ma. N.Z. = New Zealand. PETM = Paleocene/Eocene Thermal Maximum; DWBC = Deep Western Boundary Current; STF = Subtropical Front; AAIW = Antarctic Intermediate Water; VZ = volcanic zone. See caption to Figure F6, p. 88, for key to New Zealand biostratigraphic stage abbreviations.



**Figure F24.** Reconstructed frontal systems and ocean surface circulation for the Australasian Southern Ocean at 35, 20, 10, and 0 Ma. Base map tectonic reconstruction by Sutherland (after Cande et al., 1995; Sutherland, 1995; Royer and Rollet, 1997). The maps are in transverse Mercator projection and show the present-day coastline, the 2000-m isobath, and the positions of sites drilled during Legs 181 and 187. Also plotted on the 0-Ma reconstruction are the apparent paleomagnetic polar wander paths for the Australian (Veevers and Li, 1991) and Pacific (Sutherland, 1995) plates, interpolated at 5-m.y. intervals to show the relative northwestward motions. STF = Subtropical Front, AAPF = Antarctic Polar Front, AAD = Antarctic Divergence, SAF = Subantarctic Front.

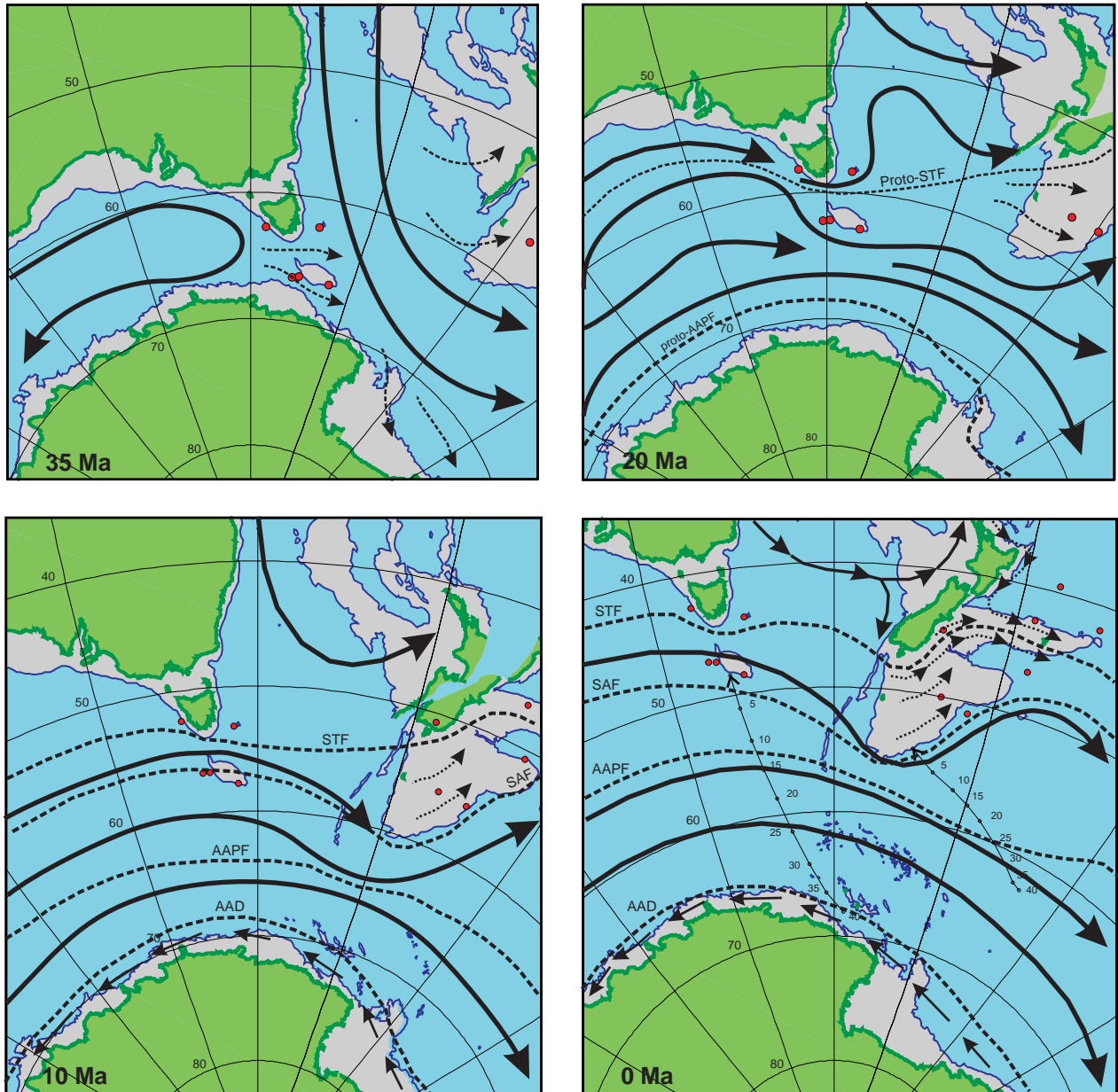


**Figure F25.** Manifestations of the Marshall Paraconformity in the ENZOSS region. This several-million-year-long current-induced unconformity is present across all sedimentary facies and water depths between the inner shelf and the lower slope, and thereby marks the early Oligocene startup of the seabed to sea-surface ACC. **A.** Outcrop view of cross-bedded, glauconitic, calcarenite sediment drifts of the early Miocene (Lw) Weka Pass Limestone, Waihao Forks. The Marshall Paraconformity outcrops nearby (cf. Ward and Lewis, 1975) but here lies obscured beneath the grassy talus slope. Figures for scale. **B.** Typical onland shallow-water outcrop of the paraconformity at its type locality, Squires Farm, Pareora district (cf. Gair, 1959). Intensely bioturbated late Oligocene (Ld) Concord Greensand overlies and infills *Thalassinoides* burrows in the underlying latest Eocene–early Oligocene (early Lwh) marly Amuri Limestone, which is also intensely bioturbated. Note bioerosional remnants of the underlying marl incorporated within the base of the greensand. Hammer handle = 32 cm. **C.** Paraconformity as developed farther south, near Dunedin. Late Oligocene (Ld) Concord Greensand penetrating via *Chondrites* burrows into underlying bioturbated late Eocene (Ak-Ar) Burnside Marl (cf. Bishop and Turnbull, 1996). Bioerosional fragments of marl are conspicuous within the basal part of the Concord Greensand. Scale in millimeters. **D.** Paraconformity developed at Site 1123. Basal sediments of the early Miocene (Po) Chatham drift overlies and fills *Chondrites* burrows in early Oligocene (early Lwh) nannofossil chalk of the pre-ENZOSS sediment apron (cf. Carter, R., McCave, Richter, Carter, L., et al., 1998). Black bar = 5 cm. **E.** Paraconformity developed at Site 1124. Basal sediments of a late Oligocene (Ld) DWBC sediment drift overlies and fills *Chondrites* burrows in early Oligocene (early Lwh) nannofossil chalk of the pre-ENZOSS sediment apron (cf. Carter, R., McCave, Richter, Carter, L., et al., 1998). Black bar = 5 cm. See caption to Figure F6, p. 88, for key to New Zealand biostratigraphic stage abbreviations.

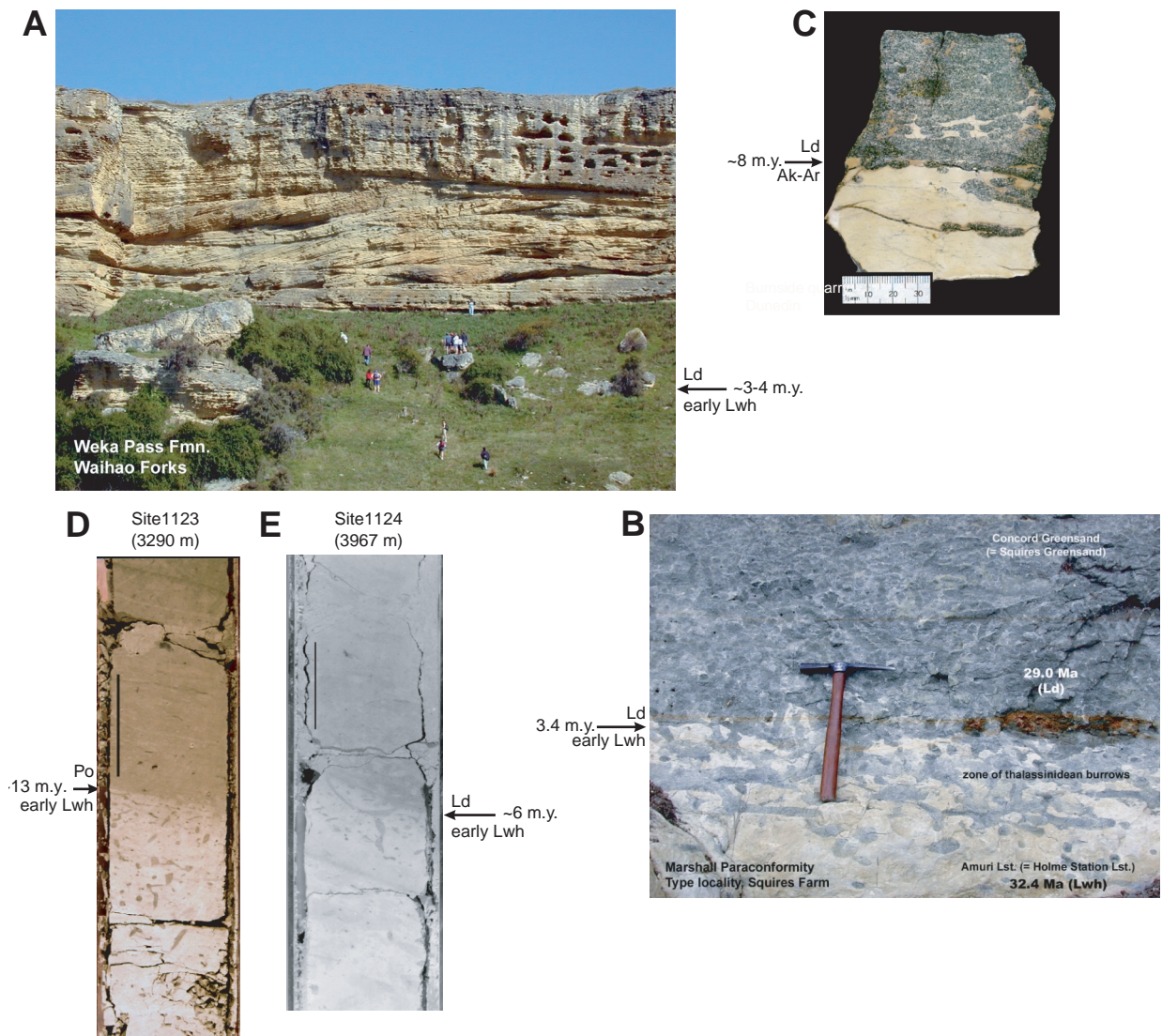


**Figure F26.** Timescales for DSDP Leg 90 Site 594 (water depth = 1204 m; south slope of Chatham Rise) and Site 1125 (water depth = 1366 m; north slope of Chatham Rise). **A.** Increasing terrigenous content, Site 594 (~170 mbsf). **B.** Appearance of marked climatic terrigenous-carbonate couplets, Site 594 (~145 mbsf). Site 594 after Kennett et al. (1986) as amended by Grant and Dickens (submitted [N5]) after Lazarus et al. (1995). Site 1125 after Carter, R., McCave, Richter, Carter, L., et al. (1999). See caption to Figure F6, p. 88, for key to New Zealand biostratigraphic stage abbreviations.

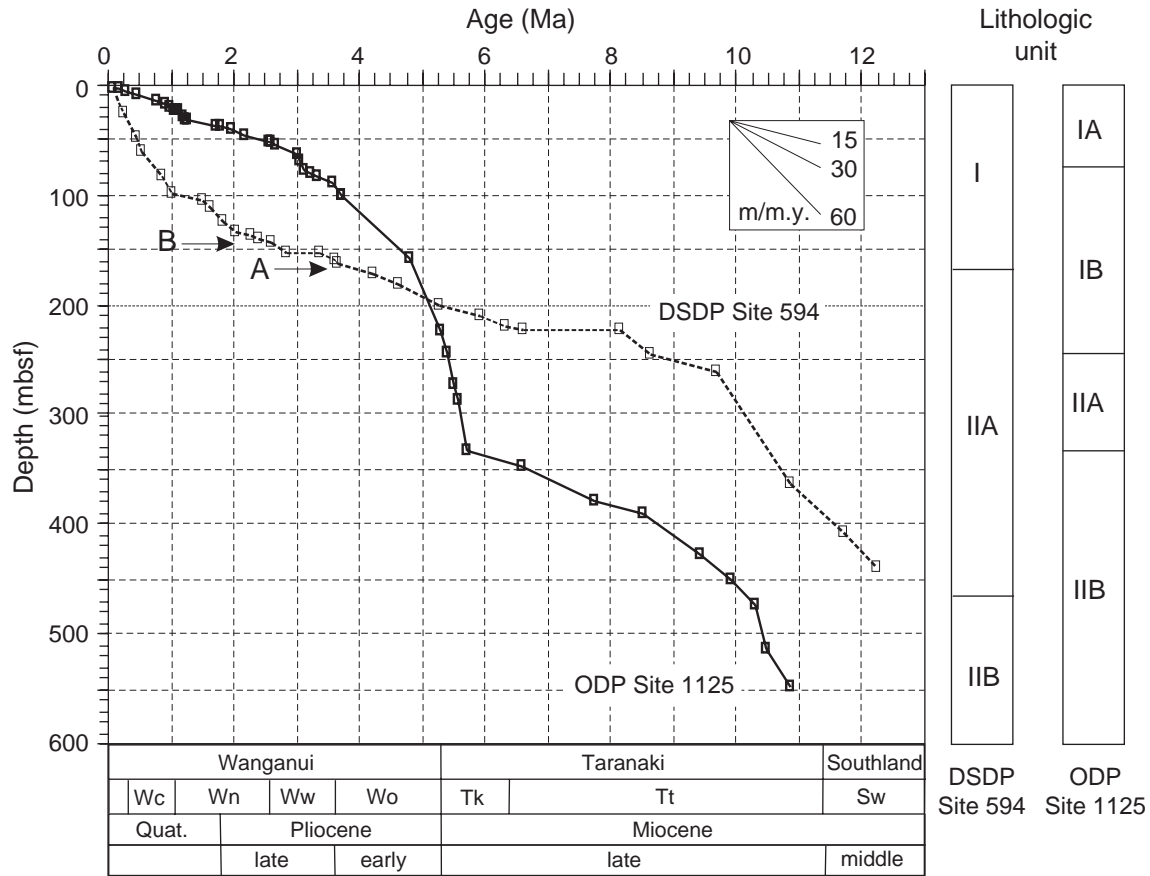


**Table T1.** Leg 181 drill sites.

Site	Latitude	Longitude	Water depth (m)	Holes	Penetration (mbsf)	Location	Target
1119	44°45.332'S	172°23.598'E	396	1119A 1119B 1119C	6.0 155.5 494.8	Upper slope, Canterbury Bight	Canterbury (SAMW/AAIW) drifts
1120	50°03.822'S	173°22.300'E	546	1120A 1120B 1120C 1120D	4.6 188.0 44.6 220.7	Central Campbell Plateau	Biopelagic platform cover
1121	50°53.876'S	176°59.862'E	4488	1121A 1121B	8.4 139.7	Foot of Campbell Plateau slope	DWBC "skin drift;" Paleogene apron
1122	46°34.780'S	177°23.622'W	4432	1122A 1122B 1122C	123.9 9.5 627.4	Left bank levee, abyssal Bounty Fan	Fan history; underlying contourites
1123	41°47.147'S	171°29.941'W	3290	1123A 1123B 1123C	158.1 489.0 632.8	Northeastern slope of Chatham Rise	North Chatham (DWBC) Drift
1124	39°29.901'S	176°31.894'W	3967	1124A 1124B 1124C 1124D	9.5 9.9 473.1 155.6	Northern edge of Hikurangi Plateau	Rekohu (DWBC) Drift
1125	42°32.979'S	178°09.988'W	1366	1125A 1125B	203.5 552.1	Northern slope of Chatham Rise	AAIW drifts and frontal biopelagites

Notes: SAMW= Subantarctic Mode Water; AAIW = Antarctic Intermediate Water; DWBC = Deep Western Boundary Current. After Carter, R., McCave, Richter, Carter, L., et al., 1999.

Table T2. Table of major water masses and other oceanographic features, ENZOSS sector of the Southwest Pacific Ocean.

Water mass	Abbrev.	Depth (mbsl)	Density (g/cm <sup>3</sup> )	Salinity	Temperature (°C)	Oxygen (mg/L)	Silica
(Warm) Subtropical Surface Water <i>Tasman Front</i>	(W)STW	Surface			>20		
			Separates CSTW/WSTW at 20° summer surface isotherm				
(Cool) Subtropical Surface Water <i>Subtropical Front</i>	(C)STW STF	Surface			>15		
			Separates CSTW/ASW at 15° summer surface isotherm				
Subantarctic (= Australasian) Surface Water <i>Subantarctic Front</i>	SAW SAF	Surface			8–15		
			Separates ASW/CSW at 8° summer surface isotherm				
Circumpolar Surface Water <i>Antarctic Polar Front (Convergence)</i>	CSW AAPF	Surface			5–8		
			Separates CSW/AAW, with icebergs (<5°C)				
Antarctic Surface Water <i>Antarctic Divergence</i>	AAW AAD	Surface			2.5–5 1.9–2.5		
Thermocline water				34.42–34.90	7.00–11.00	4.40–5.00	
Subantarctic mode water	SAMW	400–600	26.80–27.20	34.0–34.2	6–10	Very high	Very low
Antarctic Intermediate Water (S min)	AAIW	600–1450	27.20–27.35	34.50–34.36	3.20–7.00	3.20–4.70	
North Pacific Deep Water (O min)	NPDW	1450–2550		34.67–34.50	1.80–3.20	2.80–3.20	
Circumpolar Deep Water (upper)	UCDW	2550–2900	36.50–37.00	34.67–34.71	1.60–1.80	3.03–3.45	
Circumpolar Deep Water (middle) (S max)	MCDW	2900–3800	37.00–45.93	34.71–34.73	0.90–1.60	3.45–3.63	High
Circumpolar Deep Water (lower) (O max)	LCDW	>3800	45.93–46.00	<34.71	0.55–0.90	4.70–4.80	High
Antarctic Circumpolar Current	ACC	0–seafloor	Various	—	—	—	—
Weddell Sea Deep Water	WSDW				–0.30–0.00		
North Atlantic Deep Water	NADW		As for MCDW	—	—	—	—
Antarctic Bottom Water	AABW						

Notes: General term for cold water of Antarctic origin which spreads north into the major ocean basins. Bold italic text (left column) indicates surface. AAW = Antarctic Water. After Carter, R., et al., 1996. — = no data.

## CHAPTER NOTES\*

- N1. Neil, H.L., Carter, L., and Morris, M., submitted. Thermal isolation of Campbell Plateau, the Antarctic Circumpolar Current over the past 130 k.y. *Palaeoceanography*.
- N2. Wei, K.-Y., Mii, H.-S., Shu, I.-T., and Lin, Y.-J., submitted. Uppermost Cretaceous–middle Oligocene carbon and oxygen isotope stratigraphy in the Southwest Pacific: Holes 1121B and 1124C, ODP Leg 181. *N. Z. J. Geol. Geophys.*
- N3. Wei, K.-Y., and Chen, L.-L., submitted. Late Pliocene–Pleistocene calcareous nanofossil biostratigraphy of transitional sites of DSDP 594 and ODP 1125 in the middle latitudes of southwest Pacific. *Mar. Geol.*
- N4. Mii, H.-S., Wei, K.-Y., Shu, I.-T., and Lin, Y.-J., 2002. Carbon and isotope records in bulk sediments from ODP Leg 181, Holes 1121B and 1124C. Abstract [unpubl. data].
- N5. Grant, K.M., and Dickens, G.R., submitted. The late Miocene–early Pliocene ‘biogenic bloom’ at two oceanic fronts in the Southwest Pacific. *Mar. Geol.*

\*Dates reflect file corrections or revisions.